CHAPTER 4

BASEBAND PULSE TRANSMISSION

This chapter discusses the transmission of digital data over a baseband channel, with emphasis on the following topics:

- *The matched filter, which is the optimum system for detecting a known signal in additive white Gaussian noise.*
- *Calculation of the bit error rate due to the presence of channel noise.*
- *Intersymbol interference, which arises when the channel is dispersive as is commonly the case in practice.*
- *Nyquist's criterion for distortionless baseband data transmission.*
- *Correlative-level coding or partial-response signaling for combatting the effects of intersymbol interference.*
- *Digital subscriber lines.*
- *Equalization of a dispersive baseband channel.*
- *The eye pattern for displaying the combined effects of intersymbol interference and channel noise in data transmission.*

4.1 *Introduction*

In Chapter 3 we described techniques for converting an analog information-bearing signal into digital form. There is another way in which digital data can arise in practice: The data may represent the output of a source of information that is inherently discrete in nature (e.g., a digital computer). In this chapter we study the transmission of digital data (of whatever origin) over a *baseband channel.*[1] Data transmission over a band-pass channel using modulation is covered in Chapter 6.

Digital data have a broad spectrum with a significant low-frequency content. Baseband transmission of digital data therefore requires the use of a low-pass channel with a bandwidth large enough to accommodate the essential frequency content of the data stream. Typically, however, the channel is *dispersive* in that its frequency response deviates from that of an ideal low-pass filter. The result of data transmission over such a channel is that each received pulse is affected somewhat by adjacent pulses, thereby giving rise to a common form of interference called *intersymbol interference* (ISI). Intersymbol interference is a major source of bit errors in the reconstructed data stream at the receiver output. To correct for it, control has to be exercised over the pulse shape in the overall system. Thus much of the material covered in this chapter is devoted to *pulse shaping* in one form or another.

Another source of bit errors in a baseband data transmission system is the ubiquitous *channel noise*. Naturally, noise and ISI arise in the system simultaneously. However, to understand how they affect the performance of the system, we first consider them separately; later on in the chapter, we study their combined effects.

We thus begin the chapter by describing a fundamental result in communication theory, which deals with the *detection* of a pulse signal of known waveform that is immersed in additive white noise. The device for the optimum detection of such a pulse involves the use of a linear-time-invariant filter known as a *matched filter*,[2] which is so called because its impulse response is matched to the pulse signal.

4.2 Matched Filter

A basic problem that often arises in the study of communication systems is that of *detecting* a pulse transmitted over a channel that is corrupted by channel noise (i.e., additive noise at the front end of the receiver). For the purpose of the discussion presented in this section, we assume that the major source of system limitation is the channel noise.

Consider then the receiver model shown in Figure 4.1, involving a linear time-invariant filter of impulse response $h(t)$. The filter input $x(t)$ consists of a pulse signal $g(t)$ corrupted by additive channel noise $w(t)$, as shown by

$$x(t) = g(t) + w(t), \qquad 0 \le t \le T \tag{4.1}$$

where T is an arbitrary observation interval. The pulse signal $g(t)$ may represent a binary symbol 1 or 0 in a digital communication system. The $w(t)$ is the sample function of a white noise process of zero mean and power spectral density $N_0/2$. It is assumed that the receiver has knowledge of the waveform of the pulse signal $g(t)$. The source of uncertainty lies in the noise $w(t)$. The function of the receiver is to detect the pulse signal $g(t)$ in an optimum manner, given the received signal $x(t)$. To satisfy this requirement, we have to optimize the design of the filter so as to minimize the effects of noise at the filter output in some statistical sense, and thereby enhance the detection of the pulse signal $g(t)$.

Since the filter is linear, the resulting output $y(t)$ may be expressed as

$$y(t) = g_o(t) + n(t) \tag{4.2}$$

where $g_o(t)$ and $n(t)$ are produced by the signal and noise components of the input $x(t)$, respectively. A simple way of describing the requirement that the output signal component $g_o(t)$ be considerably greater than the output noise component $n(t)$ is to have the filter make the instantaneous power in the output signal $g_o(t)$, measured at time $t = T$, as large as possible compared with the average power of the output noise $n(t)$. This is equivalent to maximizing the *peak pulse signal-to-noise ratio*, defined as

$$\eta = \frac{|g_o(T)|^2}{E[n^2(t)]} \tag{4.3}$$

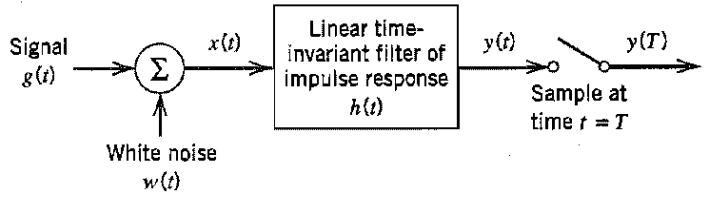

FIGURE 4.1 Linear receiver.

where $|g_o(T)|^2$ is the instantaneous power in the output signal, E is the statistical expectation operator, and $E[n^2(t)]$ is a measure of the average output noise power. The requirement is to specify the impulse response $h(t)$ of the filter such that the output signal-to-noise ratio in Equation (4.3) is maximized.

Let $G(f)$ denote the Fourier transform of the known signal $g(t)$, and $H(f)$ denote the frequency response of the filter. Then the Fourier transform of the output signal $g_o(t)$ is equal to $H(f)G(f)$, and $g_o(t)$ is itself given by the inverse Fourier transform

$$g_o(t) = \int_{-\infty}^{\infty} H(f)G(f) \exp(j2\pi ft)\, df \tag{4.4}$$

Hence, when the filter output is sampled at time $t = T$, we have (in the absence of channel noise)

$$|g_o(T)|^2 = \left| \int_{-\infty}^{\infty} H(f)G(f) \exp(j2\pi fT)\, df \right|^2 \tag{4.5}$$

Consider next the effect on the filter output due to the noise $w(t)$ acting alone. The power spectral density $S_N(f)$ of the output noise $n(t)$ is equal to the power spectral density of the input noise $w(t)$ times the squared magnitude response $|H(f)|^2$ (see Section 1.7). Since $w(t)$ is white with constant power spectral density $N_0/2$, it follows that

$$S_N(f) = \frac{N_0}{2} |H(f)|^2 \tag{4.6}$$

The average power of the output noise $n(t)$ is therefore

$$\begin{aligned} E[n^2(t)] &= \int_{-\infty}^{\infty} S_N(f)\, df \\ &= \frac{N_0}{2} \int_{-\infty}^{\infty} |H(f)|^2\, df \end{aligned} \tag{4.7}$$

Thus substituting Equations (4.5) and (4.7) into (4.3), we may rewrite the expression for the peak pulse signal-to-noise ratio as

$$\eta = \frac{\left| \int_{-\infty}^{\infty} H(f)G(f) \exp(j2\pi fT)\, df \right|^2}{\frac{N_0}{2} \int_{-\infty}^{\infty} |H(f)|^2\, df} \tag{4.8}$$

Our problem is to find, for a given $G(f)$, the particular form of the frequency response $H(f)$ of the filter that makes η a maximum. To find the solution to this optimization problem, we apply a mathematical result known as Schwarz's inequality to the numerator of Equation (4.8).

A derivation of *Schwarz's inequality* is given in Chapter 5. For now it suffices to say that if we have two complex functions $\phi_1(x)$ and $\phi_2(x)$ in the real variable x, satisfying the conditions

$$\int_{-\infty}^{\infty} |\phi_1(x)|^2\, dx < \infty$$

and

$$\int_{-\infty}^{\infty} |\phi_2(x)|^2\, dx < \infty$$

then we may write

$$\left|\int_{-\infty}^{\infty} \phi_1(x)\phi_2(x)\,dx\right|^2 \leq \int_{-\infty}^{\infty} |\phi_1(x)|^2\,dx \int_{-\infty}^{\infty} |\phi_2(x)|^2\,dx \tag{4.9}$$

The equality in (4.9) holds if, and only if, we have

$$\phi_1(x) = k\phi_2^*(x) \tag{4.10}$$

where k is an arbitrary constant, and the asterisk denotes complex conjugation.

Returning to the problem at hand, we readily see that by invoking Schwarz's inequality (4.9), and setting $\phi_1(x) = H(f)$ and $\phi_2(x) = G(f)\exp(j\pi fT)$, the numerator in Equation (4.8) may be rewritten as

$$\left|\int_{-\infty}^{\infty} H(f)G(f)\exp(j2\pi fT)\,df\right|^2 \leq \int_{-\infty}^{\infty} |H(f)|^2\,df \int_{-\infty}^{\infty} |G(f)|^2\,df \tag{4.11}$$

Using this relation in Equation (4.8), we may redefine the peak pulse signal-to-noise ratio as

$$\eta \leq \frac{2}{N_0}\int_{-\infty}^{\infty} |G(f)|^2\,df \tag{4.12}$$

The right-hand side of this relation does not depend on the frequency response $H(f)$ of the filter but only on the signal energy and the noise power spectral density. Consequently, the peak pulse signal-to-noise ratio η will be a maximum when $H(f)$ is chosen so that the equality holds; that is,

$$\eta_{\max} = \frac{2}{N_0}\int_{-\infty}^{\infty} |G(f)|^2\,df \tag{4.13}$$

Correspondingly, $H(f)$ assumes its optimum value denoted by $H_{\text{opt}}(f)$. To find this optimum value we use Equation (4.10), which, for the situation at hand, yields

$$H_{\text{opt}}(f) = kG^*(f)\exp(-j2\pi fT) \tag{4.14}$$

where $G^*(f)$ is the complex conjugate of the Fourier transform of the input signal $g(t)$, and k is a scaling factor of appropriate dimensions. This relation states that, except for the factor $k\exp(-j2\pi fT)$, the frequency response of the optimum filter is the same as the complex conjugate of the Fourier transform of the input signal.

Equation (4.14) specifies the optimum filter in the frequency domain. To characterize it in the time domain, we take the inverse Fourier transform of $H_{\text{opt}}(f)$ in Equation (4.14) to obtain the impulse response of the optimum filter as

$$h_{\text{opt}}(t) = k\int_{-\infty}^{\infty} G^*(f)\exp[-j2\pi f(T-t)]\,df \tag{4.15}$$

Since for a real signal $g(t)$ we have $G^*(f) = G(-f)$, we may rewrite Equation (4.15) as

$$\begin{aligned} h_{\text{opt}}(t) &= k\int_{-\infty}^{\infty} G(-f)\exp[-j2\pi f(T-t)]\,df \\ &= k\int_{-\infty}^{\infty} G(f)\exp[j2\pi f(T-t)]\,df \\ &= kg(T-t) \end{aligned} \tag{4.16}$$

Equation (4.16) shows that the impulse response of the optimum filter, except for the scaling factor k, is a time-reversed and delayed version of the input signal $g(t)$; that is, it

is "matched" to the input signal. A linear time-invariant filter defined in this way is called a matched filter. Note that in deriving the matched filter the only assumption we have made about the input noise $w(t)$ is that it is stationary and white with zero mean and power spectral density $N_0/2$. In other words, no assumption was made on the statistics of the channel noise $w(t)$.

Properties of Matched Filters

We note that a filter, which is matched to a pulse signal $g(t)$ of duration T, is characterized by an impulse response that is a time-reversed and delayed version of the input $g(t)$, as shown by

$$h_{\text{opt}}(t) = kg(T - t)$$

In other words, the impulse response $h_{\text{opt}}(t)$ is uniquely defined, except for the delay T and the scaling factor k, by the waveform of the pulse signal $g(t)$ to which the filter is matched. In the frequency domain, the matched filter is characterized by a frequency response that is, except for a delay factor, the complex conjugate of the Fourier transform of the input $g(t)$, as shown by

$$H_{\text{opt}}(f) = kG^*(f) \exp(-j2\pi fT)$$

The most important result in the calculation of the performance of signal processing systems using matched filters is perhaps the following:

The peak pulse signal-to-noise ratio of a matched filter depends only on the ratio of the signal energy to the power spectral density of the white noise at the filter input.

To demonstrate this property, consider a filter matched to a known signal $g(t)$. The Fourier transform of the resulting matched filter output $g_o(t)$ is

$$\begin{aligned} G_o(f) &= H_{\text{opt}}(f)G(f) \\ &= kG^*(f)G(f) \exp(-j2\pi fT) \\ &= k|G(f)|^2 \exp(-j2\pi fT) \end{aligned} \tag{4.17}$$

Using Equation (4.17) in the formula for the inverse Fourier transform, we find that the matched filter output at time $t = T$ is

$$\begin{aligned} g_o(T) &= \int_{-\infty}^{\infty} G_o(f) \exp(j2\pi fT)\, df \\ &= k \int_{-\infty}^{\infty} |G(f)|^2\, df \end{aligned}$$

According to *Rayleigh's energy theorem, the integral of the squared magnitude spectrum of a pulse signal with respect to frequency is equal to the signal energy* E:

$$E = \int_{-\infty}^{\infty} g^2(t)dt = \int_{-\infty}^{\infty} |G(f)|^2\, df$$

Hence

$$g_o(T) = kE \tag{4.18}$$

Substituting Equation (4.14) into (4.7), we find that the average output noise power is

$$\begin{aligned} E[n^2(t)] &= \frac{k^2N_0}{2} \int_{-\infty}^{\infty} |G(f)|^2\, df \\ &= k^2N_0E/2 \end{aligned} \tag{4.19}$$

where again we have made use of Rayleigh's energy theorem. Therefore, the peak pulse signal-to-noise ratio has the maximum value

$$\eta_{\max} = \frac{(kE)^2}{(k^2 N_0 E/2)} = \frac{2E}{N_0} \tag{4.20}$$

From Equation (4.20) we see that dependence on the waveform of the input $g(t)$ has been completely removed by the matched filter. Accordingly, in evaluating the ability of a matched-filter receiver to combat additive white noise, we find that all signals that have the same energy are equally effective. Note that the signal energy E is in joules and the noise spectral density $N_0/2$ is in watts per Hertz, so that the ratio $2E/N_0$ is dimensionless; however, the two quantities have different physical meaning. We refer to E/N_0 as the *signal energy-to-noise spectral density ratio*.

▶ EXAMPLE 4.1 Matched Filter for Rectangular Pulse

Consider a signal $g(t)$ in the form of a rectangular pulse of amplitude A and duration T, as shown in Figure 4.2*a*. In this example, the impulse response $h(t)$ of the matched filter has exactly the same waveform as the signal itself. The output signal $g_o(t)$ of the matched filter produced in response to the input signal $g(t)$ has a triangular waveform, as shown in Figure 4.2*b*.

The maximum value of the output signal $g_o(t)$ is equal to kA^2T, which is the energy of the input signal $g(t)$ scaled by the factor k; this maximum value occurs at $t = T$, as indicated in Figure 4.2*b*.

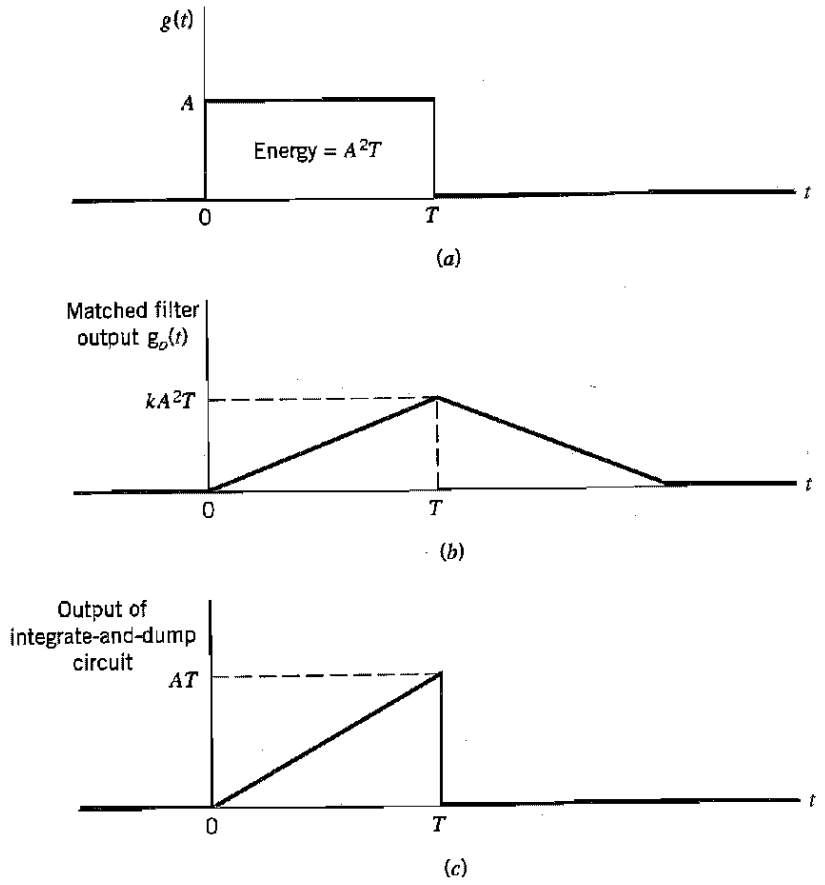

FIGURE 4.2 (*a*) Rectangular pulse. (*b*) Matched filter output. (*c*) Integrator output.

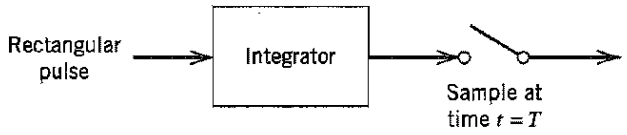

FIGURE 4.3 Integrate-and-dump circuit.

For the special case of a rectangular pulse, the matched filter may be implemented using a circuit known as the *integrate-and-dump circuit*, a block diagram of which is shown in Figure 4.3. The integrator computes the area under the rectangular pulse, and the resulting output is then sampled at time $t = T$, where T is the duration of the pulse. Immediately after $t = T$, the integrator is restored to its initial condition; hence the name of the circuit. Figure 4.2*c* shows the output waveform of the integrate-and-dump circuit for the rectangular pulse of Figure 4.2*a*. We see that for $0 \leq t \leq T$, the output of this circuit has the *same waveform* as that appearing at the output of the matched filter; the difference in the notations used to describe their peak values is of no practical significance. ◀

4.3 Error Rate Due to Noise

In Section 3.8 we presented a qualitative discussion of the effect of channel noise on the performance of a binary PCM system. Now that we are equipped with the matched filter as the optimum detector of a known pulse in additive white noise, we are ready to derive a formula for the error rate in such a system due to noise.

To proceed with the analysis, consider a binary PCM system based on *polar nonreturn-to-zero (NRZ) signaling*. In this form of signaling, symbols 1 and 0 are represented by positive and negative rectangular pulses of equal amplitude and equal duration. The channel noise is modeled as *additive white Gaussian noise* $w(t)$ of zero mean and power spectral density $N_0/2$; the Gaussian assumption is needed for later calculations. In the signaling interval $0 \leq t \leq T_b$, the received signal is thus written as follows:

$$x(t) = \begin{cases} +A + w(t), & \text{symbol 1 was sent} \\ -A + w(t), & \text{symbol 0 was sent} \end{cases} \tag{4.21}$$

where T_b is the *bit duration*, and A is the *transmitted pulse amplitude*. It is assumed that the receiver has acquired knowledge of the starting and ending times of each transmitted pulse; in other words, the receiver has prior knowledge of the pulse shape, but not its polarity. Given the noisy signal $x(t)$, the receiver is required to make a decision in each signaling interval as to whether the transmitted symbol is a 1 or a 0.

The structure of the receiver used to perform this decision-making process is shown in Figure 4.4. It consists of a matched filter followed by a sampler, and then finally a

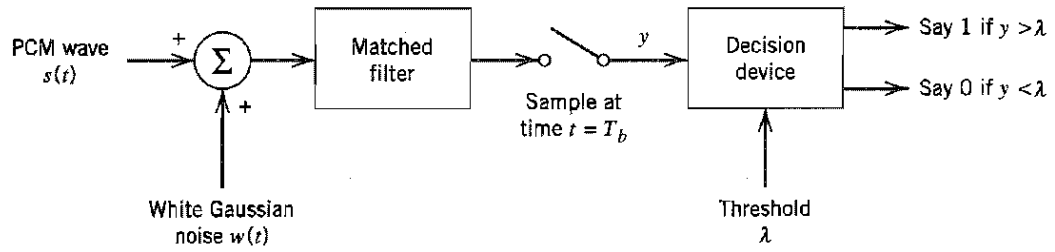

FIGURE 4.4 Receiver for baseband transmission of binary-encoded PCM wave using polar NRZ signaling.

decision device. The filter is matched to a rectangular pulse of amplitude A and duration T_b, exploiting the bit-timing information available to the receiver. The resulting matched filter output is sampled at the end of each signaling interval. The presence of channel noise $w(t)$ adds randomness to the matched filter output.

Let y denote the sample value obtained at the end of a signaling interval. The sample value y is compared to a preset *threshold* λ in the decision device. If the threshold is exceeded, the receiver makes a decision in favor of symbol 1; if not, a decision is made in favor of symbol 0. We adopt the convention that when the sample value y is exactly equal to the threshold λ, the receiver just makes a guess as to which symbol was transmitted; such a decision is the same as that obtained by flipping a fair coin, the outcome of which will not alter the average probability of error.

There are two possible kinds of error to be considered:

1. Symbol 1 is chosen when a 0 was actually transmitted; we refer to this error as an *error of the first kind.*
2. Symbol 0 is chosen when a 1 was actually transmitted; we refer to this error as an *error of the second kind.*

To determine the average probability of error, we consider these two situations separately.

Suppose that symbol 0 was sent. Then, according to Equation (4.21), the received signal is

$$x(t) = -A + w(t), \qquad 0 \le t \le T_b \tag{4.22}$$

Correspondingly, the matched filter output, sampled at time $t = T_b$, is given by (in light of Example 4.1 with kAT_b set equal to unity for convenience of presentation)

$$\begin{aligned} y &= \int_0^{T_b} x(t)\, dt \\ &= -A + \frac{1}{T_b}\int_0^{T_b} w(t)\, dt \end{aligned} \tag{4.23}$$

which represents the sample value of a random variable Y. By virtue of the fact that the noise $w(t)$ is white and Gaussian, we may characterize the random variable Y as follows:

- The random variable Y is Gaussian distributed with a mean of $-A$.
- The variance of the random variable Y is

$$\begin{aligned} \sigma_Y^2 &= E[(Y + A)^2] \\ &= \frac{1}{T_b^2} E\left[\int_0^{T_b}\int_0^{T_b} w(t)w(u)\, dt\, du\right] \\ &= \frac{1}{T_b^2}\int_0^{T_b}\int_0^{T_b} E[w(t)w(u)]\, dt\, du \\ &= \frac{1}{T_b^2}\int_0^{T_b}\int_0^{T_b} R_W(t, u)\, dt\, du \end{aligned} \tag{4.24}$$

where $R_W(t, u)$ is the autocorrelation function of the white noise $w(t)$. Since $w(t)$ is white with a power spectral density $N_0/2$, we have

$$R_W(t, u) = \frac{N_0}{2}\delta(t - u) \tag{4.25}$$

a 3-dB increase in E_b/N_0 is much easier to implement when E_b has a small value than when its value is orders of magnitude larger.

4.4 Intersymbol Interference

The next source of bit errors in a baseband-pulse transmission system that we wish to study is intersymbol interference (ISI), which arises when the communication channel is *dispersive*. First of all, however, we need to address a key question: Given a pulse shape of interest, how do we use it to transmit data in M-ary form? The answer lies in the use of *discrete pulse modulation*, in which the amplitude, duration, or position of the transmitted pulses is varied in a discrete manner in accordance with the given data stream. However, for the baseband transmission of digital data, the use of *discrete pulse-amplitude modulation* (PAM) is one of the most efficient schemes in terms of power and bandwidth utilization. Accordingly, we confine our attention to discrete PAM systems. We begin the study by first considering the case of binary data; later in the chapter, we consider the more general case of M-ary data.

Consider then a *baseband binary PAM system*, a generic form of which is shown in Figure 4.7. The incoming binary sequence $\{b_k\}$ consists of symbols 1 and 0, each of duration T_b. The *pulse-amplitude modulator* modifies this binary sequence into a new sequence of short pulses (approximating a unit impulse), whose amplitude a_k is represented in the polar form

$$a_k = \begin{cases} +1 & \text{if symbol } b_k \text{ is 1} \\ -1 & \text{if symbol } b_k \text{ is 0} \end{cases} \tag{4.42}$$

The sequence of short pulses so produced is applied to a *transmit filter* of impulse response $g(t)$, producing the transmitted signal

$$s(t) = \sum_k a_k g(t - kT_b) \tag{4.43}$$

The signal $s(t)$ is modified as a result of transmission through the *channel* of impulse response $h(t)$. In addition, the channel adds random noise to the signal at the receiver input. The noisy signal $x(t)$ is then passed through a *receive filter* of impulse response $c(t)$. The resulting filter output $y(t)$ is sampled *synchronously* with the transmitter, with the sampling instants being determined by a *clock* or *timing signal* that is usually extracted from the receive filter output. Finally, the sequence of samples thus obtained is used to reconstruct the original data sequence by means of a *decision device*. Specifically, the amplitude of each sample is compared to a *threshold* λ. If the threshold λ is exceeded, a decision is made in favor of symbol 1. If the threshold λ is not exceeded, a decision is made in favor of symbol 0. If the sample amplitude equals the threshold exactly, the flip of a

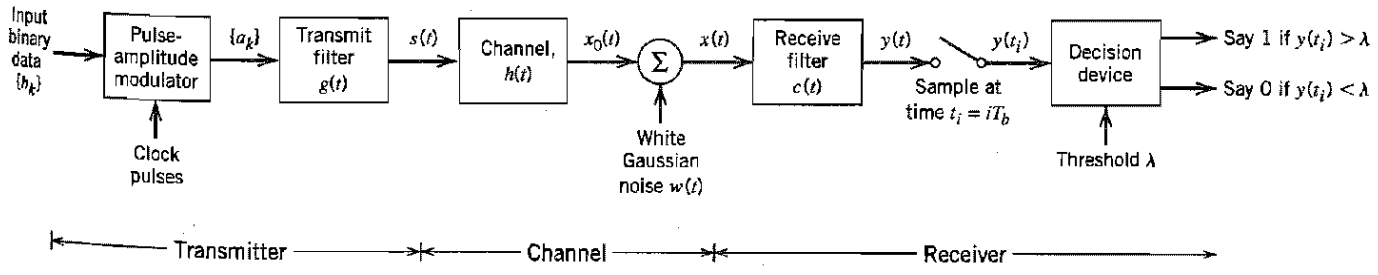

FIGURE 4.7 Baseband binary data transmission system.

fair coin will determine which symbol was transmitted (i.e., the receiver simply makes a random guess).

The receive filter output is written as

$$y(t) = \mu \sum_k a_k p(t - kT_b) + n(t) \tag{4.44}$$

where μ is a scaling factor, and the pulse $p(t)$ is to be defined. To be precise, an arbitrary time delay t_0 should be included in the argument of the pulse $p(t - kT_b)$ in Equation (4.44) to represent the effect of transmission delay through the system. To simplify the exposition, we have put this delay equal to zero in Equation (4.44) without loss of generality.

The scaled pulse $\mu p(t)$ is obtained by a double convolution involving the impulse response $g(t)$ of the transmit filter, the impulse response $h(t)$ of the channel, and the impulse response $c(t)$ of the receive filter, as shown by

$$\mu p(t) = g(t) \bigstar h(t) \bigstar c(t) \tag{4.45}$$

where the star denotes convolution. We assume that the pulse $p(t)$ is *normalized* by setting

$$p(0) = 1 \tag{4.46}$$

which justifies the use of μ as a scaling factor to account for amplitude changes incurred in the course of signal transmission through the system.

Since convolution in the time domain is transformed into multiplication in the frequency domain, we may use the Fourier transform to change Equation (4.45) into the equivalent form

$$\mu P(f) = G(f)H(f)C(f) \tag{4.47}$$

where $P(f)$, $G(f)$, $H(f)$, and $C(f)$ are the Fourier transforms of $p(t)$, $g(t)$, $h(t)$, and $c(t)$, respectively.

Finally, the term $n(t)$ in Equation (4.44) is the noise produced at the output of the receive filter due to the channel noise $w(t)$. It is customary to model $w(t)$ as a white Gaussian noise of zero mean.

The receive filter output $y(t)$ is sampled at time $t_i = iT_b$ (with i taking on integer values), yielding [in light of Equation (4.46)]

$$\begin{aligned} y(t_i) &= \mu \sum_{k=-\infty}^{\infty} a_k p[(i - k)T_b] + n(t_i) \\ &= \mu a_i + \mu \sum_{\substack{k=-\infty \\ k \neq i}}^{\infty} a_k p[(i - k)T_b] + n(t_i) \end{aligned} \tag{4.48}$$

In Equation (4.48), the first term μa_i represents the contribution of the ith transmitted bit. The second term represents the residual effect of all other transmitted bits on the decoding of the ith bit; this residual effect due to the occurrence of pulses before and after the sampling instant t_i is called intersymbol interference (ISI). The last term $n(t_i)$ represents the noise sample at time t_i.

In the absence of both ISI and noise, we observe from Equation (4.48) that

$$y(t_i) = \mu a_i$$

which shows that, under these ideal conditions, the ith transmitted bit is decoded correctly. The unavoidable presence of ISI and noise in the system, however, introduces errors in the decision device at the receiver output. Therefore, in the design of the transmit and receive filters, the objective is to minimize the effects of noise and ISI and thereby deliver the digital data to their destination with the smallest error rate possible.

When the signal-to-noise ratio is high, as is the case in a telephone system, for example, the operation of the system is largely limited by ISI rather than noise; in other words, we may ignore $n(t_i)$. In the next couple of sections, we assume that this condition holds so that we may focus our attention on ISI and the techniques for its control. In particular, the issue we wish to consider is to determine the pulse waveform $p(t)$ for which the ISI is completely eliminated.

4.5 Nyquist's Criterion for Distortionless Baseband Binary Transmission

Typically, the frequency response of the channel and the transmitted pulse shape are specified, and the problem is to determine the frequency responses of the transmit and receive filters so as to reconstruct the original binary data sequence $\{b_k\}$. The receiver does this by *extracting* and then *decoding* the corresponding sequence of coefficients, $\{a_k\}$, from the output $y(t)$. The *extraction* involves sampling the output $y(t)$ at time $t = iT_b$. The *decoding* requires that the weighted pulse contribution $a_k p(iT_b - kT_b)$ for $k = i$ be *free* from ISI due to the overlapping tails of all other weighted pulse contributions represented by $k \neq i$. This, in turn, requires that we *control* the overall pulse $p(t)$, as shown by

$$p(iT_b - kT_b) = \begin{cases} 1, & i = k \\ 0, & i \neq k \end{cases} \tag{4.49}$$

where $p(0) = 1$, by normalization. If $p(t)$ satisfies the conditions of Equation (4.49), the receiver output $y(t_i)$ given in Equation (4.48) simplifies to (ignoring the noise term)

$$y(t_i) = \mu a_i \qquad \text{for all } i$$

which implies zero intersymbol interference. Hence, the two conditions of Equation (4.49) ensure *perfect reception in the absence of noise.*

From a design point of view, it is informative to transform the conditions of Equation (4.49) into the frequency domain. Consider then the sequence of samples $\{p(nT_b)\}$, where $n = 0, \pm 1, \pm 2, \cdots$. From the discussion presented in Chapter 3 on the sampling process, we recall that sampling in the time domain produces periodicity in the frequency domain. In particular, we may write

$$P_\delta(f) = R_b \sum_{n=-\infty}^{\infty} P(f - nR_b) \tag{4.50}$$

where $R_b = 1/T_b$ is the *bit rate* in bits per second (b/s); $P_\delta(f)$ is the Fourier transform of an infinite periodic sequence of delta functions of period T_b, whose individual areas are weighted by the respective sample values of $p(t)$. That is, $P_\delta(f)$ is given by

$$P_\delta(f) = \int_{-\infty}^{\infty} \sum_{m=-\infty}^{\infty} [p(mT_b)\, \delta(t - mT_b)] \exp(-j2\pi ft)\, dt \tag{4.51}$$

Let the integer $m = i - k$. Then, $i = k$ corresponds to $m = 0$, and likewise $i \neq k$ corresponds to $m \neq 0$. Accordingly, imposing the conditions of Equation (4.49) on the sample values of $p(t)$ in the integral of Equation (4.51), we get

$$\begin{aligned} P_\delta(f) &= \int_{-\infty}^{\infty} p(0)\, \delta(t) \exp(-j2\pi ft)\, dt \\ &= p(0) \end{aligned} \tag{4.52}$$

where we have made use of the sifting property of the delta function. Since from Equation (4.46) we have $p(0) = 1$, it follows from Equations (4.50) and (4.52) that the condition for zero intersymbol interference is satisfied if

$$\sum_{n=-\infty}^{\infty} P(f - nR_b) = T_b \tag{4.53}$$

We may now state the *Nyquist criterion*[4] *for distortionless baseband transmission* in the absence of noise: *The frequency function $P(f)$ eliminates intersymbol interference for samples taken at intervals T_b provided that it satisfies Equation (4.53).* Note that $P(f)$ refers to the overall system, incorporating the transmit filter, the channel, and the receive filter in accordance with Equation (4.47).

■ IDEAL NYQUIST CHANNEL

The simplest way of satisfying Equation (4.53) is to specify the frequency function $P(f)$ to be in the form of a *rectangular function*, as shown by

$$\begin{aligned} P(f) &= \begin{cases} \dfrac{1}{2W}, & -W < f < W \\ 0, & |f| > W \end{cases} \\ &= \frac{1}{2W}\,\mathrm{rect}\left(\frac{f}{2W}\right) \end{aligned} \tag{4.54}$$

where $\mathrm{rect}(f)$ stands for a *rectangular function* of unit amplitude and unit support centered on $f = 0$, and the overall system bandwidth W is defined by

$$W = \frac{R_b}{2} = \frac{1}{2T_b} \tag{4.55}$$

According to the solution described by Equations (4.54) and (4.55), no frequencies of absolute value exceeding half the bit rate are needed. Hence, from Fourier-transform pair 2 of Table A6.3 we find that a signal waveform that produces zero intersymbol interference is defined by the *sinc function*:

$$\begin{aligned} p(t) &= \frac{\sin(2\pi Wt)}{2\pi Wt} \\ &= \mathrm{sinc}(2Wt) \end{aligned} \tag{4.56}$$

The special value of the bit rate $R_b = 2W$ is called the *Nyquist rate*, and W is itself called the *Nyquist bandwidth*. Correspondingly, the ideal baseband pulse transmission system described by Equation (4.54) in the frequency domain or, equivalently, Equation (4.56) in the time domain, is called the *ideal Nyquist channel*.

Figures 4.8*a* and 4.8*b* show plots of $P(f)$ and $p(t)$, respectively. In Figure 4.8*a*, the normalized form of the frequency function $P(f)$ is plotted for positive and negative frequencies. In Figure 4.8*b*, we have also included the signaling intervals and the corresponding centered sampling instants. The function $p(t)$ can be regarded as the impulse response of an ideal low-pass filter with passband magnitude response $1/2W$ and bandwidth W. The function $p(t)$ has its peak value at the origin and goes through zero at integer multiples of the bit duration T_b. It is apparent that if the received waveform $y(t)$ is sampled at the

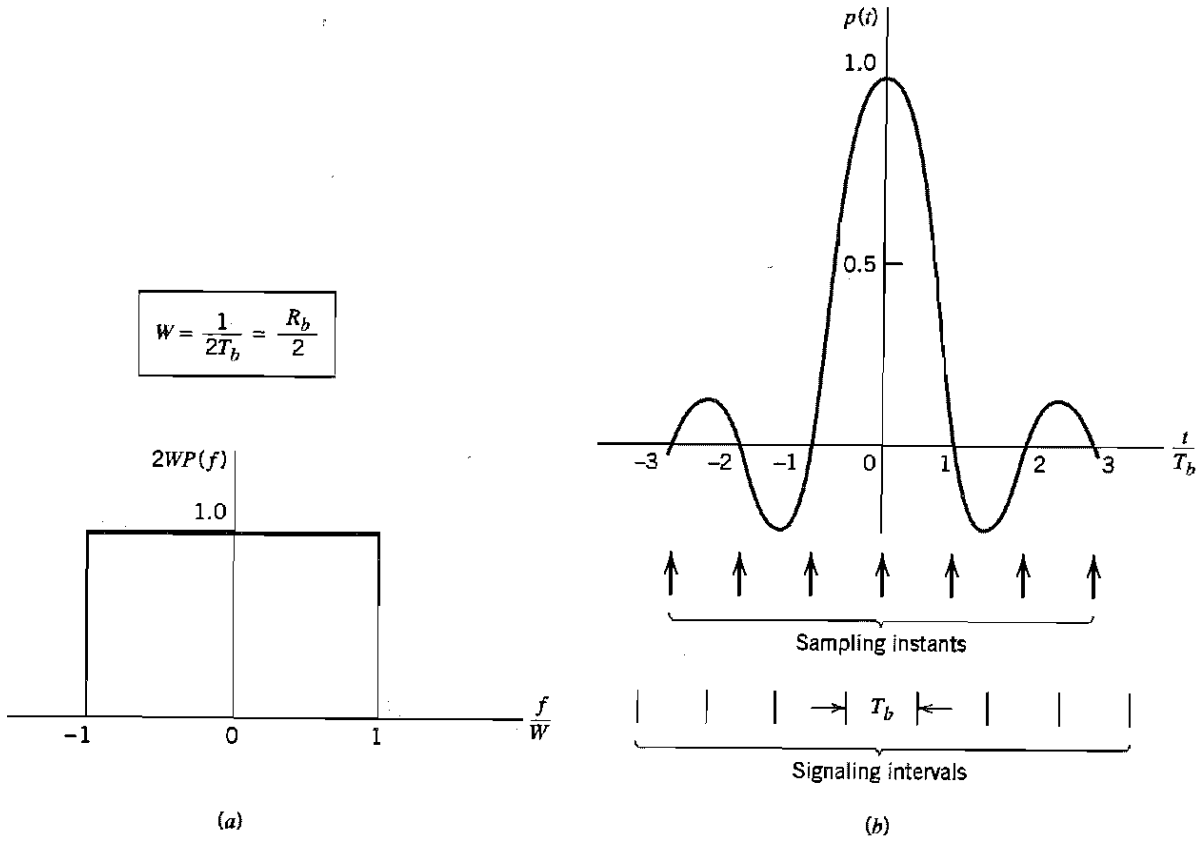

FIGURE 4.8 (*a*) Ideal magnitude response. (*b*) Ideal basic pulse shape.

instants of time $t = 0, \pm T_b, \pm 2T_b, \cdots$, then the pulses defined by $\mu p(t - iT_b)$ with arbitrary amplitude μ and index $i = 0, \pm 1, \pm 2, \cdots$, will not interfere with each other. This condition is illustrated in Figure 4.9 for the binary sequence 1011010.

Although the use of the ideal Nyquist channel does indeed achieve economy in bandwidth in that it solves the problem of zero intersymbol interference with the minimum

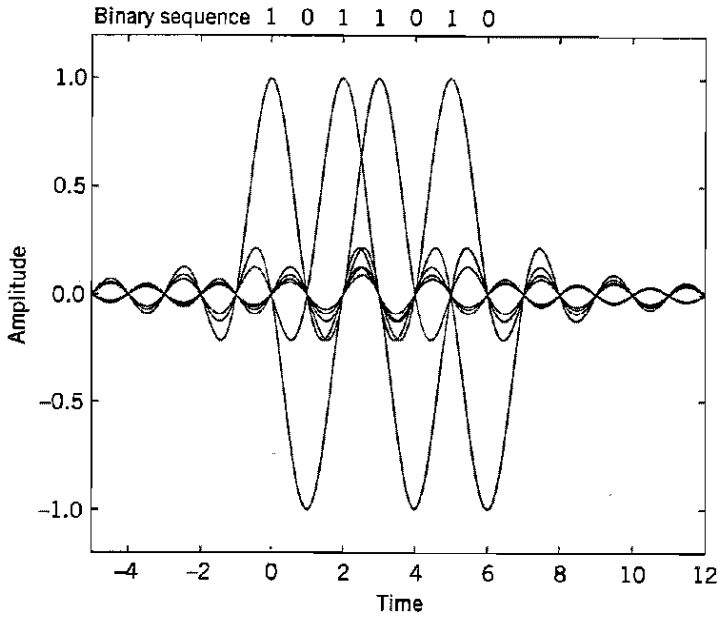

FIGURE 4.9 A series of sinc pulses corresponding to the sequence 1011010.

bandwidth possible, there are two practical difficulties that make it an undesirable objective for system design:

1. It requires that the magnitude characteristic of $P(f)$ be flat from $-W$ to W, and zero elsewhere. This is physically unrealizable because of the abrupt transitions at the band edges $\pm W$.
2. The function $p(t)$ decreases as $1/|t|$ for large $|t|$, resulting in a slow rate of decay. This is also caused by the discontinuity of $P(f)$ at $\pm W$. Accordingly, there is practically no margin of error in sampling times in the receiver.

To evaluate the effect of this *timing error*, consider the sample of $y(t)$ at $t = \Delta t$, where Δt is the timing error. To simplify the exposition, we may put the correct sampling time t_i equal to zero. In the absence of noise, we thus have (from Equation (4.48))

$$\begin{aligned} y(\Delta t) &= \mu \sum_k a_k p(\Delta t - kT_b) \\ &= \mu \sum_k a_k \frac{\sin[2\pi W(\Delta t - kT_b)]}{2\pi W(\Delta t - kT_b)} \end{aligned} \tag{4.57}$$

Since $2WT_b = 1$, by definition, we may rewrite Equation (4.57) as

$$y(\Delta t) = \mu a_0 \operatorname{sinc}(2W\,\Delta t) + \frac{\mu \sin(2\pi W\,\Delta t)}{\pi} \sum_{\substack{k \\ k \neq 0}} \frac{(-1)^k a_k}{(2W\,\Delta t - k)} \tag{4.58}$$

The first term on the right-hand side of Equation (4.58) defines the desired symbol, whereas the remaining series represents the intersymbol interference caused by the timing error Δt in sampling the output $y(t)$. Unfortunately, it is possible for this series to diverge, thereby causing erroneous decisions in the receiver.

■ RAISED COSINE SPECTRUM

We may overcome the practical difficulties encountered with the ideal Nyquist channel by extending the bandwidth from the minimum value $W = R_b/2$ to an adjustable value between W and $2W$. We now specify the overall frequency response $P(f)$ to satisfy a condition more elaborate than that for the ideal Nyquist channel; specifically, we retain three terms of Equation (4.53) and restrict the frequency band of interest to $[-W, W]$, as shown by

$$P(f) + P(f - 2W) + P(f + 2W) = \frac{1}{2W}, \qquad -W \leq f \leq W \tag{4.59}$$

We may devise several band-limited functions that satisfy Equation (4.59). A particular form of $P(f)$ that embodies many desirable features is provided by a *raised cosine spectrum*. This frequency response consists of a *flat* portion and a *rolloff* portion that has a sinusoidal form, as follows:

$$P(f) = \begin{cases} \dfrac{1}{2W}, & 0 \leq |f| < f_1 \\ \dfrac{1}{4W}\left\{1 - \sin\left[\dfrac{\pi(|f| - W)}{2W - 2f_1}\right]\right\}, & f_1 \leq |f| < 2W - f_1 \\ 0, & |f| \geq 2W - f_1 \end{cases} \tag{4.60}$$

The frequency parameter f_1 and bandwidth W are related by

$$\alpha = 1 - \frac{f_1}{W} \tag{4.61}$$

The parameter α is called the *rolloff factor*; it indicates the *excess bandwidth* over the ideal solution, W. Specifically, the transmission bandwidth B_T is defined by

$$\begin{aligned} B_T &= 2W - f_1 \\ &= W(1 + \alpha) \end{aligned}$$

The frequency response $P(f)$, normalized by multiplying it by $2W$, is plotted in Figure 4.10*a* for three values of α, namely, 0, 0.5, and 1. We see that for $\alpha = 0.5$ or 1, the

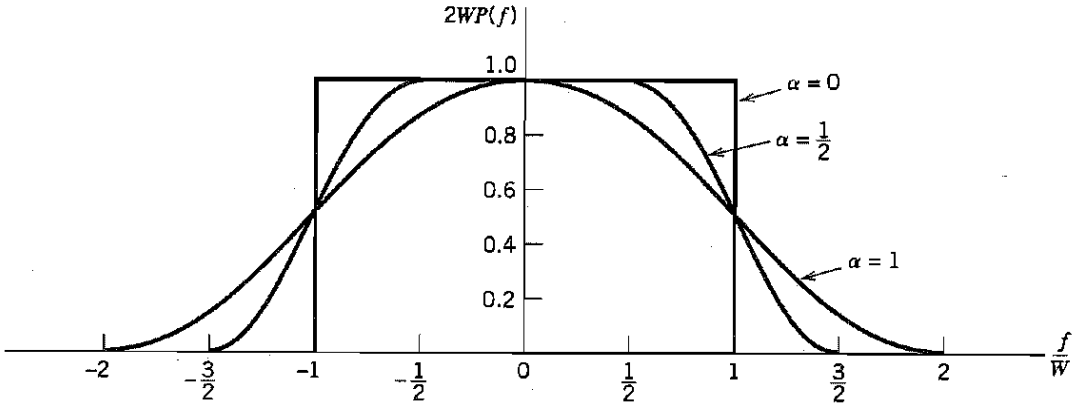

(*a*)

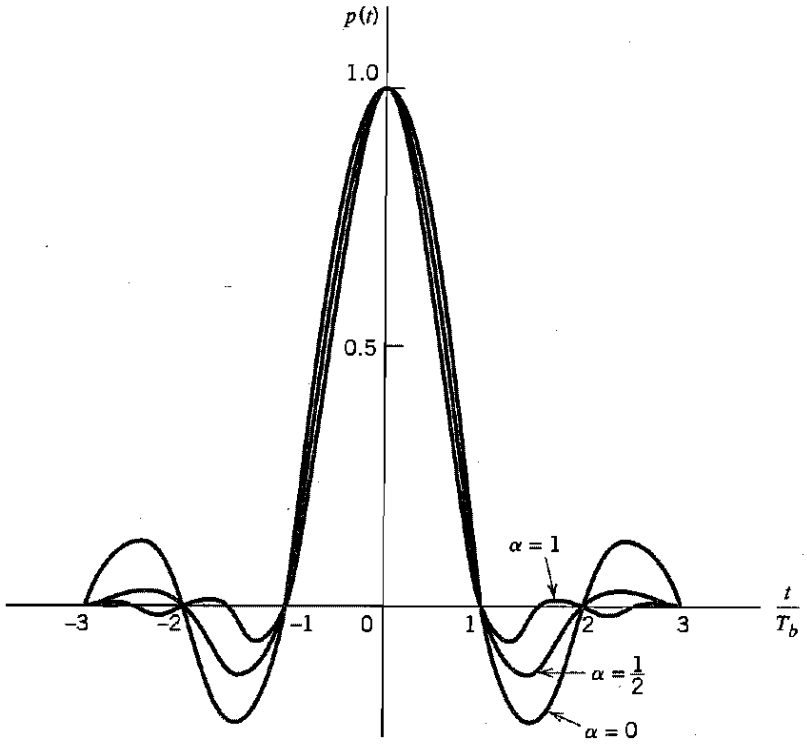

(*b*)

FIGURE 4.10 Responses for different rolloff factors. (*a*) Frequency response. (*b*) Time response.

function $P(f)$ cuts off gradually as compared with the ideal Nyquist channel (i.e., $\alpha = 0$) and is therefore easier to implement in practice. Also the function $P(f)$ exhibits odd symmetry with respect to the Nyquist bandwidth W, making it possible to satisfy the condition of Equation (4.59).

The time response $p(t)$ is the inverse Fourier transform of the frequency response $P(f)$. Hence, using the $P(f)$ defined in Equation (4.60), we obtain the result (see Problem 4.13)

$$p(t) = (\text{sinc}(2Wt))\left(\frac{\cos(2\pi\alpha Wt)}{1 - 16\alpha^2 W^2 t^2}\right) \tag{4.62}$$

which is plotted in Figure 4.10*b* for $\alpha = 0$, 0.5, and 1.

The time response $p(t)$ consists of the product of two factors: the factor $\text{sinc}(2Wt)$ characterizing the ideal Nyquist channel and a second factor that decreases as $1/|t|^2$ for large $|t|$. The first factor ensures zero crossings of $p(t)$ at the desired sampling instants of time $t = iT$ with i an integer (positive and negative). The second factor reduces the tails of the pulse considerably below that obtained from the ideal Nyquist channel, so that the transmission of binary waves using such pulses is relatively insensitive to sampling time errors. In fact, for $\alpha = 1$ we have the most gradual rolloff in that the amplitudes of the oscillatory tails of $p(t)$ are smallest. Thus the amount of intersymbol interference resulting from timing error decreases as the rolloff factor α is increased from zero to unity.

The special case with $\alpha = 1$ (i.e., $f_1 = 0$) is known as the *full-cosine rolloff* characteristic, for which the frequency response of Equation (4.60) simplifies to

$$P(f) = \begin{cases} \dfrac{1}{4W}\left[1 + \cos\left(\dfrac{\pi f}{2W}\right)\right], & 0 < |f| < 2W \\ 0, & |f| \geq 2W \end{cases} \tag{4.63}$$

Correspondingly, the time response $p(t)$ simplifies to

$$p(t) = \frac{\text{sinc}(4Wt)}{1 - 16W^2 t^2} \tag{4.64}$$

This time response exhibits two interesting properties:

1. At $t = \pm T_b/2 = \pm 1/4W$, we have $p(t) = 0.5$; that is, the pulse width measured at half amplitude is exactly equal to the bit duration T_b.
2. There are zero crossings at $t = \pm 3T_b/2, \pm 5T_b/2, \cdots$ in addition to the usual zero crossings at the sampling times $t = \pm T_b, \pm 2T_b, \cdots$.

These two properties are extremely useful in extracting a timing signal from the received signal for the purpose of synchronization. However, the price paid for this desirable property is the use of a channel bandwidth double that required for the ideal Nyquist channel corresponding to $\alpha = 0$.

▶ EXAMPLE 4.2 Bandwidth Requirement of the T1 System

In Example 3.2 of Chapter 3, we described the signal format for the T1 carrier system that is used to multiplex 24 independent voice inputs, based on an 8-bit PCM word. It was shown

that the bit duration of the resulting time-division multiplexed signal (including a framing bit) is

$$T_b = 0.647\ \mu s$$

Assuming the use of an ideal Nyquist channel, it follows that the minimum transmission bandwidth B_T of the T1 system is (for $\alpha = 0$)

$$B_T = W = \frac{1}{2T_b} = 772\ \text{kHz}$$

However, a more realistic value for the necessary transmission bandwidth is obtained by using a full-cosine rolloff characteristic with $\alpha = 1$. In this case, we find that

$$B_T = W(1 + \alpha) = 2W = \frac{1}{T_b} = 1.544\ \text{MHz}$$

◀

4.6 Correlative-Level Coding

Thus far we have treated intersymbol interference as an undesirable phenomenon that produces a degradation in system performance. Indeed, its very name connotes a nuisance effect. Nevertheless, by adding intersymbol interference to the transmitted signal in a controlled manner, it is possible to achieve a signaling rate equal to the Nyquist rate of $2W$ symbols per second in a channel of bandwidth W Hertz. Such schemes are called *correlative-level coding* or *partial-response signaling* schemes.[5] The design of these schemes is based on the following premise: Since intersymbol interference introduced into the transmitted signal is known, its effect can be interpreted at the receiver in a deterministic way. Thus correlative-level coding may be regarded as a practical method of achieving the theoretical maximum signaling rate of $2W$ symbols per second in a bandwidth of W Hertz, as postulated by Nyquist, using realizable and perturbation-tolerant filters.

Duobinary Signaling

The basic idea of correlative-level coding will now be illustrated by considering the specific example of *duobinary signaling*, where "duo" implies doubling of the transmission capacity of a straight binary system. This particular form of correlative-level coding is also called *class I partial response*.

Consider a binary input sequence $\{b_k\}$ consisting of uncorrelated binary symbols 1 and 0, each having duration T_b. As before, this sequence is applied to a pulse-amplitude modulator producing a two-level sequence of short pulses (approximating a unit impulse), whose amplitude a_k is defined by

$$a_k = \begin{cases} +1 & \text{if symbol } b_k \text{ is 1} \\ -1 & \text{if symbol } b_k \text{ is 0} \end{cases} \tag{4.65}$$

When this sequence is applied to a *duobinary encoder*, it is converted into a *three-level output*, namely, −2, 0, and +2. To produce this transformation, we may use the scheme shown in Figure 4.11. The two-level sequence $\{a_k\}$ is first passed through a simple filter involving a single delay element and summer. For every unit impulse applied to the

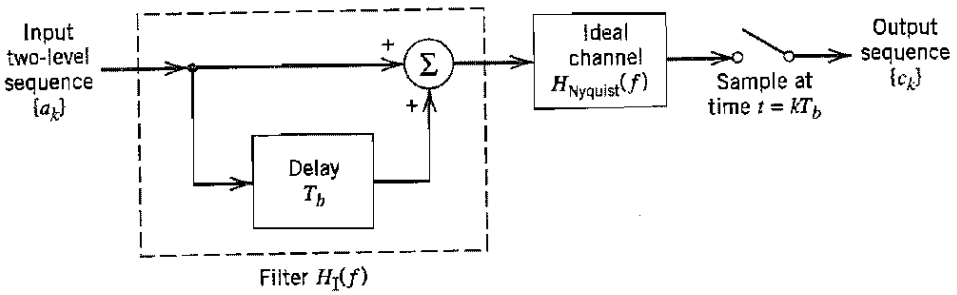

FIGURE 4.11 Duobinary signaling scheme.

input of this filter, we get two unit impulses spaced T_b seconds apart at the filter output. We may therefore express the duobinary coder output c_k as the sum of the present input pulse a_k and its previous value a_{k-1}, as shown by

$$c_k = a_k + a_{k-1} \tag{4.66}$$

One of the effects of the transformation described by Equation (4.66) is to change the input sequence $\{a_k\}$ of uncorrelated two-level pulses into a sequence $\{c_k\}$ of correlated three-level pulses. This correlation between the adjacent pulses may be viewed as introducing intersymbol interference into the transmitted signal in an artificial manner. However, the intersymbol interference so introduced is under the designer's control, which is the basis of correlative coding.

An ideal delay element, producing a delay of T_b seconds, has the frequency response $\exp(-j2\pi fT_b)$, so that the frequency response of the simple delay-line filter in Figure 4.11 is $1 + \exp(-j2\pi fT_b)$. Hence, the overall frequency response of this filter connected in cascade with an ideal Nyquist channel is

$$\begin{aligned} H_I(f) &= H_{Nyquist}(f)[1 + \exp(-j2\pi fT_b)] \\ &= H_{Nyquist}(f)[\exp(j\pi fT_b) + \exp(-j\pi fT_b)] \exp(-j\pi fT_b) \\ &= 2H_{Nyquist}(f) \cos(\pi fT_b) \exp(-j\pi fT_b) \end{aligned} \tag{4.67}$$

where the subscript I in $H_I(f)$ indicates the pertinent class of partial response. For an ideal Nyquist channel of bandwidth $W = 1/2T_b$, we have (ignoring the scaling factor T_b)

$$H_{Nyquist}(f) = \begin{cases} 1, & |f| \leq 1/2T_b \\ 0, & \text{otherwise} \end{cases} \tag{4.68}$$

Thus the overall frequency response of the duobinary signaling scheme has the form of a half-cycle cosine function, as shown by

$$H_I(f) = \begin{cases} 2\cos(\pi fT_b) \exp(-j\pi fT_b), & |f| \leq 1/2T_b \\ 0, & \text{otherwise} \end{cases} \tag{4.69}$$

for which the magnitude response and phase response are as shown in Figures 4.12*a* and 4.12*b*, respectively. An advantage of this frequency response is that it can be easily approximated, in practice, by virtue of the fact that there is continuity at the band edges.

From the first line in Equation (4.67) and the definition of $H_{Nyquist}(f)$ in Equation (4.68), we find that the impulse response corresponding to the frequency response $H_I(f)$

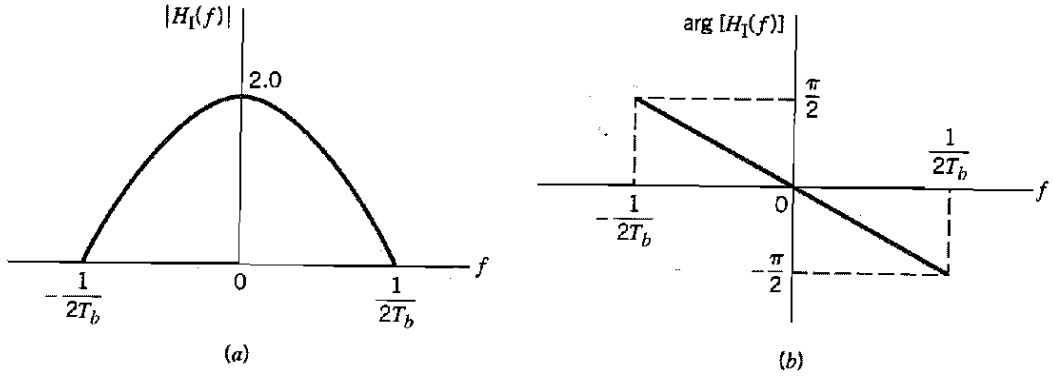

FIGURE 4.12 Frequency response of the duobinary conversion filter. (*a*) Magnitude response. (*b*) Phase response.

consists of two sinc (Nyquist) pulses that are time-displaced by T_b seconds with respect to each other, as shown by (except for a scaling factor)

$$\begin{aligned} h_I(t) &= \frac{\sin(\pi t/T_b)}{\pi t/T_b} + \frac{\sin[\pi(t - T_b)/T_b]}{\pi(t - T_b)/T_b} \\ &= \frac{\sin(\pi t/T_b)}{\pi t/T_b} - \frac{\sin(\pi t/T_b)}{\pi(t - T_b)/T_b} \\ &= \frac{T_b^2 \sin(\pi t/T_b)}{\pi t(T_b - t)} \end{aligned} \tag{4.70}$$

The impulse response $h_I(t)$ is plotted in Figure 4.13, where we see that it has only *two* distinguishable values at the sampling instants. The form of $h_I(t)$ shown here explains why we also refer to this type of correlative coding as partial-response signaling. The response to an input pulse is spread over more than one signaling interval; stated in another way, the response in any signaling interval is "partial." Note also that the tails of $h_I(t)$ decay as $1/|t|^2$, which is a faster rate of decay than the $1/|t|$ encountered in the ideal Nyquist channel.

The original two-level sequence $\{a_k\}$ may be detected from the duobinary-coded sequence $\{c_k\}$ by invoking the use of Equation (4.66). Specifically, let $\hat{a}_k$ represent the *estimate* of the original pulse a_k as conceived by the receiver at time $t = kt_b$. Then, subtracting the previous estimate $\hat{a}_{k-1}$ from c_k, we get

$$\hat{a}_k = c_k - \hat{a}_{k-1} \tag{4.71}$$

It is apparent that if c_k is received without error and if also the previous estimate $\hat{a}_{k-1}$ at time $t = (k - 1)T_b$ corresponds to a correct decision, then the current estimate $\hat{a}_k$ will be

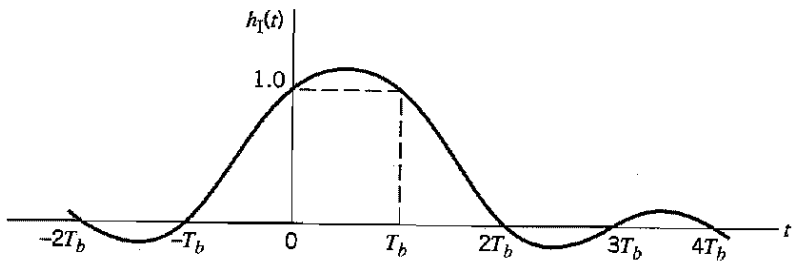

FIGURE 4.13 Impulse response of the duobinary conversion filter.

correct too. The technique of using a stored estimate of the previous symbol is called *decision feedback*.

We observe that the detection procedure just described is essentially an inverse of the operation of the simple delay-line filter at the transmitter. However, a major drawback of this detection procedure is that once errors are made, they tend to *propagate* through the output because a decision on the current input a_k depends on the correctness of the decision made on the previous input a_{k-1}.

A practical means of avoiding the error-propagation phenomenon is to use *precoding* before the duobinary coding, as shown in Figure 4.14. The precoding operation performed on the binary data sequence $\{b_k\}$ converts it into another binary sequence $\{d_k\}$ defined by

$$d_k = b_k \oplus d_{k-1} \tag{4.72}$$

where the symbol $\oplus$ denotes *modulo-two addition* of the binary digits b_k and d_{k-1}. This addition is equivalent to a two-input EXCLUSIVE OR operation, which is performed as follows:

$$d_k = \begin{cases} \text{symbol 1} & \text{if either symbol } b_k \text{ or symbol } d_{k-1} \text{ (but not both) is 1} \\ \text{symbol 0} & \text{otherwise} \end{cases} \tag{4.73}$$

The precoded binary sequence $\{d_k\}$ is applied to a pulse-amplitude modulator, producing a corresponding two-level sequence of short pulses $\{a_k\}$, where $a_k = \pm 1$ as before. This sequence of short pulses is next applied to the duobinary coder, thereby producing the sequence $\{c_k\}$ that is related to $\{a_k\}$ as follows:

$$c_k = a_k + a_{k-1} \tag{4.74}$$

Note that unlike the linear operation of duobinary coding, the precoding described by Equation (4.72) is a *nonlinear* operation.

The combined use of Equations (4.72) and (4.74) yields

$$c_k = \begin{cases} 0 & \text{if data symbol } b_k \text{ is 1} \\ \pm 2 & \text{if data symbol } b_k \text{ is 0} \end{cases} \tag{4.75}$$

which is illustrated in Example 4.3. From Equation (4.75) we deduce the following decision rule for detecting the original binary sequence $\{b_k\}$ from $\{c_k\}$:

$$\begin{aligned} &\text{If } |c_k| < 1, && \text{say symbol } b_k \text{ is 1} \\ &\text{If } |c_k| > 1, && \text{say symbol } b_k \text{ is 0} \end{aligned} \tag{4.76}$$

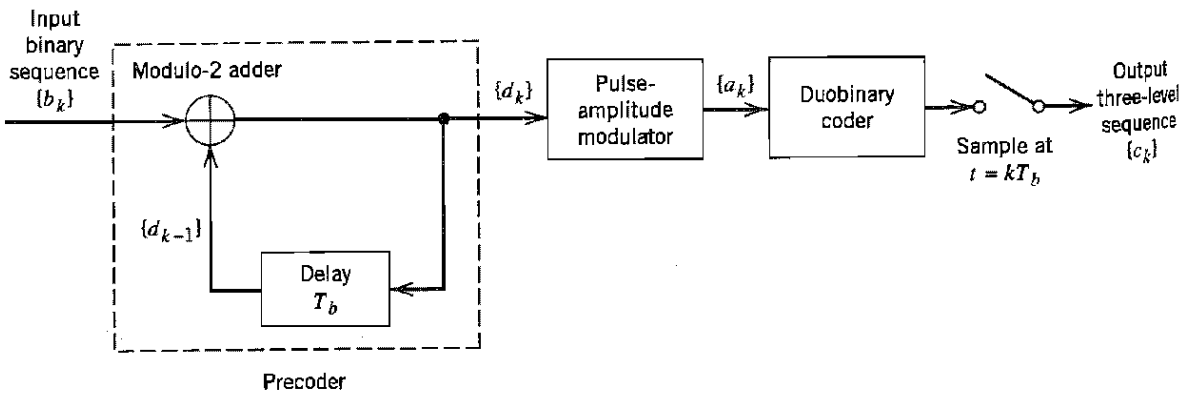

FIGURE 4.14 A precoded duobinary scheme; details of the duobinary coder are given in Figure 4.11.

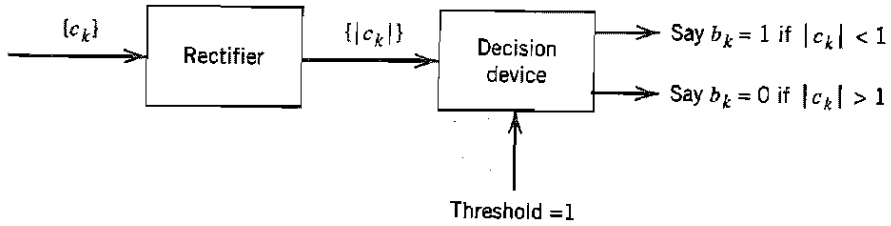

FIGURE 4.15 Detector for recovering original binary sequence from the precoded duobinary coder output.

When $|c_k| = 1$, the receiver simply makes a random guess in favor of symbol 1 or 0. According to this decision rule, the detector consists of a rectifier, the output of which is compared in a decision device to a threshold of 1. A block diagram of the detector is shown in Figure 4.15. A useful feature of this detector is that no knowledge of any input sample other than the present one is required. Hence, error propagation cannot occur in the detector of Figure 4.15.

▶ EXAMPLE 4.3 Duobinary Coding with Precoding

Consider the binary data sequence 0010110. To proceed with the precoding of this sequence, which involves feeding the precoder output back to the input, we add an extra bit to the precoder output. This extra bit is chosen arbitrarily to be 1. Hence, using Equation (4.73), we find that the sequence $\{d_k\}$ at the precoder output is as shown in row 2 of Table 4.1. The polar representation of the precoded sequence $\{d_k\}$ is shown in row 3 of Table 4.1. Finally, using Equation (4.74), we find that the duobinary coder output has the amplitude levels given in row 4 of Table 4.1.

To detect the original binary sequence, we apply the decision rule of Equation (4.76), and so obtain the binary sequence given in row 5 of Table 4.1. This latter result shows that, in the absence of noise, the original binary sequence is detected correctly. ◀

■ MODIFIED DUOBINARY SIGNALING

In the duobinary signaling technique the frequency response $H(f)$, and consequently the power spectral density of the transmitted pulse, is nonzero at the origin. This is considered to be an undesirable feature in some applications, since many communications channels cannot transmit a DC component. We may correct for this deficiency by using the *class IV partial response* or *modified duobinary* technique, which involves a correlation span of two binary digits. This special form of correlation is achieved by subtracting amplitude-modulated pulses spaced $2T_b$ seconds apart, as indicated in the block diagram of Figure

TABLE 4.1 *Illustrating Example 4.3 on duobinary coding*

Binary sequence $\{b_k\}$		0	0	1	0	1	1	0
Precoded sequence $\{d_k\}$	1	1	1	0	0	1	0	0
Two-level sequence $\{a_k\}$	+1	+1	+1	−1	−1	+1	−1	−1
Duobinary coder output $\{c_k\}$		+2	+2	0	−2	0	0	−2
Binary sequence obtained by applying decision rule of Eq. (4.76)		0	0	1	0	1	1	0

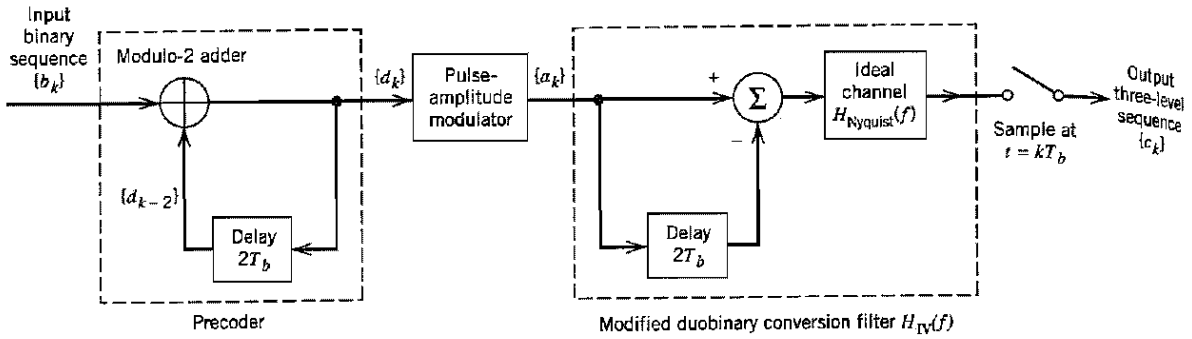

FIGURE 4.16 Modified duobinary signaling scheme.

4.16. The precoder involves a delay of $2T_b$ seconds. The output of the modified duobinary conversion filter is related to the input two-level sequence $\{a_k\}$ at the pulse-amplitude modulator output as follows:

$$c_k = a_k - a_{k-2} \tag{4.77}$$

Here, again, we find that a three-level signal is generated. With $a_k = \pm 1$, we find that c_k takes on one of three values: $+2$, 0, and -2.

The overall frequency response of the delay-line filter connected in cascade with an ideal Nyquist channel, as in Figure 4.16, is given by

$$\begin{aligned} H_{\text{IV}}(f) &= H_{\text{Nyquist}}(f)[1 - \exp(-j4\pi f T_b)] \\ &= 2jH_{\text{Nyquist}}(f)\sin(2\pi f T_b)\exp(-j2\pi f T_b) \end{aligned} \tag{4.78}$$

where the subscript IV in $H_{\text{IV}}(f)$ indicates the pertinent class of partial response and $H_{\text{Nyquist}}(f)$ is as defined in Equation (4.68). We therefore have an overall frequency response in the form of a half-cycle sine function, as shown by

$$H_{\text{IV}}(f) = \begin{cases} 2j\sin(2\pi f T_b)\exp(-j2\pi f T_b), & |f| \le 1/2T_b \\ 0, & \text{elsewhere} \end{cases} \tag{4.79}$$

The corresponding magnitude response and phase response of the modified duobinary coder are shown in Figures 4.17*a* and 4.17*b*, respectively. A useful feature of the modified duobinary coder is the fact that its output has no DC component. Note also that this

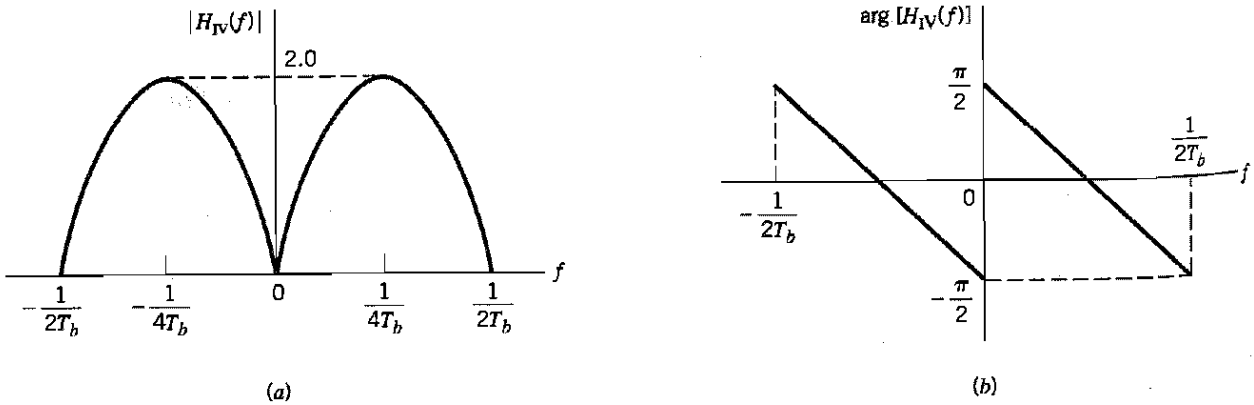

FIGURE 4.17 Frequency response of the modified duobinary conversion filter. (*a*) Magnitude response. (*b*) Phase response.

second form of correlative-level coding exhibits the same continuity at the band edges as in duobinary signaling.

From the first line of Equation (4.78) and the definition of $H_{\text{Nyquist}}(f)$ in Equation (4.68), we find that the impulse response of the modified duobinary coder consists of two sinc (Nyquist) pulses that are time-displaced by $2T_b$ seconds with respect to each other, as shown by (except for a scaling factor)

$$\begin{aligned} h_{\text{IV}}(t) &= \frac{\sin(\pi t/T_b)}{\pi t/T_b} - \frac{\sin[\pi(t - 2T_b)/T_b)]}{\pi(t - 2T_b)/T_b} \\ &= \frac{\sin(\pi t/T_b)}{\pi t/T_b} - \frac{\sin(\pi t/T_b)}{\pi(t - 2T_b)/T_b} \\ &= \frac{2T_b^2 \sin(\pi t/T_b)}{\pi t(2T_b - t)} \end{aligned} \tag{4.80}$$

This impulse response is plotted in Figure 4.18, which shows that it has *three* distinguishable levels at the sampling instants. Note also that, as with duobinary signaling, the tails of $h_{\text{IV}}(t)$ for the modified duobinary signaling decay as $1/|t|^2$.

To eliminate the possibility of error propagation in the modified duobinary system, we use a precoding procedure similar to that used for the duobinary case. Specifically, prior to the generation of the modified duobinary signal, a modulo-two logical addition is used on signals $2T_b$ seconds apart, as shown by (see the front end of Figure 4.16)

$$\begin{aligned} d_k &= b_k \oplus d_{k-2} \\ &= \begin{cases} \text{symbol 1} & \text{if either symbol } b_k \text{ or symbol } d_{k-2} \text{ (but not both) is 1} \\ \text{symbol 0} & \text{otherwise} \end{cases} \end{aligned} \tag{4.81}$$

where $\{b_k\}$ is the incoming binary data sequence and $\{d_k\}$ is the sequence at the precoder output. The precoded sequence $\{d_k\}$ thus produced is then applied to a pulse-amplitude modulator and then to the modified duobinary conversion filter.

In Figure 4.16, the output digit c_k equals -2, 0, or $+2$, assuming that the pulse-amplitude modulator uses a polar representation for the precoded sequence $\{d_k\}$. Also we find that the detected digit $\hat{b}_k$ at the receiver output may be extracted from c_k by disregarding the polarity of c_k. Specifically, we may formulate the following decision rule:

$$\begin{aligned} &\text{If } |c_k| > 1, \quad \text{say symbol } b_k \text{ is 1} \\ &\text{If } |c_k| < 1, \quad \text{say symbol } b_k \text{ is 0} \end{aligned} \tag{4.82}$$

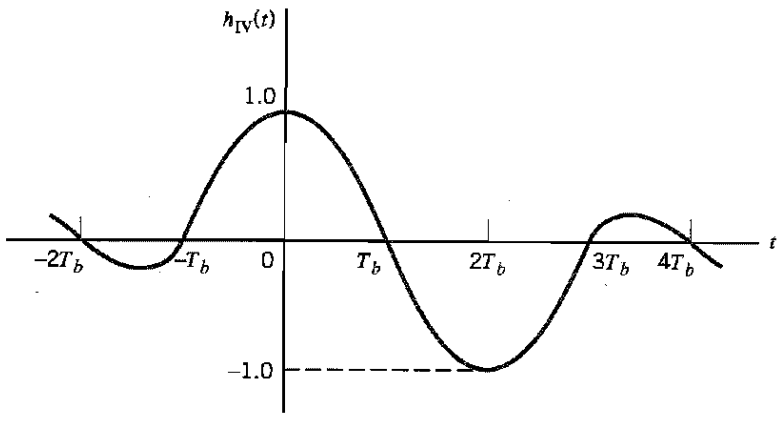

FIGURE 4.18 Impulse response of the modified duobinary conversion filter.

When $|c_k| = 1$, the receiver makes a random guess in favor of symbol 1 or 0. As with the duobinary signaling, we may note the following:

- In the absence of channel noise, the detected binary sequence $\{\hat{b}_k\}$ is exactly the same as the original binary sequence $\{b_k\}$ at the transmitter input.
- The use of Equation (4.81) requires the addition of two extra bits to the precoded sequence $\{a_k\}$. The composition of the decoded sequence $\{\hat{b}_k\}$ using Equation (4.82) is invariant to the selection made for these two bits.

■ GENERALIZED FORM OF CORRELATIVE-LEVEL CODING (PARTIAL-RESPONSE SIGNALING)

The duobinary and modified duobinary techniques have correlation spans of 1 binary digit and 2 binary digits, respectively. It is a straightforward matter to generalize these two techniques to other schemes, which are known collectively as *correlative-level coding* or *partial-response signaling* schemes. This generalization is shown in Figure 4.19, where $H_{\text{Nyquist}}(f)$ is defined in Equation (4.68). It involves the use of a tapped-delay-line filter with tap-weights $w_0, w_1, \cdots, w_{N-1}$. Specifically, different classes of partial-response sig-

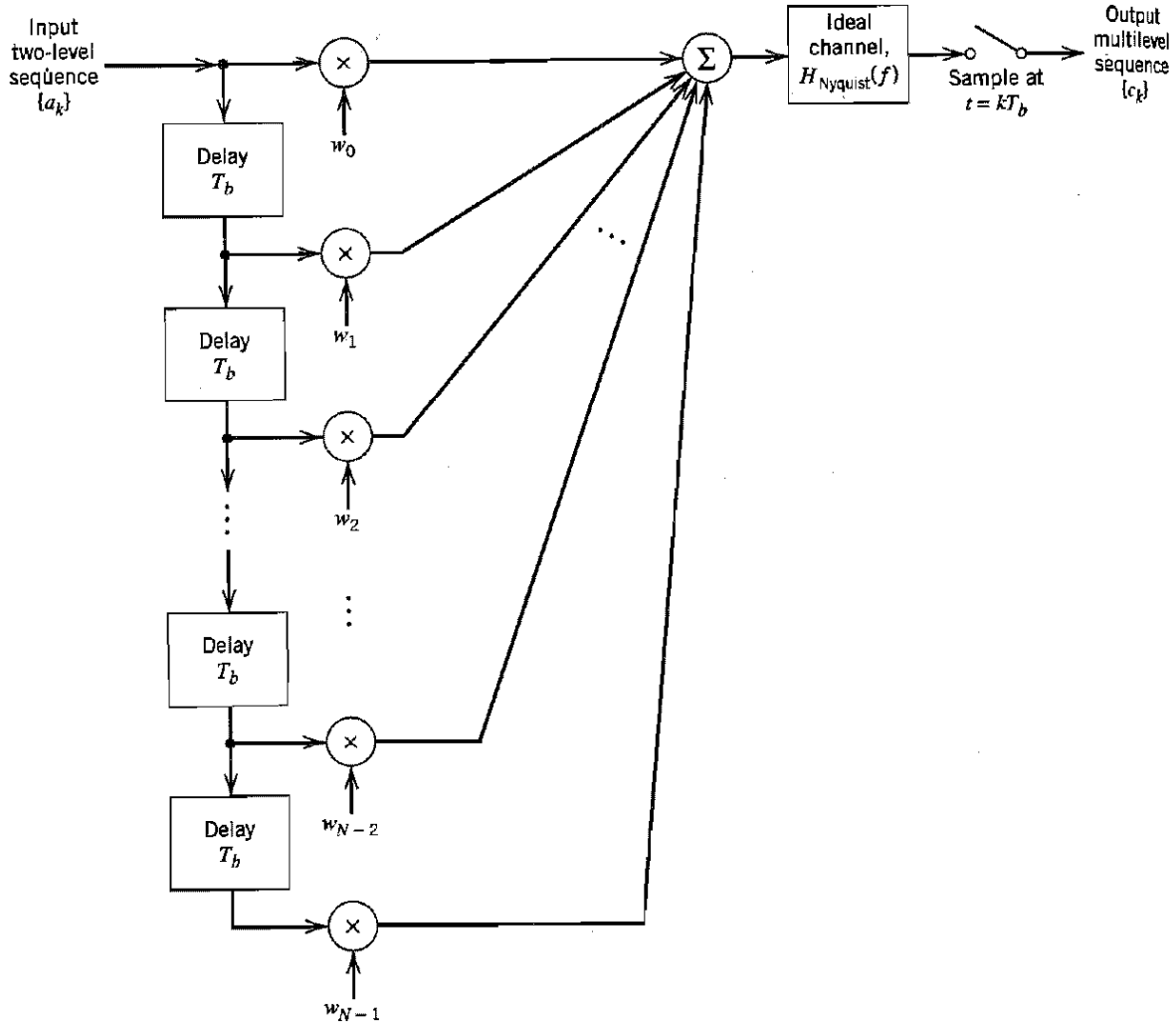

FIGURE 4.19 Generalized correlative coding scheme.

TABLE 4.2 *Different classes of partial-response signaling schemes referring to Figure 4.19*

Type of Class	N	w_0	w_1	w_2	w_3	w_4	*Comments*
I	2	1	1				Duobinary coding
II	3	1	2	1			
III	3	2	1	−1			
IV	3	1	0	−1			Modified duobinary coding
V	5	−1	0	2	0	−1	

naling schemes may be achieved by using a weighted linear combination of N ideal Nyquist (sinc) pulses, as shown by

$$h(t) = \sum_{n=0}^{N-1} w_n \operatorname{sinc}\left(\frac{t}{T_b} - n\right) \tag{4.83}$$

An appropriate choice of the tap-weights in Equation (4.83) results in a variety of spectral shapes designed to suit individual applications. Table 4.2 presents the specific details of five different classes of partial-response signaling schemes. For example, in the duobinary case (class I partial response), we have

$$w_0 = +1$$
$$w_1 = +1$$

and $w_n = 0$ for $n \geq 2$. In the modified duobinary case (class IV partial response), we have

$$w_0 = +1$$
$$w_1 = 0$$
$$w_2 = -1$$

and $w_n = 0$ for $n \geq 3$.

The useful characteristics of partial-response signaling schemes may now be summarized as follows:

- Binary data transmission over a physical baseband channel can be accomplished at a rate close to the Nyquist rate, using realizable filters with gradual cutoff characteristics.
- Different spectral shapes can be produced, appropriate for the application at hand.

However, these desirable characteristics are achieved at a price: A larger signal-to-noise ratio is required to yield the same average probability of symbol error in the presence of noise as in the corresponding binary PAM systems because of an increase in the number of signal levels used.

4.7 *Baseband M-ary PAM Transmission*

In the baseband binary PAM system of Figure 4.7, the pulse-amplitude modulator produces binary pulses, that is, pulses with one of two possible amplitude levels. On the other

switched telephone network, we find that two factors contribute to the distribution of pulse distortion on different link connections:

- Differences in the transmission characteristics of the individual links that may be switched together.
- Differences in the number of links in a connection.

The result is that the telephone channel is random in the sense of being one of an ensemble of possible physical realizations. Consequently, the use of a fixed pair of matched filter and equalizer designed on the basis of average channel characteristics may not adequately reduce the effects of intersymbol interference and channel noise. To realize the full transmission capability of the telephone channel, we need an *adaptive receiver*[9] that provides for the *adaptive implementation of both the matched filter and the equalizer in a combined manner*. The receiver is adaptive in the sense that the equalizer coefficients are adjusted automatically in accordance with a built-in algorithm.

Another point of interest is that it may be desirable to have the taps of the equalizer spaced by an amount closer than the symbol period; typically, the spacing between adjacent taps is set equal to $T/2$. The resulting structure is known as a *fractionally spaced equalizer* (*FSE*). An FSE has the capability of compensating for delay distortion much more effectively than a conventional synchronous equalizer. Another advantage of the FSE is the fact that data transmission may begin with an arbitrary sampling phase. However, mathematical analysis of the FSE is more complicated than for a synchronous equalizer and will therefore not be pursued here.[10]

4.10 *Adaptive Equalization*

In this section we develop a simple and yet effective algorithm for the adaptive equalization of a linear channel of unknown characteristics. Figure 4.28 shows the structure of an adaptive synchronous equalizer, which incorporates the matched filtering action. The algorithm used to adjust the equalizer coefficients assumes the availability of a desired response. One's first reaction to the availability of a replica of the transmitted signal is: If such a signal is available at the receiver, why do we need adaptive equalization? To answer this question, we first note that a typical telephone channel changes little during an average data call. Accordingly, prior to data transmission, the equalizer is adjusted under the guid-

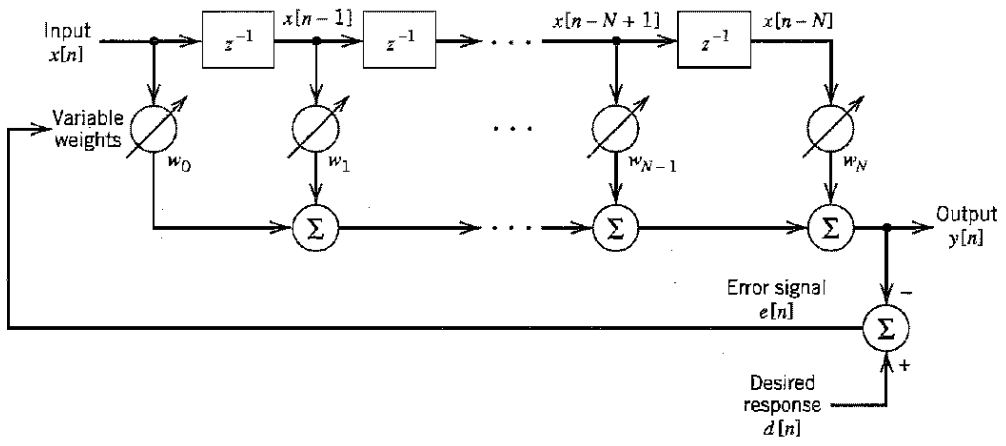

FIGURE 4.28 Block diagram of adaptive equalizer.

ance of a *training sequence* transmitted through the channel. A synchronized version of this training sequence is generated at the receiver, where (after a time shift equal to the transmission delay through the channel) it is applied to the equalizer as the desired response. A training sequence commonly used in practice is the *pseudonoise (PN) sequence*, which consists of a deterministic periodic sequence with noise-like characteristics. Two identical PN sequence generators are used, one at the transmitter and the other at the receiver. When the training process is completed, the PN sequence generator is switched off, and the adaptive equalizer is ready for normal data transmission. Detailed description of PN sequence generators is presented in Chapter 7.

■ LEAST-MEAN-SQUARE ALGORITHM (REVISITED)

To simplify notational matters, we let

$$x[n] = x(nT)$$
$$y[n] = y(nT)$$

Then, the output $y[n]$ of the tapped-delay-line equalizer in response to the input sequence $\{x[n]\}$ is defined by the discrete convolution sum (see Figure 4.28)

$$y[n] = \sum_{k=0}^{N} w_k x[n-k] \tag{4.112}$$

where w_k is the weight at the kth tap, and $N + 1$ is the total number of taps. The tap-weights constitute the adaptive filter coefficients. We assume that the input sequence $\{x[n]\}$ has finite energy. We have used a notation for the equalizer weights in Figure 4.28 that is different from the corresponding notation in Figure 4.27 to emphasize the fact that the equalizer in Figure 4.28 also incorporates matched filtering.

The adaptation may be achieved by observing the error between the desired pulse shape and the actual pulse shape at the filter output, measured at the sampling instants, and then using this error to estimate the direction in which the tap-weights of the filter should be changed so as to approach an optimum set of values. For the adaptation, we may use a criterion based on minimizing the *peak distortion*, defined as the worst-case intersymbol interference at the output of the equalizer. The development of an adaptive equalizer using such a criterion builds on the zero-forcing concept described briefly in Section 4.9. However, the equalizer is optimum only when the peak distortion at its input is less than 100 percent (i.e., the intersymbol interference is not too severe). A better approach is to use a mean-square error criterion, which is more general in application; also an adaptive equalizer based on the mean-square error criterion appears to be less sensitive to timing perturbations than one based on the peak distortion criterion. Accordingly, in what follows we use the mean-square error criterion to derive the adaptive equalization algorithm.

Let $a[n]$ denote the *desired response* defined as the polar representation of the nth transmitted binary symbol. Let $e[n]$ denote the *error signal* defined as the difference between the desired response $a[n]$ and the actual response $y[n]$ of the equalizer, as shown by

$$e[n] = a[n] - y[n] \tag{4.113}$$

In the *least-mean-square (LMS) algorithm*[11] for adaptive equalization, the error signal $e[n]$ actuates the adjustments applied to the individual tap weights of the equalizer as the algorithm proceeds from one iteration to the next. A derivation of the LMS algorithm for

adaptive prediction was presented in Section 3.13. Recasting Equation (3.72) into its most general form, we may state the formula for the LMS algorithm in words as follows:

$$\begin{pmatrix}\text{Updated value}\\ \text{of } k\text{th tap-}\\ \text{weight}\end{pmatrix} = \begin{pmatrix}\text{Old value}\\ \text{of } k\text{th tap-}\\ \text{weight}\end{pmatrix} + \begin{pmatrix}\text{Step-size}\\ \text{parameter}\end{pmatrix} \cdot \begin{pmatrix}\text{Input signal}\\ \text{applied to}\\ k\text{th tap-}\\ \text{weight}\end{pmatrix}\begin{pmatrix}\text{Error}\\ \text{signal}\end{pmatrix} \tag{4.114}$$

Let μ denote the step-size parameter. From Figure 4.28 we see that the input signal applied to the kth tap-weight at time step n is $x[n-k]$. Hence, using $\hat{w}_k(n)$ as the old value of the kth tap-weight at time step n, the updated value of this tap-weight at time step $n+1$ is, in light of Equation (4.114), defined by

$$\hat{w}_k[n+1] = \hat{w}_k[n] + \mu x[n-k]e[n], \qquad k = 0, 1, \ldots, N \tag{4.115}$$

where

$$e[n] = a[n] - \sum_{k=0}^{N} \hat{w}_k[n]x[n-k] \tag{4.116}$$

These two equations constitute the *LMS algorithm for adaptive equalization.* Note that the length of the adaptive equalizer in Figure 4.28 is not to be confused with the length of the equalizer in Figure 4.27.

We may simplify the formulation of the LMS algorithm using matrix notation. Let the $(N+1)$-by-1 vector $\mathbf{x}[n]$ denote the tap-inputs of the equalizer:

$$\mathbf{x}[n] = [x[n], \ldots, x[n-N+1], x[n-N]]^T \tag{4.117}$$

where the superscript T denotes matrix transposition. Correspondingly, let the $(N+1)$-by-1 vector $\hat{\mathbf{w}}[n]$ denote the tap-weights of the equalizer:

$$\hat{\mathbf{w}}[n] = [\hat{w}_0[n], \hat{w}_1[n], \ldots, \hat{w}_N[n]]^T \tag{4.118}$$

We may then use matrix notation to recast the convolution sum of Equation (4.112) in the compact form

$$y[n] = \mathbf{x}^T[n]\hat{\mathbf{w}}[n] \tag{4.119}$$

where $\mathbf{x}^T[n]\hat{\mathbf{w}}[n]$ is referred to as the *inner product* of the vectors $\mathbf{x}[n]$ and $\hat{\mathbf{w}}[n]$. We may now summarize the LMS algorithm for adaptive equalization as follows:

1. Initialize the algorithm by setting $\hat{\mathbf{w}}[1] = 0$ (i.e., set all the tap-weights of the equalizer to zero at $n = 1$, which corresponds to time $t = T$).
2. For $n = 1, 2, \ldots$, compute

$$\begin{aligned} y[n] &= \mathbf{x}^T[n]\hat{\mathbf{w}}[n] \\ e[n] &= a[n] - y[n] \\ \hat{\mathbf{w}}[n+1] &= \hat{\mathbf{w}}[n] + \mu e[n]\mathbf{x}[n] \end{aligned}$$

   where μ is the step-size parameter.
3. Continue the iterative computation until the equalizer reaches a "steady state," by which we mean that the actual mean-square error of the equalizer essentially reaches a constant value.

The LMS algorithm is an example of a feedback system, as illustrated in the block diagram of Figure 4.29, which pertains to the kth filter coefficient. It is therefore possible

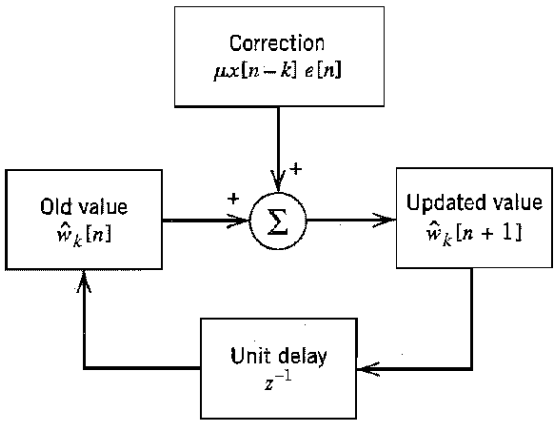

FIGURE 4.29 Signal-flow graph representation of the LMS algorithm involving the kth tap weight.

for the algorithm to diverge (i.e., for the adaptive equalizer to become unstable). Unfortunately, the convergence behavior of the LMS algorithm is difficult to analyze. Nevertheless, provided that the step-size parameter μ is assigned a small value, we find that after a large number of iterations the behavior of the LMS algorithm is roughly similar to that of the *steepest-descent algorithm*, which uses the actual gradient rather than a noisy estimate for the computation of the tap-weights. (The steepest-descent algorithm was discussed in Section 3.13.)

■ OPERATION OF THE EQUALIZER

There are two modes of operation for an adaptive equalizer, namely, the training mode and decision-directed mode, as shown in Figure 4.30. During the *training mode*, as explained previously, a known PN sequence is transmitted and a synchronized version of it is generated in the receiver, where (after a time shift equal to the transmission delay) it is applied to the adaptive equalizer as the desired response; the tap-weights of the equalizer are thereby adjusted in accordance with the LMS algorithm.

When the training process is completed, the adaptive equalizer is switched to its second mode of operation: the *decision-directed mode*. In this mode of operation, the error signal is defined by

$$e[n] = \hat{a}[n] - y[n] \tag{4.120}$$

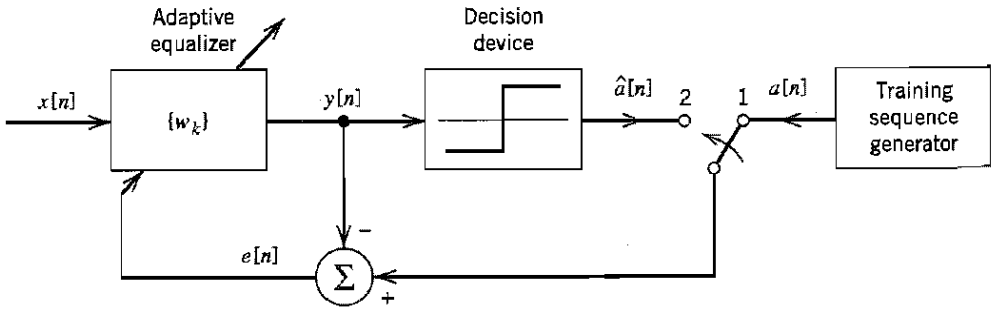

FIGURE 4.30 Illustrating the two operating modes of an adaptive equalizer: For the training mode, the switch is in position 1; and for the tracking mode, it is moved to position 2.

where $y[n]$ is the equalizer output at time $t = nT$, and $\hat{a}[n]$ is the final (not necessarily) correct estimate of the transmitted symbol $a[n]$. Now, in normal operation the decisions made by the receiver are correct with high probability. This means that the error estimates are correct most of the time, thereby permitting the adaptive equalizer to operate satisfactorily. Furthermore, an adaptive equalizer operating in a decision-directed mode is able to *track* relatively slow variations in channel characteristics.

It turns out that the larger the step-size parameter μ, the faster the tracking capability of the adaptive equalizer. However, a large step-size parameter μ may result in an unacceptably high *excess mean-square error*, defined as that part of the mean-square value of the error signal in excess of the minimum attainable value $J_{\min}$ (which results when the tap-weights are at their optimum settings). We therefore find that in practice the choice of a suitable value for the step-size parameter μ involves making a compromise between fast tracking and reducing the excess mean-square error.

Decision-Feedback Equalization

To develop further insight into adaptive equalization, consider a baseband channel with impulse response denoted in its sampled form by the sequence $\{h[n]\}$ where $h[n] = h(nT)$. The response of this channel to an input sequence $\{x[n]\}$, in the absence of noise, is given by the discrete convolution sum

$$\begin{aligned} y[n] &= \sum_k h[k]x[n-k] \\ &= h[0]x[n] + \sum_{k<0} h[k]x[n-k] + \sum_{k>0} h[k]x[n-k] \end{aligned} \tag{4.121}$$

The first term of Equation (4.121) represents the desired data symbol. The second term is due to the *precursors* of the channel impulse response that occur before the main sample $h[0]$ associated with the desired data symbol. The third term is due to the *postcursors* of the channel impulse response that occur after the main sample $h[0]$. The precursors and postcursors of a channel impluse response are illustrated in Figure 4.31. The idea of *decision-feedback equalization*[12] is to use data decisions made on the basis of precursors of the channel impulse response to take care of the postcursors; for the idea to work, however, the decisions would obviously have to be correct. Provided that this condition is satisfied,

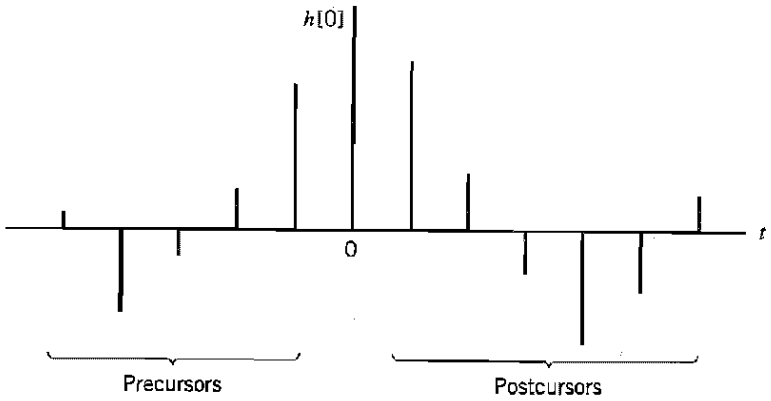

Figure 4.31 Impulse response of a discrete-time channel, depicting the precursors and postcursors.

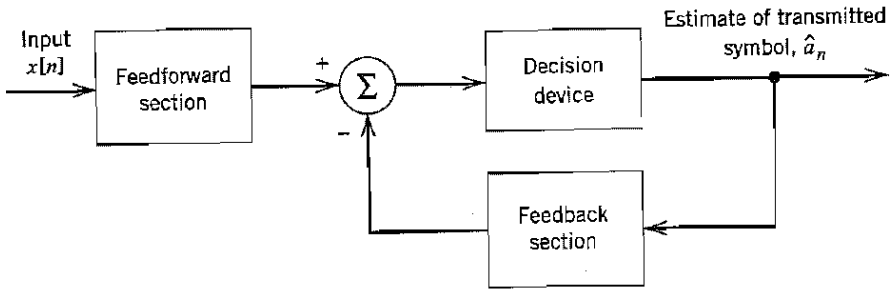

FIGURE 4.32 Block diagram of decision-feedback equalizer.

a decision-feedback equalizer is able to provide an improvement over the performance of the tapped-delay-line equalizer.

A *decision-feedback equalizer* (DFE) consists of a feedforward section, a feedback section, and a decision device connected together as shown in Figure 4.32. The feedforward section consists of a tapped-delay-line filter whose taps are spaced at the reciprocal of the signaling rate. The data sequence to be equalized is applied to this section. The feedback section consists of another tapped-delay-line filter whose taps are also spaced at the reciprocal of the signaling rate. The input applied to the feedback section consists of the decisions made on previously detected symbols of the input sequence. The function of the feedback section is to subtract out that portion of the intersymbol interference produced by previously detected symbols from the estimates of future samples.

Note that the inclusion of the decision device in the feedback loop makes the equalizer intrinsically *nonlinear* and therefore more difficult to analyze than an ordinary tapped-delay-line equalizer. Nevertheless, the mean-square error criterion can be used to obtain a mathematically tractable optimization of a decision-feedback equalizer. Indeed, the LMS algorithm can be used to jointly adapt both the feedforward tap-weights and the feedback tap-weights based on a *common* error signal; see Problem 4.37.

On the basis of extensive comparative evaluations of a linear equalizer and decision-feedback equalizer reported in the literature,[13] we may report that when the frequency response of a linear channel is characterized by severe amplitude distortion or relatively sharp amplitude cutoff, the decision-feedback equalizer offers a significant improvement in performance over a linear equalizer for an equal number of taps. It is presupposed here that the feedback decisions in the DFE are all correct. For an example of sharp amplitude cutoff, see the frequency response of a telephone channel depicted in Figure 8 in the Background and Preview chapter.

Unlike a linear equalizer, a decision-feedback equalizer suffers from *error propagation*. However, despite the fact that the DFE is a feedback system, error propagation will not persist indefinitely. Rather, decision errors tend to occur in *bursts*. To justify this kind of behavior, we offer the following intuitive reasoning:[14]

- Let L denote the number of taps in the feedback section of a DFE. After a sequence of L consecutive correct decisions, all decision errors in the feedback section will be flushed out. This points to an error propagation of finite duration.
- When a decision error is made, the probability of the next decision being erroneous too is clearly no worse than 1/2.
- Let K denote the duration of error propagation, that is, the number of symbols needed to make L consecutive correct decisions. Then the average error rate is $(K/2)P_0$, where $K/2$ is the average number of errors produced by a single decision error, and P_0 is the probability of error given that the past L decisions are all correct.

- In a fair-coin tossing experiment, the average number of coin tosses, K, needed to get L successive heads (representing no errors) turns out to be $2(2^L - 1)$.

It follows therefore that the effect of error propagation in a decision-feedback equalizer is to increase the average error rate by a factor approximately equal to 2^L, compared to the probability of making the first error. For example, for $L = 3$ the average error rate is increased by less than an order of magnitude due to error propagation.

4.11 Computer Experiments: Eye Patterns

In previous sections of this chapter we have discussed various techniques for dealing with the effects of channel noise and intersymbol interference on the performance of a baseband pulse-transmission system. In the final analysis, what really matters is how to evaluate the combined effect of these impairments on overall system performance in an operational environment. An experimental tool for such an evaluation in an insightful manner is the so-called *eye pattern*, which is defined as the synchronized superposition of all possible realizations of the signal of interest (e.g., received signal, receiver output) viewed within a particular signaling interval. The eye pattern derives its name from the fact that it resembles the human eye for binary waves. The interior region of the eye pattern is called the *eye opening*.

An eye pattern provides a great deal of useful information about the performance of a data transmission system, as described in Figure 4.33. Specifically, we make the following statements:

- The width of the eye opening defines the *time interval over which the received signal can be sampled without error from intersymbol interference*; it is apparent that the preferred time for sampling is the instant of time at which the eye is open the widest.
- The *sensitivity of the system to timing errors* is determined by the rate of closure of the eye as the sampling time is varied.
- The height of the eye opening, at a specified sampling time, defines the *noise margin* of the system.

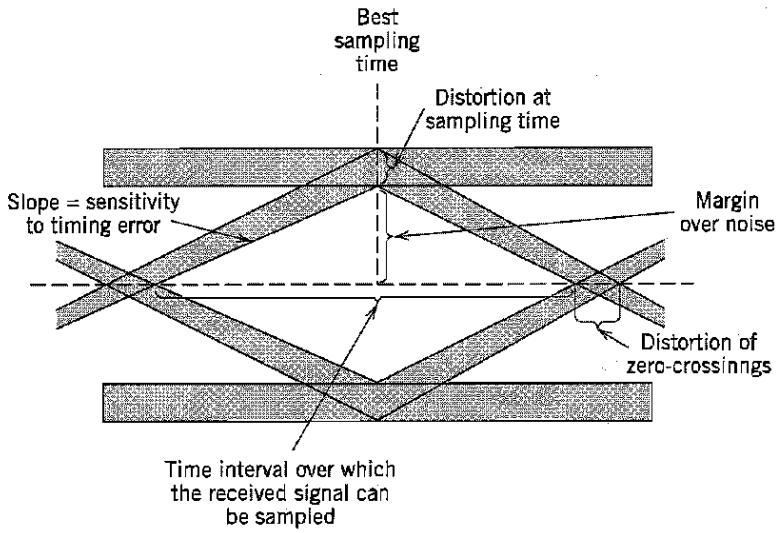

FIGURE 4.33 Interpretation of the eye pattern.

When the effect of intersymbol interference is severe, traces from the upper portion of the eye pattern cross traces from the lower portion, with the result that the eye is completely closed. In such a situation, it is impossible to avoid errors due to the combined presence of intersymbol interference and noise in the system.

In the case of an M-ary system, the eye pattern contains $(M - 1)$ eye openings stacked up vertically one on the other, where M is the number of discrete amplitude levels used to construct the transmitted signal. In a strictly linear system with truly random data, all these eye openings would be identical.

In the next two experiments, we use computer simulations to study the eye patterns for a quaternary ($M = 4$) baseband PAM transmission system under noiseless, noisy, and band-limited conditions. The effect of channel nonlinearity on eye patterns is discussed in Problem 4.38.

Experiment 1: Effect of Channel Noise

Figure 4.34*a* shows the eye diagram of the system under idealized conditions: no channel noise and no bandwidth limitation. The source symbols used are randomly generated on a computer, with raised cosine pulse-shaping. The system parameters used for the generation of the eye diagram are as follows: Nyquist bandwidth $W = 0.5$ Hz, rolloff factor $\alpha = 0.5$, and symbol duration $T = T_b \log_2 M = 2T_b$. The openings in Figure 4.34 are perfect, indicating reliable operation of the system. Note that this figure has $M - 1 = 3$ openings.

Figures 4.34*b* and 4.34*c* show the eye diagrams for the system, but this time with channel noise corrupting the received signal. These two figures were simulated for signal-to-noise ratio SNR = 20 dB and 10 dB, respectively, with the SNR being measured at the channel output. When SNR = 20 dB the effect of channel noise is hardly discernible in Figure 4.34*b*, but when SNR = 10 dB the openings of the eye diagram in Figure 4.34*c* are barely visible.

Experiment 2: Effect of Bandwidth Limitation

Figures 4.35*a* and 4.35*b* show the eye diagrams for the quaternary system using the same parameters as before, but this time under a bandwidth-limited condition and a noiseless channel. Specifically, the channel is now modeled by a low-pass *Butterworth filter*, whose squared magnitude response is defined by

$$|H(f)|^2 = \frac{1}{1 + (f/f_0)^{2N}}$$

where N is the *order* of the filter, and f_0 is its 3-dB cutoff frequency. For the computer experiment described in Figure 4.35*a*, the following values are used:

$$N = 25 \text{ and } f_0 = 0.975 \text{ Hz}$$

The bandwidth required by the PAM trasmission system is computed to be

$$B_T = W(1 + \alpha) = 0.75 \text{ Hz}$$

Although the channel bandwidth (i.e., cutoff frequency) is greater than absolutely necessary, its effect on the passband is observed as a decrease in the size of the eye openings compared to those in Figure 4.34*a*. Instead of the distinct values at time $t = 1$ s (as shown in Figure 4.34*a*), now there is a blurred region.

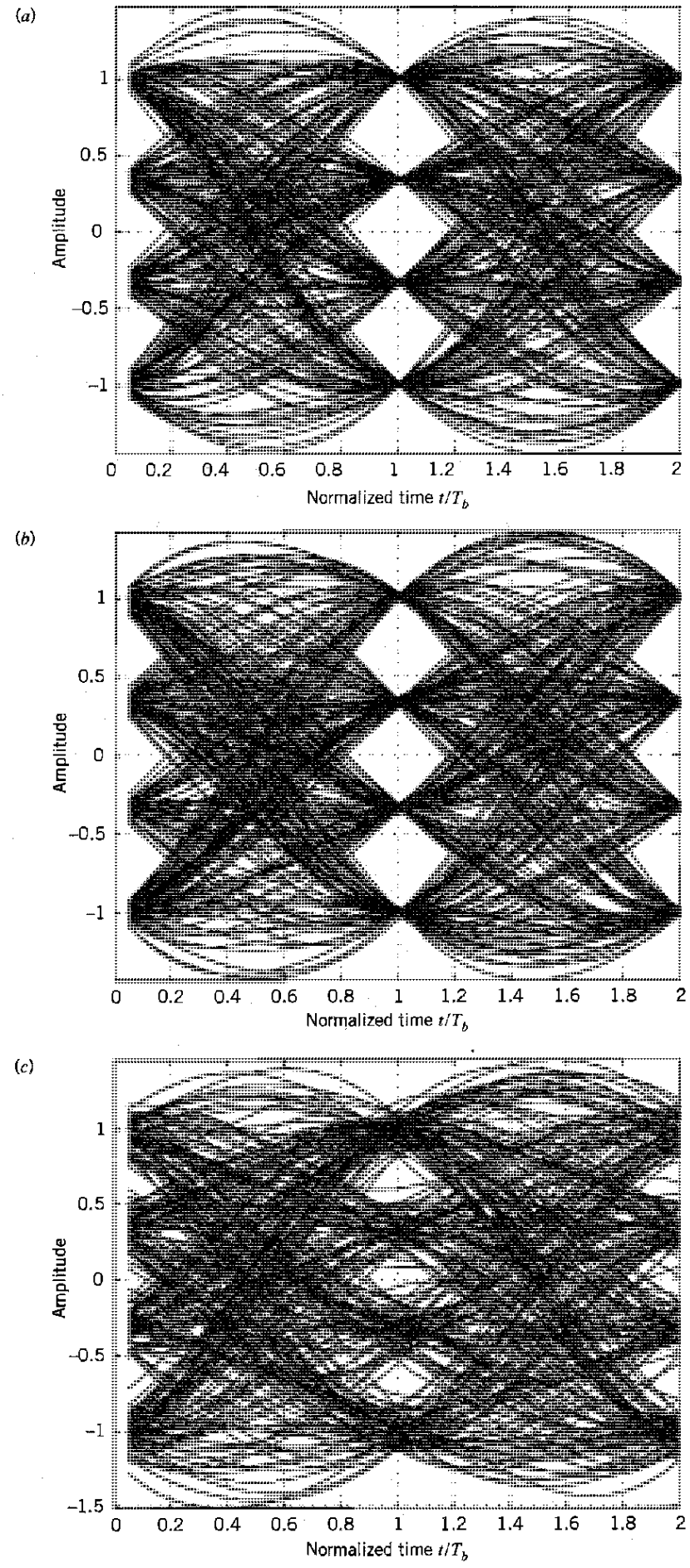

FIGURE 4.34 (*a*) Eye diagram for noiseless quaternary system. (*b*) Eye diagram for quaternary system with SNR = 20 dB. (*c*) Eye diagram for quaternary system with SNR = 10 dB.

modification may result in a significant increase in transmit power; modulo arithmetic is used to overcome most of this power increase.

13. For performance comparison between linear equalizers and decision-feedback equalizers, see Gitlin et al. (1992) and Proakis (1995).

14. The intuitive discussion on error propagation in decision-feedback equalizers presented in Section 4.10 follows Gitlin et al. (1992).

    For a rigorous evaluation of the probability of symbol error P_e in a decision-feedback equalizer with error propagation, see Duttweiler et al. (1974). In this paper it is shown that in the worst-case intersymbol interference, P_e is multiplied by a factor of 2^L relative to the probability of error that results in the absence of decision errors at high signal-to-noise ratios, where L is the number of taps in the feedback section. The result derived by Duttweiler et al. provides theoretical justification for the intuitive arguments presented in Section 4.10.

PROBLEMS

Matched Filters

4.1 Consider the signal $s(t)$ shown in Figure P4.1.

(a) Determine the impulse response of a filter matched to this signal and sketch it as a function of time.

(b) Plot the matched filter output as a function of time.

(c) What is the peak value of the output?

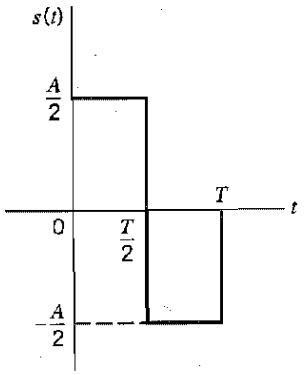

FIGURE P4.1

4.2 Figure P4.2*a* shows a pair of pulses that are orthogonal to each other over the interval $[0, T]$. In this problem we investigate the use of this pulse-pair to study a *two-dimensional matched filter*.

(a) Determine the matched filters for the pulses $s_1(t)$ and $s_2(t)$ considered individually; for $s_1(t)$ the filter is the same as that considered in Problem 4.1.

(b) Form a two-dimensional matched filter by connecting the two matched filters of Part (a) in parallel, as shown in Figure P4.2*b*. Hence, demonstrate the following:

(i) When the pulse $s_1(t)$ is applied to this two-dimensional filter, the response of the lower matched filter is zero.

(ii) When the pulse $s_2(t)$ is applied to the two-dimensional filter, the response of the upper matched filter is zero.

Generalize the results of your investigation.

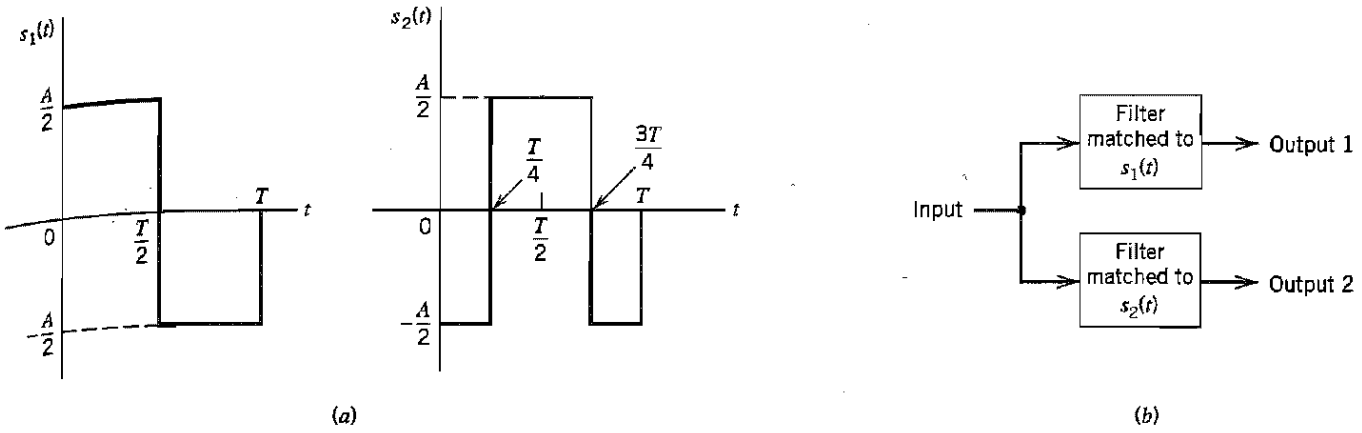

FIGURE P4.2

4.3 Consider a rectangular pulse defined by

$$g(t) = \begin{cases} A, & 0 \leq t \leq T \\ 0, & \text{otherwise} \end{cases}$$

It is proposed to approximate the matched filter for $g(t)$ by an ideal low-pass filter of bandwidth B; maximization of the peak pulse signal-to-noise ratio is the primary objective.

(a) Determine the optimum value of B for which the ideal low-pass filter provides the best approximation to the matched filter.

(b) By how many decibels is the ideal low-pass filter worse off than the matched filter?

4.4 In this problem we explore another method for the approximate realization of a matched filter, this time using the simple resistance-capacitance (RC) low-pass filter shown in Figure P4.4. The frequency resonse of this filter is

$$H(f) = \frac{1}{1 + jf/f_0}$$

where $f_0 = 1/2\pi RC$. The input signal $g(t)$ is a rectangular pulse of amplitude A and duration T. The requirement is to optimize the selection of the 3-dB cutoff frequency f_0 of the filter so that the peak pulse signal-to-noise ratio at the filter output is maximized. With this objective in mind, show that the optimum value of f_0 is $0.2/T$, for which the loss in signal-to-noise ratio compared to the matched filter is about 1 dB.

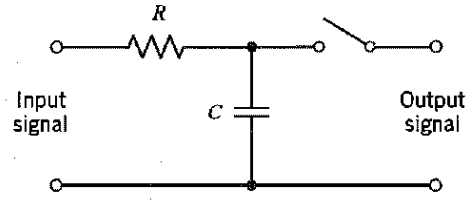

FIGURE P4.4

Probability of Error Calculation

4.5 The formula for the optimum threshold in the receiver of Figure 4.4 is, in general, given by Equation (4.37). Discuss, in graphical terms, how this optimum choice affects the

contributions of the two terms in Equation (4.35) for the average probability of symbol error P_e by considering the following two cases:

(a) $p_0 > p_1$

(b) $p_1 < p_0$

where p_0 and p_1 are the *a priori* probabilities of symbols 0 and 1, respectively.

4.6 In a binary PCM system, symbols 0 and 1 have *a priori probabilities* p_0 and p_1, respectively. The conditional probability density function of the random variable Y (with sample value y) obtained by sampling the matched filter output in the receiver of Figure 4.4 at the end of a signaling interval, given that symbol 0 was transmitted, is denoted by $f_Y(y|0)$. Similarly, $f_Y(y|1)$ denotes the conditional probability density function of Y, given that symbol 1 was transmitted. Let λ denote the threshold used in the receiver, so that if the sample value y exceeds λ, the receiver decides in favor of symbol 1; otherwise, it decides in favor of symbol 0. Show that the optimum threshold λ_{opt}, for which the average probability of error is a minimum, is given by the solution of

$$\frac{f_Y(\lambda_{opt}|1)}{f_Y(\lambda_{opt}|0)} = \frac{p_0}{p_1}$$

4.7 A binary PCM system using polar NRZ signaling operates just above the error threshold with an average probability of error equal to 10^{-6}. Suppose that the signaling rate is doubled. Find the new value of the average probability of error. You may use Table A6.6 to evaluate the complementary error function.

4.8 A continuous-time signal is sampled and then transmitted as a PCM signal. The random variable at the input of the decision device in the receiver has a variance of 0.01 volts^2.

(a) Assuming the use of polar NRZ signaling, determine the pulse amplitude that must be transmitted for the average error rate not to exceed 1 bit in 10^8 bits.

(b) If the added presence of interference causes the error rate to increase to 1 bit in 10^6 bits, what is the variance of the interference?

4.9 A binary PCM wave uses unipolar NRZ signaling to transmit symbols 1 and 0; symbol 1 is represented by a rectangular pulse of amplitude A and duration T_b. The channel noise is modeled as additive, white and Gaussian, with zero mean and power spectral density $N_0/2$. Assuming that symbols 1 and 0 occur with equal probability, find an expression for the average probability of error at the receiver output, using a matched filter as described in Section 4.3.

4.10 Repeat Problem 4.9 for the case of unipolar return-to-zero signaling, in which case symbol 1 is represented by a pulse of amplitude A and duration $T_b/2$ and symbol 0 is represented by transmitting no pulse.

Hence show that this unipolar type of signaling requires twice the average power of unipolar nonreturn-to-zero (i.e., on-off) signaling for the same average probability of symbol error.

4.11 In this problem, we revisit the PCM receiver of Figure 4.4, but this time we consider the use of bipolar nonreturn-to-zero signaling, in which case the transmitted signal $s(t)$ is defined by

Binary symbol 1: $s(t) = \pm A$ for $0 < t \leq T$

Binary symbol 0: $s(t) = 0$, $0 < t \leq T$

Determine the average probability of symbol error P_e for this receiver assuming that the binary symbols 0 and 1 are equiprobable.

Raised Cosine Spectrum

4.12 The nonreturn-to-zero pulse of Figure P4.12 may be viewed as a very crude form of a Nyquist pulse. Compare the spectral characteristics of these two pulses.

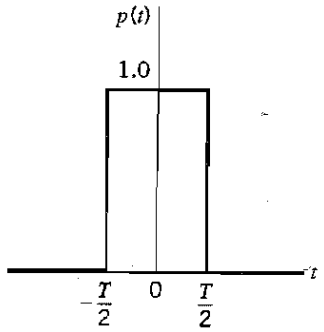

FIGURE P4.12

4.13 Determine the inverse Fourier transform of the frequency function $P(f)$ defined in Equation (4.60).

4.14 An analog signal is sampled, quantized, and encoded into a binary PCM wave. The specifications of the PCM system include the following:

Sampling rate = 8 kHz

Number of representation levels = 64

The PCM wave is transmitted over a baseband channel using discrete pulse-amplitude modulation. Determine the minimum bandwidth required for transmitting the PCM wave if each pulse is allowed to take on the following number of amplitude levels: 2, 4, or 8.

4.15 Consider a baseband binary PAM system that is designed to have a raised-cosine spectrum $P(f)$. The resulting pulse $p(t)$ is defined in Equation (4.62). How would this pulse be modified if the system was designed to have a linear phase response?

4.16 A computer puts out binary data at the rate of 56 kb/s. The computer output is transmitted using a baseband binary PAM system that is designed to have a raised-cosine spectrum. Determine the transmission bandwidth required for each of the following rolloff factors: $\alpha = 0.25, 0.5, 0.75, 1.0$.

4.17 Repeat Problem 4.16, given that each set of three successive binary digits in the computer output are coded into one of eight possible amplitude levels, and the resulting signal is transmitted using an eight-level PAM system designed to have a raised-cosine spectrum.

4.18 An analog signal is sampled, quantized, and encoded into a binary PCM wave. The number of representation levels used is 128. A synchronizing pulse is added at the end of each code word representing a sample of the analog signal. The resulting PCM wave is transmitted over a channel of bandwidth 12 kHz using a quaternary PAM system with raised-cosine spectrum. The rolloff factor is unity.

(a) Find the rate (b/s) at which information is transmitted through the channel.

(b) Find the rate at which the analog signal is sampled. What is the maximum possible value for the highest frequency component of the analog signal?

4.19 A binary PAM wave is to be transmitted over a baseband channel with an absolute maximum bandwidth of 75 kHz. The bit duration is 10 μs. Find a raised-cosine spectrum that satisfies these requirements.

Correlative-Level Coding

4.20 The duobinary, ternary, and bipolar signaling techniques have one common feature: They all employ three amplitude levels. In what way does the duobinary technique differ from the other two?

4.21 The binary data stream 001101001 is applied to the input of a duobinary system.

(a) Construct the duobinary coder output and corresponding receiver output, without a precoder.

(b) Suppose that owing to error during transmission, the level at the receiver input produced by the second digit is reduced to zero. Construct the new receiver output.

4.22 Repeat Problem 4.21, assuming the use of a precoder in the transmitter.

4.23 The scheme shown in Figure P4.23 may be viewed as a differential encoder (consisting of the modulo-2 adder and the 1-unit delay element) connected in cascade with a special form of correlative coder (consisting of the 1-unit delay element and summer). A single-delay element is shown in Figure P4.23 since it is common to both the differential encoder and the correlative coder. In this differential encoder, a transition is represented by symbol 0 and no transition by symbol 1.

(a) Find the frequency response and impulse response of the correlative coder part of the scheme shown in Figure P4.23.

(b) Show that this scheme may be used to convert the on–off representation of a binary sequence (applied to the input) into the bipolar representation of the sequence at the output. You may illustrate this conversion by considering the sequence 010001101.

For descriptions of on–off, bipolar, and differential encoding of binary sequences, see Section 3.7.

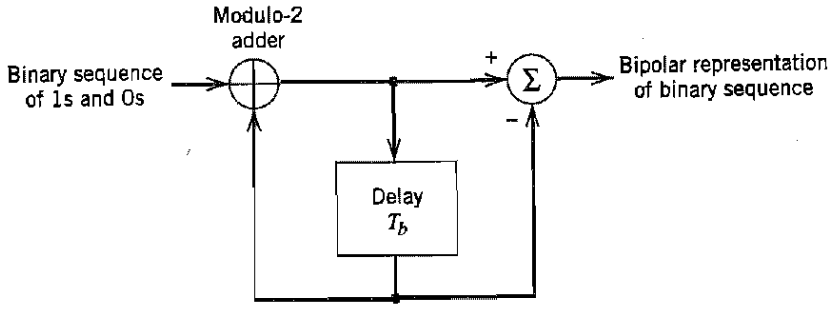

FIGURE P4.23

4.24 Consider a random binary wave $x(t)$ in which the 1s and 0s occur with equal probability, the symbols in adjacent time slots are statistically independent, and symbol 1 is represented by A volts and symbol 0 by zero volts. This on–off binary wave is applied to the circuit of Figure P4.23.

(a) Using the result of Problem 4.23, show that the power spectral density of the bipolar wave $y(t)$ appearing at the output of the circuit equals

$$S_X(f) = T_b A^2 \sin^2(\pi f T_b) \operatorname{sinc}^2(f T_b)$$

(b) Plot the power spectral densities of the on–off and bipolar binary waves, and compare them.

4.25 The binary data stream 011100101 is applied to the input of a modified duobinary system.

(a) Construct the modified duobinary coder output and corresponding receiver output, without a precoder.

(b) Suppose that due to error during transmission, the level produced by the third digit is reduced to zero. Construct the new receiver output.

4.26 Repeat Problem 4.25 assuming the use of a precoder in the transmitter.

M-ary PAM Systems

4.27 Consider a baseband M-ary system using M discrete amplitude levels. The receiver model is as shown in Figure P4.27, the operation of which is governed by the following assumptions:

4.31 In this problem we use the LMS algorithm to formulate an adaptive echo canceller for use in a digital subscriber line. The basic principle of adaptive echo cancellation is to synthesize a replica of the echo and subtract it from the returned signal in an adaptive manner, as illustrated in Figure P4.31. The synthesized echo, denoted by $\hat{r}[n]$, is generated by passing the transmitted signal through an adaptive filter that ideally matches the transfer function of the echo path. The returned signal, consisting of the sum of actual echo $r[n]$ and the received signal $x[n]$, may be viewed as the desired response for the adaptive filtering process.

Using the LMS algorithm, formulate the equations that define the operation of the adaptive echo canceller in Figure P4.31.

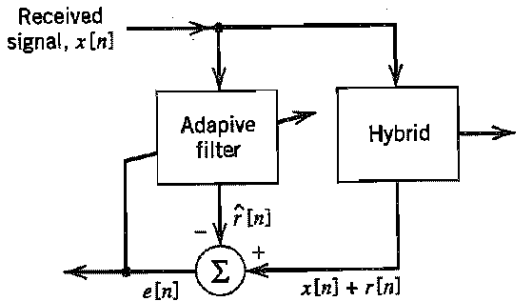

FIGURE P4.31

Equalization

4.32 Figure P4.32 shows the cascade connection of a linear channel and a synchronous tapped-delay-line equalizer. The impulse response of the channel is denoted by $c(t)$, and that of the equalizer is denoted by $h(t)$. The $h(t)$ is defined by

$$h(t) = \sum_{k=-N}^{N} w_k \, \delta(t - kT)$$

where T is the spacing between adjacent taps of the equalizer, and the w_k are its tap-weights (coefficients). The impulse response of the cascaded system of Figure P4.32 is denoted by $p(t)$. The $p(t)$ is sampled uniformly at the rate $1/T$. To eliminate intersymbol interference, we require that the Nyquist criterion for distortionless transmission be satisfied, as shown by

$$p(nT) = \begin{cases} 1, & n = 0 \\ 0, & n \neq 0 \end{cases}$$

(a) By imposing this condition, show that the $(2N + 1)$ tap-weights of the resulting zero-forcing equalizer satisfy the following set of $(2N + 1)$ simultaneous equations:

$$\sum_{k=-N}^{N} w_k c_{n-k} = \begin{cases} 1, & n = 0 \\ 0, & n \neq \pm 1, \pm 2, \ldots, \pm N \end{cases}$$

where $c_n = c(nT)$. Hence, show that the zero-forcing equalizer is an *inverse filter* in that its transfer function is equal to the reciprocal of the transfer function of the channel.

(b) A shortcoming of the zero-forcing equalizer is *noise enhancement* that can result in poor performance in the presence of channel noise. To explore this phenomenon, consider a low-pass channel with a notch at the Nyquist frequency, that is, $H(f)$ is zero at $f = 1/2T$. Assuming that the channel noise is additive and white, show that the power spectral density of the noise at the equalizer output approaches infinity at $f = 1/2T$.

CHAPTER 5

SIGNAL-SPACE ANALYSIS

This chapter discusses some basic issues that pertain to the transmission of signals over an additive white Gaussian noise (AWGN) channel. Specifically, it addresses the following topics:

- *Geometric representation of signals with finite energy, which provides a mathematically elegant and highly insightful tool for the study of data transmission.*
- *Maximum likelihood procedure for the detection of a signal in AWGN channel.*
- *Derivation of the correlation receiver that is equivalent to the matched filter receiver discussed in the previous chapter.*
- *Probability of symbol error and the union bound for its approximate calculation.*

The material presented herein naturally leads to the study of passband data transmission covered in Chapter 6.

5.1 Introduction

Consider the most basic form of a digital communication system depicted in Figure 5.1. A *message source* emits one *symbol* every T seconds, with the symbols belonging to an alphabet of M symbols denoted by $m_1, m_2, \ldots, m_M$. Consider, for example, the remote connection of two digital computers, with one computer acting as an information source that calculates digital outputs based on observations and inputs fed into it. The resulting computer output is expressed as a sequence of 0s and 1s, which are transmitted to a second computer over a communication channel. In this case, the alphabet consists simply of two binary symbols: 0 and 1. A second example is that of a quaternary PCM encoder with an alphabet consisting of four possible symbols: 00, 01, 10, and 11. In any event, the *a priori* probabilities $p_1, p_2, \ldots, p_M$ specify the message source output. In the absence of prior information, it is customary to assume that the M symbols of the alphabet are *equally likely*. Then we may express the probability that symbol m_i is emitted by the source as

$$\begin{aligned} p_i &= P(m_i) \\ &= \frac{1}{M} \text{ for } i = 1, 2, \ldots, M \end{aligned} \tag{5.1}$$

The transmitter takes the message source output m_i and codes it into a *distinct* signal $s_i(t)$ suitable for transmission over the channel. The signal $s_i(t)$ occupies the full duration T allotted to symbol m_i. Most important, $s_i(t)$ is a real-valued *energy signal* (i.e., a signal with finite energy), as shown by

$$E_i = \int_0^T s_i^2(t)\, dt, \qquad i = 1, 2, \ldots, M \tag{5.2}$$

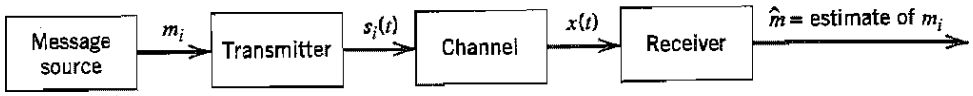

FIGURE 5.1 Block diagram of a generic digital communication system.

The channel is assumed to have two characteristics:

1. The channel is *linear*, with a bandwidth that is wide enough to accommodate the transmission of signal $s_i(t)$ with negligible or no distortion.
2. The channel noise, $w(t)$, is the sample function of a *zero-mean white Gaussian noise process*. The reasons for this second assumption are that it makes receiver calculations tractable, and it is a reasonable description of the type of noise present in many practical communication systems.

We refer to such a channel as an *additive white Gaussian noise* (AWGN) *channel*. Accordingly, we may express the *received signal* $x(t)$ as

$$x(t) = s_i(t) + w(t), \qquad \begin{cases} 0 \le t \le T \\ i = 1, 2, \ldots, M \end{cases} \tag{5.3}$$

and thus model the channel as in Figure 5.2.

The receiver has the task of observing the received signal $x(t)$ for a duration of T seconds and making a best *estimate* of the transmitted signal $s_i(t)$ or, equivalently, the symbol m_i. However, owing to the presence of channel noise, this decision-making process is statistical in nature, with the result that the receiver will make occasional errors. The requirement is therefore to design the receiver so as to minimize the *average probability of symbol error*, defined as

$$P_e = \sum_{i=1}^{M} p_i P(\hat{m} \neq m_i \,|m_i) \tag{5.4}$$

where m_i is the transmitted symbol, $\hat{m}$ is the estimate produced by the receiver, and $P(\hat{m} \neq m_i \,|m_i)$ is the conditional error probability given that the ith symbol was sent. The resulting receiver is said to be *optimum in the minimum probability of error* sense.

This model provides a basis for the design of the optimum receiver, for which we will use geometric representation of the known set of transmitted signals, $\{s_i(t)\}$. This method, discussed in Section 5.2, provides a great deal of insight, with considerable simplification of detail.

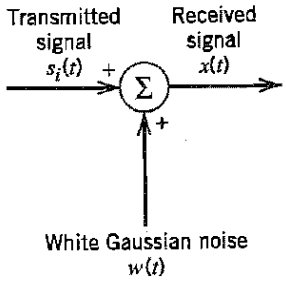

FIGURE 5.2 Additive white Gaussian noise (AWGN) model of a channel.

5.2 Geometric Representation of Signals

The essence of *geometric representation of signals*[1] is to represent any set of M energy signals $\{s_i(t)\}$ as linear combinations of N *orthonormal basis functions*, where $N \leq M$. That is to say, given a set of real-valued energy signals $s_1(t), s_2(t), \ldots, s_M(t)$, each of duration T seconds, we write

$$s_i(t) = \sum_{j=1}^{N} s_{ij}\phi_j(t), \qquad \begin{cases} 0 \leq t \leq T \\ i = 1, 2, \ldots, M \end{cases} \tag{5.5}$$

where the coefficients of the expansion are defined by

$$s_{ij} = \int_0^T s_i(t)\phi_j(t)\, dt, \qquad \begin{cases} i = 1, 2, \ldots, M \\ j = 1, 2, \ldots, N \end{cases} \tag{5.6}$$

The real-valued basis functions $\phi_1(t), \phi_2(t), \ldots, \phi_N(t)$ are *orthonormal*, by which we mean

$$\int_0^T \phi_i(t)\phi_j(t)\, dt = \delta_{ij} = \begin{cases} 1 \text{ if } i = j \\ 0 \text{ if } i \neq j \end{cases} \tag{5.7}$$

where δ_{ij} is the *Kronecker delta*. The first condition of Equation (5.7) states that each basis function is *normalized* to have unit energy. The second condition states that the basis functions $\phi_1(t), \phi_2(t), \ldots, \phi_N(t)$ are *orthogonal* with respect to each other over the interval $0 \leq t \leq T$.

The set of coefficients $\{s_{ij}\}_{j=1}^N$ may naturally be viewed as an *N-dimensional vector*, denoted by $\mathbf{s}_i$. The important point to note here is that the vector $\mathbf{s}_i$ bears a *one-to-one* relationship with the transmitted signal $s_i(t)$:

- Given the N elements of the vectors $\mathbf{s}_i$ (i.e., $s_{i1}, s_{i2}, \ldots, s_{iN}$) operating as input, we may use the scheme shown in Figure 5.3*a* to generate the signal $s_i(t)$, which follows

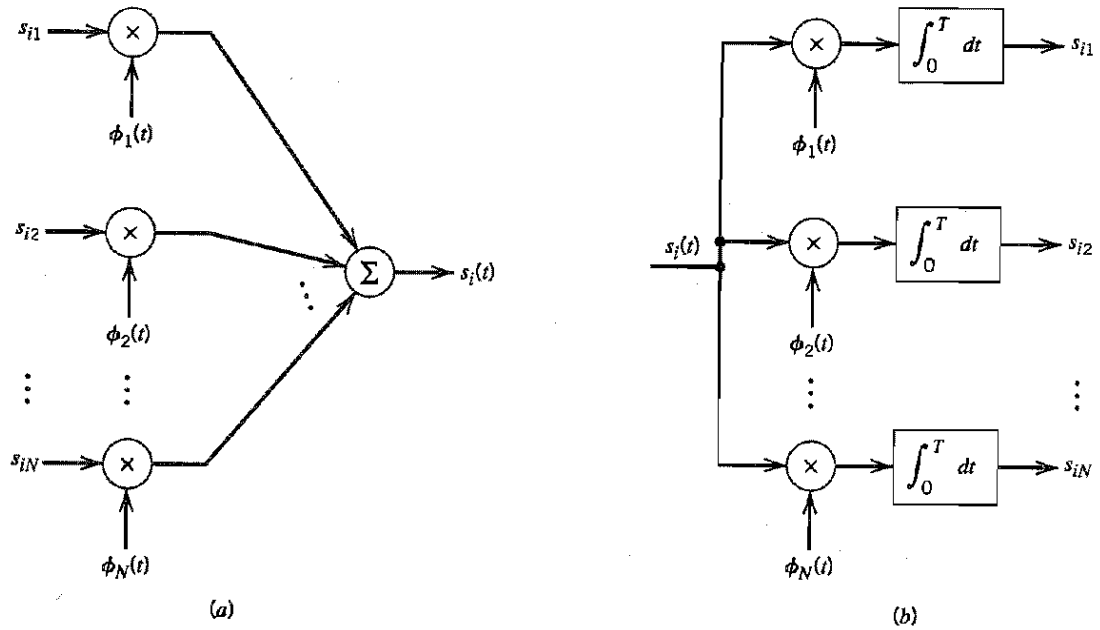

FIGURE 5.3 (*a*) Synthesizer for generating the signal $s_i(t)$. (*b*) Analyzer for generating the set of signal vectors $\{s_i\}$.

directly from Equation (5.5). It consists of a bank of N multipliers, with each multiplier having its own basis function, followed by a summer. This scheme may be viewed as a *synthesizer*.

- Conversely, given the signals $s_i(t)$, $i = 1, 2, \ldots, M$, operating as input, we may use the scheme shown in Figure 5.3*b* to calculate the coefficients $s_{i1}, s_{i2}, \ldots, s_{iN}$ which follows directly from Equation (5.6). This second scheme consists of a bank of N *product-integrators* or *correlators* with a common input, and with each one of them supplied with its own basis function. The scheme of Figure 5.3*b* may be viewed as an *analyzer*.

Accordingly, we may state that each signal in the set $\{s_i(t)\}$ is completely determined by the *vector* of its coefficients

$$\mathbf{s}_i = \begin{bmatrix} s_{i1} \\ s_{i2} \\ \vdots \\ s_{iN} \end{bmatrix}, \qquad i = 1, 2, \ldots, M \tag{5.8}$$

The vector $\mathbf{s}_i$ is called a *signal vector*. Furthermore, if we conceptually extend our conventional notion of two- and three-dimensional Euclidean spaces to an *N-dimensional Euclidean space*, we may visualize the set of signal vectors $\{\mathbf{s}_i \mid i = 1, 2, \ldots, M\}$ as defining a corresponding set of M points in an N-dimensional Euclidean space, with N mutually perpendicular axes labeled $\phi_1, \phi_2, \ldots, \phi_N$. This N-dimensional Euclidean space is called the *signal space*.

The idea of visualizing a set of energy signals geometrically, as just described, is of profound importance. It provides the mathematical basis for the geometric representation of energy signals, thereby paving the way for the noise analysis of digital communication systems in a conceptually satisfying manner. This form of representation is illustrated in Figure 5.4 for the case of a two-dimensional signal space with three signals, that is, $N = 2$ and $M = 3$.

In an N-dimensional Euclidean space, we may define *lengths* of vectors and *angles* between vectors. It is customary to denote the length (also called the *absolute value* or *norm*) of a signal vector $\mathbf{s}_i$ by the symbol $\| \mathbf{s}_i \|$. The squared-length of any signal vector $\mathbf{s}_i$ is defined to be the *inner product* or *dot product* of $\mathbf{s}_i$ with itself, as shown by

$$\begin{aligned} \| \mathbf{s}_i \|^2 &= \mathbf{s}_i^T \mathbf{s}_i \\ &= \sum_{j=1}^{N} s_{ij}^2, \qquad i = 1, 2, \ldots, M \end{aligned} \tag{5.9}$$

where s_{ij} is the jth element of $\mathbf{s}_i$, and the superscript T denotes matrix transposition.

There is an interesting relationship between the energy content of a signal and its representation as a vector. By definition, the energy of a signal $s_i(t)$ of duration T seconds is

$$E_i = \int_0^T s_i^2(t)\, dt \tag{5.10}$$

Therefore, substituting Equation (5.5) into (5.10), we get

$$E_i = \int_0^T \left[\sum_{j=1}^{N} s_{ij} \phi_j(t) \right] \left[\sum_{k=1}^{N} s_{ik} \phi_k(t) \right] dt$$

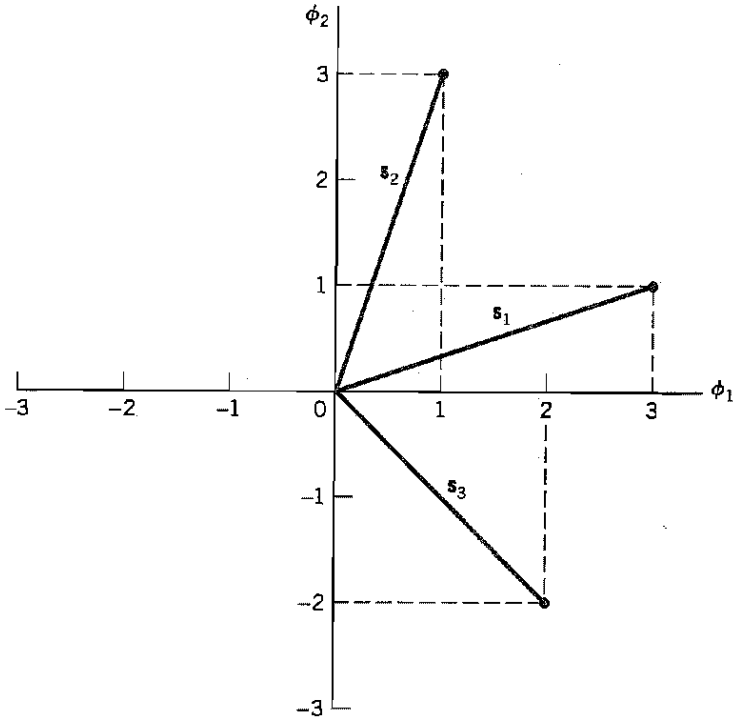

FIGURE 5.4 Illustrating the geometric representation of signals for the case when $N = 2$ and $M = 3$.

Interchanging the order of summation and integration, and then rearranging terms, we get

$$E_i = \sum_{j=1}^{N} \sum_{k=1}^{N} s_{ij} s_{ik} \int_0^T \phi_j(t)\phi_k(t)dt \tag{5.11}$$

But since the $\phi_j(t)$ form an orthonormal set, in accordance with the two conditions of Equation (5.7), we find that Equation (5.11) reduces simply to

$$\begin{aligned} E_i &= \sum_{j=1}^{N} s_{ij}^2 \\ &= \| \mathbf{s}_i \|^2 \end{aligned} \tag{5.12}$$

Thus Equations (5.9) and (5.12) show that the energy of a signal $s_i(t)$ is equal to the squared length of the signal vector $\mathbf{s}_i(t)$ representing it.

In the case of a pair of signals $s_i(t)$ and $s_k(t)$, represented by the signal vectors $\mathbf{s}_i$ and $\mathbf{s}_k$, respectively, we may also show that

$$\int_0^T s_i(t)s_k(t)\, dt = \mathbf{s}_i^T \mathbf{s}_k \tag{5.13}$$

Equation (5.13) states that the *inner product* of the signals $s_i(t)$ and $s_k(t)$ over the interval $[0, T]$, using their time-domain representations, is equal to the inner product of their respective vector representations $\mathbf{s}_i$ and $\mathbf{s}_k$. Note that the inner product of $s_i(t)$ and $s_k(t)$ is *invariant* to the choice of basis functions $\{\phi_j(t)\}_{j=1}^N$ in that it only depends on the components of the signals $s_i(t)$ and $s_k(t)$ projected onto each of the basis functions.

Yet another useful relation involving the vector representations of the signals $s_i(t)$ and $s_k(t)$ is described by

$$\begin{aligned} \| \mathbf{s}_i - \mathbf{s}_k \|^2 &= \sum_{j=1}^{N} (s_{ij} - s_{kj})^2 \\ &= \int_0^T (s_i(t) - s_k(t))^2 dt \end{aligned} \tag{5.14}$$

where $\| \mathbf{s}_i - \mathbf{s}_k \|$ is the *Euclidean distance*, d_{ik}, between the points represented by the signal vectors $\mathbf{s}_i$ and $\mathbf{s}_k$.

To complete the geometric representation of energy signals, we need to have a representation for the angle θ_{ik} subtended between two signal vectors $\mathbf{s}_i$ and $\mathbf{s}_k$. By definition, the *cosine of the angle* θ_{ik} is equal to the inner product of these two vectors divided by the product of their individual norms, as shown by

$$\cos \theta_{ik} = \frac{\mathbf{s}_i^T \mathbf{s}_k}{\| \mathbf{s}_i \| \, \| \mathbf{s}_k \|} \tag{5.15}$$

The two vectors $\mathbf{s}_i$ and $\mathbf{s}_k$ are thus *orthogonal* or *perpendicular* to each other if their inner product $\mathbf{s}_i^T \mathbf{s}_k$ is zero, in which case $\theta_{ik} = 90$ degrees; this condition is intuitively satisfying.

▶ EXAMPLE 5.1 Schwarz Inequality

Consider any pair of energy signals $s_1(t)$ and $s_2(t)$. The *Schwarz inequality* states that

$$\left(\int_{-\infty}^{\infty} s_1(t) s_2(t) dt \right)^2 \leq \left(\int_{-\infty}^{\infty} s_1^2(t) dt \right) \left(\int_{-\infty}^{\infty} s_2^2(t) dt \right) \tag{5.16}$$

The equality holds if and only if $s_2(t) = cs_1(t)$, where c is any constant.

To prove this important inequality, let $s_1(t)$ and $s_2(t)$ be expressed in terms of the pair of orthonormal basis functions $\phi_1(t)$ and $\phi_2(t)$ as follows:

$$\begin{aligned} s_1(t) &= s_{11}\phi_1(t) + s_{12}\phi_2(t) \\ s_2(t) &= s_{21}\phi_1(t) + s_{22}\phi_2(t) \end{aligned}$$

where $\phi_1(t)$ and $\phi_2(t)$ satisfy the orthonormality conditions over the entire time interval $(-\infty, \infty)$:

$$\int_{-\infty}^{\infty} \phi_i(t)\phi_j(t) dt = \delta_{ij} = \begin{cases} 1 & \text{for } j = i \\ 0 & \text{otherwise} \end{cases}$$

On this basis, we may represent the signals $s_1(t)$ and $s_2(t)$ by the following respective pair of vectors, as illustrated in Figure 5.5:

$$\begin{aligned} \mathbf{s}_1 &= \begin{bmatrix} s_{11} \\ s_{12} \end{bmatrix} \\ \mathbf{s}_2 &= \begin{bmatrix} s_{21} \\ s_{22} \end{bmatrix} \end{aligned}$$

From Figure 5.5 we readily see that angle θ subtended between the vectors $\mathbf{s}_1$ and $\mathbf{s}_2$ is

$$\begin{aligned} \cos \theta &= \frac{\mathbf{s}_1^T \mathbf{s}_2}{\| \mathbf{s}_1 \| \, \| \mathbf{s}_2 \|} \\ &= \frac{\int_{-\infty}^{\infty} s_1(t) s_2(t) dt}{\left(\int_{-\infty}^{\infty} s_1^2(t) dt \right)^{1/2} \left(\int_{-\infty}^{\infty} s_2^2(t) dt \right)^{1/2}} \end{aligned} \tag{5.17}$$

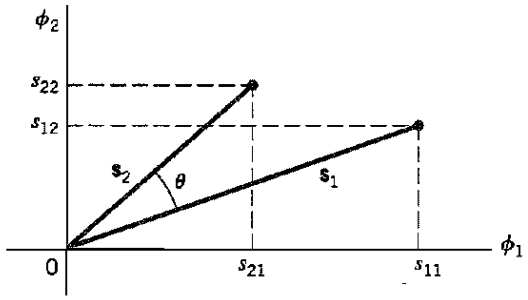

FIGURE 5.5 Vector representations of signals $s_1(t)$ and $s_2(t)$, providing the background picture for proving the Schwarz inequality.

where we have made use of Equations (5.15), (5.13) and (5.9). Recognizing that $|\cos\theta| \leq 1$, the Schwarz inequality of Equation (5.16) immediately follows from Equation (5.17). Moreover, from the first line of Equation (5.17) we note that $|\cos\theta| = 1$ if and only if $\mathbf{s}_2 = c\mathbf{s}_1$, that is, $s_2(t) = cs_1(t)$, where c is an arbitrary constant.

The proof of the Schwarz inequality, as presented here, applies to real-valued signals. It may be readily extended to complex-valued signals, in which case Equation (5.16) is reformulated as

$$\left|\int_{-\infty}^{\infty} s_1(t)s_2^*(t)dt\right|^2 \leq \left(\int_{-\infty}^{\infty} |s_1(t)|^2 dt\right)\left(\int_{-\infty}^{\infty} |s_2(t)|^2 dt\right) \tag{5.18}$$

where the equality holds if and only if $s_2(t) = cs_1(t)$, where c is a constant; see Problem 5.9. It is the complex form of the Schwarz inequality that was used in Chapter 4 to derive the matched filter. ◀

■ GRAM-SCHMIDT ORTHOGONALIZATION PROCEDURE

Having demonstrated the elegance of the geometric representation of energy signals, how do we justify it in mathematical terms? The answer lies in the *Gram-Schmidt orthogonalization procedure*, for which we need a *complete orthonormal set of basis functions*. To proceed with the formulation of this procedure, suppose we have a set of M energy signals denoted by $s_1(t), s_2(t), \ldots, s_M(t)$. Starting with $s_1(t)$ chosen from this set arbitrarily, the first basis function is defined by

$$\phi_1(t) = \frac{s_1(t)}{\sqrt{E_1}} \tag{5.19}$$

where E_1 is the energy of the signal $s_1(t)$. Then, clearly, we have

$$\begin{aligned} s_1(t) &= \sqrt{E_1}\phi_1(t) \\ &= s_{11}\phi_1(t) \end{aligned} \tag{5.20}$$

where the coefficient $s_{11} = \sqrt{E_1}$ and $\phi_1(t)$ has unit energy, as required.

Next, using the signal $s_2(t)$, we define the coefficient s_{21} as

$$s_{21} = \int_0^T s_2(t)\phi_1(t)dt \tag{5.21}$$

We may thus introduce a new intermediate function

$$g_2(t) = s_2(t) - s_{21}\phi_1(t) \tag{5.22}$$

which is orthogonal to $\phi_1(t)$ over the interval $0 \le t \le T$ by virtue of Equation (5.21) and the fact that the basis function $\phi_1(t)$ has unit energy. Now, we are ready to define the second basis function as

$$\phi_2(t) = \frac{g_2(t)}{\sqrt{\int_0^T g_2^2(t)dt}} \tag{5.23}$$

Substituting Equation (5.22) into (5.23) and simplifying, we get the desired result

$$\phi_2(t) = \frac{s_2(t) - s_{21}\phi_1(t)}{\sqrt{E_2 - s_{21}^2}} \tag{5.24}$$

where E_2 is the energy of the signal $s_2(t)$. It is clear from Equation (5.23) that

$$\int_0^T \phi_2^2(t)dt = 1$$

and from Equation (5.24) that

$$\int_0^T \phi_1(t)\phi_2(t)dt = 0$$

That is to say, $\phi_1(t)$ and $\phi_2(t)$ form an orthonormal pair, as required.

Continuing in this fashion, we may in general define

$$g_i(t) = s_i(t) - \sum_{j=1}^{i-1} s_{ij}\phi_j(t) \tag{5.25}$$

where the coefficients s_{ij} are themselves defined by

$$s_{ij} = \int_0^T s_i(t)\phi_j(t)dt, \qquad j = 1, 2, \ldots, i-1 \tag{5.26}$$

Equation (5.22) is a special case of Equation (5.25) with $i = 2$. Note also that for $i = 1$, the function $g_i(t)$ reduces to $s_i(t)$.

Given the $g_i(t)$, we may now define the set of basis functions

$$\phi_i(t) = \frac{g_i(t)}{\sqrt{\int_0^T g_i^2(t)dt}}, \qquad i = 1, 2, \ldots, N \tag{5.27}$$

which form an orthonormal set. The dimension N is less than or equal to the number of given signals, M, depending on one of two possibilities:

- The signals $s_1(t), s_2(t), \ldots, s_M(t)$ form a *linearly independent set*, in which case $N = M$.
- The signals $s_1(t), s_2(t), \ldots, s_M(t)$ are *not* linearly independent, in which case $N < M$, and the intermediate function $g_i(t)$ is zero for $i > N$.

TABLE 5.1 *Amplitude Levels of the 2B1Q Code*

Signal		Gray code
Symbol	*Amplitude*	
$s_1(t)$	−3	00
$s_2(t)$	−1	01
$s_3(t)$	+1	11
$s_4(t)$	+3	10

Note that the conventional Fourier series expansion of a periodic signal is an example of a particular expansion of the type described herein. Also, the representation of a band-limited signal in terms of its samples taken at the Nyquist rate may be viewed as another sample of a particular expansion of this type. However, two important distinctions should be made:

1. The form of the basis functions $\phi_1(t), \phi_2(t), \ldots, \phi_N(t)$ has not been specified. That is to say, unlike the Fourier series expansion of a periodic signal or the sampled representation of a band-limited signal, we have not restricted the Gram-Schmidt orthogonalization procedure to be in terms of sinusoidal functions or sinc functions of time.
2. The expansion of the signal $s_i(t)$ in terms of a finite number of terms is not an approximation wherein only the first N terms are significant but rather an *exact* expression where N and only N terms are significant.

▶ EXAMPLE 5.2 2B1Q Code

The 2B1Q code was described in Chapter 4 as the North American line code for digital subscriber lines. It represents a quaternary PAM signal as shown in the Gray-encoded alphabet of Table 5.1. The four possible signals, $s_1(t)$, $s_2(t)$, $s_3(t)$, and $s_4(t)$, are amplitude-scaled versions of a Nyquist pulse. Each signal represents a dibit. We wish to find the vector representation of the 2B1Q code.

This example is simple enough for us to solve it by inspection. Let $\phi_1(t)$ denote the Nyquist pulse, normalized to have unit energy. The $\phi_1(t)$ so defined is the only basis function for the vector representation of the 2B1Q code. Accordingly, the signal-space representation of this code is as shown in Figure 5.6. It consists of four signal vectors s_1, s_2, s_3, and s_4, which are located on the ϕ_1-axis in a symmetric manner about the origin. In this example, we thus have $M = 4$ and $N = 1$.

We may generalize the result depicted in Figure 5.6 for the 2B1Q code as follows. The signal-space diagram of an M-ary pulse-amplitude modulated signal, in general, is one-dimensional with M signal points uniformly positioned on the only axis of the diagram. ◀

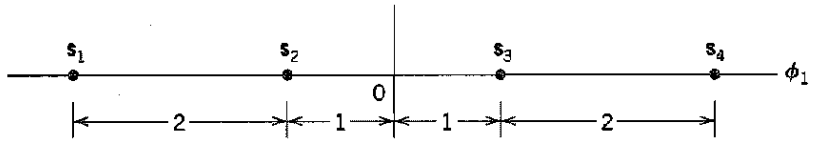

FIGURE 5.6 Signal-space representation of the 2B1Q code.

5.3 Conversion of the Continuous AWGN Channel into a Vector Channel

Suppose that the input to the bank of N product integrators or correlators in Figure 5.3*b* is not the transmitted signal $s_i(t)$ but rather the received signal $x(t)$ defined in accordance with the idealized AWGN channel of Figure 5.2. That is to say,

$$x(t) = s_i(t) + w(t), \qquad \begin{cases} 0 \le t \le T \\ i = 1, 2, \ldots, M \end{cases} \tag{5.28}$$

where $w(t)$ is a sample function of a white Gaussian noise process $W(t)$ of zero mean and power spectral density $N_0/2$. Correspondingly, we find that the output of correlator j, say, is the sample value of a random variable X_j, as shown by

$$\begin{aligned} x_j &= \int_0^T x(t)\phi_j(t)dt \\ &= s_{ij} + w_j, \qquad j = 1, 2, \ldots, N \end{aligned} \tag{5.29}$$

The first component, s_{ij}, is a deterministic quantity contributed by the transmitted signal $s_i(t)$; it is defined by

$$s_{ij} = \int_0^T s_i(t)\phi_j(t)dt \tag{5.30}$$

The second component, w_j, is the sample value of a random variable W_j that arises because of the presence of the channel noise $w(t)$; it is defined by

$$w_j = \int_0^T w(t)\phi_j(t)dt \tag{5.31}$$

Consider next a new random process $X'(t)$ whose sample function $x'(t)$ is related to the received signal $x(t)$ as follows:

$$x'(t) = x(t) - \sum_{j=1}^{N} x_j\phi_j(t) \tag{5.32}$$

Substituting Equations (5.28) and (5.29) into (5.32), and then using the expansion of Equation (5.5), we get

$$\begin{aligned} x'(t) &= s_i(t) + w(t) - \sum_{j=1}^{N} (s_{ij} + w_j)\phi_j(t) \\ &= w(t) - \sum_{j=1}^{N} w_j\phi_j(t) \\ &= w'(t) \end{aligned} \tag{5.33}$$

The sample function $x'(t)$ therefore depends solely on the channel noise $w(t)$. On the basis of Equations (5.32) and (5.33), we may thus express the received signal as

$$\begin{aligned} x(t) &= \sum_{j=1}^{N} x_j\phi_j(t) + x'(t) \\ &= \sum_{j=1}^{N} x_j\phi_j(t) + w'(t) \end{aligned} \tag{5.34}$$

Accordingly, we may view $w'(t)$ as a sort of *remainder* term that must be included on the right to preserve the equality in Equation (5.34). It is informative to contrast the expansion

of the received signal $x(t)$ given in Equation (5.34) with the corresponding expansion of the transmitted signal $s_i(t)$ given in Equation (5.5). The latter expansion is entirely deterministic, whereas that of Equation (5.34) is random (stochastic), which is to be expected.

Statistical Characterization of the Correlator Outputs

We now wish to develop a statistical characterization of the set of N correlator outputs. Let $X(t)$ denote the random process, a sample function of which is represented by the received signal $x(t)$. Correspondingly, let X_j denote the random variable whose sample value is represented by the correlator output x_j, $j = 1, 2, \ldots, N$. According to the AWGN model of Figure 5.2, the random process $X(t)$ is a Gaussian process. It follows therefore that X_j is a Gaussian random variable for all j (see Property 1 of a Gaussian process, Section 1.8). Hence, X_j is characterized completely by its mean and variance, which are determined next.

Let W_j denote the random variable represented by the sample value w_j produced by the jth correlator in response to the white Gaussian noise component $w(t)$. The random variable W_j has zero mean, because the noise process $W(t)$ represented by $w(t)$ in the AWGN model of Figure 5.2 has zero mean by definition. Consequently, the mean of X_j depends only on s_{ij}, as shown by

$$\begin{aligned} \mu_{X_j} &= E[X_j] \\ &= E[s_{ij} + W_j] \\ &= s_{ij} + E[W_j] \\ &= s_{ij} \end{aligned} \tag{5.35}$$

To find the variance of X_j, we note that

$$\begin{aligned} \sigma_{X_j}^2 &= \text{var}[X_j] \\ &= E[(X_j - s_{ij})^2] \\ &= E[W_j^2] \end{aligned} \tag{5.36}$$

where the last line follows from Equation (5.29) with x_j and w_j replaced by X_j and W_j, respectively. According to Equation (5.31), the random variable W_j is defined by

$$W_j = \int_0^T W(t)\phi_j(t)dt$$

We may therefore expand Equation (5.36) as follows:

$$\begin{aligned} \sigma_{X_j}^2 &= E\left[\int_0^T W(t)\phi_j(t)dt \int_0^T W(u)\phi_j(u)du\right] \\ &= E\left[\int_0^T \int_0^T \phi_j(t)\phi_j(u)W(t)W(u)dtdu\right] \end{aligned} \tag{5.37}$$

Interchanging the order of integration and expectation:

$$\begin{aligned} \sigma_{X_j}^2 &= \int_0^T \int_0^T \phi_j(t)\phi_j(u)E[W(t)W(u)]dtdu \\ &= \int_0^T \int_0^T \phi_j(t)\phi_j(u)R_W(t, u)dtdu \end{aligned} \tag{5.38}$$

where $R_W(t, u)$ is the autocorrelation function of the noise process $W(t)$. Since this noise is stationary, $R_W(t, u)$ depends only on the time difference $t - u$. Furthermore, since the noise $W(t)$ is white with a constant power spectral density $N_0/2$, we may express $R_W(t, u)$ as follows [see Equation (1.95)]:

$$R_W(t, u) = \frac{N_0}{2}\,\delta(t - u) \tag{5.39}$$

Therefore, substituting Equation (5.39) into (5.38), and then using the sifting property of the delta function $\delta(t)$, we get

$$\begin{aligned}\sigma_{X_j}^2 &= \frac{N_0}{2}\int_0^T\int_0^T \phi_j(t)\phi_j(u)\,\delta(t - u)dtdu \\ &= \frac{N_0}{2}\int_0^T \phi_j^2(t)dt\end{aligned} \tag{5.40}$$

Since the $\phi_j(t)$ have unit energy, by definition, we finally get the simple result

$$\sigma_{X_j}^2 = \frac{N_0}{2} \qquad \text{for all } j \tag{5.41}$$

This important result shows that all the correlator outputs denoted by X_j with $j = 1, 2, \ldots, N$, have a variance equal to the power spectral density $N_0/2$ of the noise process $W(t)$.

Moreover, since the $\phi_j(t)$ form an orthogonal set, we find that the X_j are mutually uncorrelated, as shown by

$$\begin{aligned}\text{cov}[X_jX_k] &= E[(X_j - \mu_{X_j})(X_k - \mu_{X_k})] \\ &= E[(X_j - s_{ij})(X_k - s_{ik})] \\ &= E[W_jW_k] \\ &= E\left[\int_0^T W(t)\phi_j(t)dt \int_0^T W(u)\phi_k(u)du\right] \\ &= \int_0^T\int_0^T \phi_j(t)\phi_k(u)R_W(t, u)dtdu \\ &= \frac{N_0}{2}\int_0^T\int_0^T \phi_j(t)\phi_k(u)\,\delta(t - u)dtdu \\ &= \frac{N_0}{2}\int_0^T \phi_j(t)\phi_k(t)dt \\ &= 0, \qquad j \neq k\end{aligned} \tag{5.42}$$

Since the X_j are Gaussian random variables, Equation (5.42) implies that they are also statistically independent (see Property 4 of a Gaussian Process, Section 1.8).

Define the vector of N random variables

$$\mathbf{X} = \begin{bmatrix} X_1 \\ X_2 \\ \vdots \\ X_N \end{bmatrix} \tag{5.43}$$

whose elements are independent Gaussian random variables with mean values equal to s_{ij} and variances equal to $N_0/2$. Since the elements of the vector $\mathbf{X}$ are statistically indepen-

dent, we may express the conditional probability density function of the vector **X**, given that the signal $s_i(t)$ or correspondingly the symbol m_i was transmitted, as the product of the conditional probability density functions of its individual elements as shown by

$$f_{\mathbf{X}}(\mathbf{x}|m_i) = \prod_{j=1}^{N} f_{X_j}(x_j|m_i), \qquad i = 1, 2, \ldots, M \tag{5.44}$$

where the vector $\mathbf{x}$ and scalar x_j are sample values of the random vector **X** and random variable X_j, respectively. The vector $\mathbf{x}$ is called the *observation vector*; correspondingly, x_i is called an *observable element*. Any channel that satisfies Equation (5.44) is called a *memoryless channel*.

Since each X_j is a Gaussian random variable with mean s_{ij} and variance $N_0/2$, we have

$$f_{X_j}(x_j|m_i) = \frac{1}{\sqrt{\pi N_0}} \exp\left[-\frac{1}{N_0}(x_j - s_{ij})^2\right], \qquad \begin{matrix} j = 1, 2, \ldots, N \\ i = 1, 2, \ldots, M \end{matrix} \tag{5.45}$$

Therefore, substituting Equation (5.45) into (5.44) yields

$$f_{\mathbf{X}}(\mathbf{x}|m_i) = (\pi N_0)^{-N/2} \exp\left[-\frac{1}{N_0}\sum_{j=1}^{N}(x_j - s_{ij})^2\right], \qquad i = 1, 2, \ldots, M \tag{5.46}$$

It is now clear that the elements of the random vector **X** completely characterize the summation term $\Sigma_j X_j \phi_j(t)$, whose sample value is represented by the first term in Equation (5.34). However, there remains the noise term $w'(t)$ in this equation, which depends only on the channel noise $w(t)$. Since the noise process $W(t)$ represented by $w(t)$ is Gaussian with zero mean, it follows that the noise process $W'(t)$ represented by the sample function $w'(t)$ is also a zero-mean Gaussian process. Finally, we note that any random variable $W'(t_k)$, say, derived from the noise process $W'(t)$ by sampling it at time t_k, is in fact statistically independent of the set of random variables $\{X_j\}$; that is to say (see Problem 5.10),

$$E[X_j W'(t_k)] = 0, \qquad \begin{cases} j = 1, 2, \ldots, N \\ 0 \le t_k \le T \end{cases} \tag{5.47}$$

Since any random variable based on the remainder noise process $W'(t)$ is independent of the set of random variables $\{X_j\}$ as well as the set of transmitted signals $\{s_i(t)\}$, Equation (5.47) states that the random variable $W'(t_k)$ is irrelevant to the decision as to which particular signal was actually transmitted. In other words, the correlator outputs determined by the received signal $x(t)$ are the only data that are useful for the decision-making process and, hence, represent *sufficient statistics* for the problem at hand. By definition, sufficient statistics summarize the whole of the relevant information supplied by an observation vector.

We may now summarize the results presented in this section by formulating the *theorem of irrelevance*:

> Insofar as signal detection in additive white Gaussian noise is concerned, only the projections of the noise onto the basis functions of the signal set $\{s_i(t)\}_{i=1}^{M}$ affects the sufficient statistics of the detection problem; the remainder of the noise is irrelevant.

As a corollary to this theorem, we may state that the AWGN channel of Figure 5.2 is equivalent to an N-dimensional *vector channel* described by the observation vector

$$\mathbf{x} = \mathbf{s}_i + \mathbf{w}, \qquad i = 1, 2, \ldots, M \tag{5.48}$$

where the dimension N is the number of basis functions involved in formulating the signal vector $\mathbf{s}_i$. The individual components of the signal vector $\mathbf{s}_i$ and noise vector $\mathbf{w}$ are defined by Equations (5.6) and (5.31), respectively. The theorem of irrelevance and its corollary are indeed basic to the understanding of the signal detection problem as described next.

5.4 Likelihood Functions

The conditional probability density functions $f_{\mathbf{X}}(\mathbf{x}|m_i)$, $i = 1, 2, \ldots, M$, are the very characterization of an AWGN channel. Their derivation leads to a functional dependence on the observation vector $\mathbf{x}$, given the transmitted message symbol m_i. However, at the receiver we have the exact opposite situation: We are given the observation vector $\mathbf{x}$ and the requirement is to estimate the message symbol m_i that is responsible for generating $\mathbf{x}$. To emphasize this latter viewpoint, we introduce the idea of a *likelihood function*, denoted by $L(m_i)$ and defined by

$$L(m_i) = f_{\mathbf{X}}(\mathbf{x}|m_i), \qquad i = 1, 2, \ldots, M \tag{5.49}$$

It is important however to recognize that although the $L(m_i)$ and $f_{\mathbf{X}}(\mathbf{x}|m_i)$ have exactly the same mathematical form, their individual meanings are different.

In practice, we find it more convenient to work with the *log-likelihood function*, denoted by $l(m_i)$ and defined by

$$l(m_i) = \log L(m_i), \qquad i = 1, 2, \ldots, M \tag{5.50}$$

The log-likelihood function bears a one-to-one relationship to the likelihood function for two reasons:

1. By definition, a probability density function is always nonnegative. It follows therefore that the likelihood function is likewise a nonnegative quantity.
2. The logarithmic function is a monotonically increasing function of its argument.

The use of Equation (5.46) in (5.50) yields the log-likelihood functions for an AWGN channel as

$$l(m_i) = -\frac{1}{N_0}\sum_{j=1}^{N}(x_j - s_{ij})^2, \qquad i = 1, 2, \ldots, M \tag{5.51}$$

where we have ignored the constant term $-(N/2)\log(\pi N_0)$ as it bears no relation whatsoever to the message symbol m_i. Note that the s_{ij}, $j = 1, 2, \ldots, N$, are the elements of the signal vector $\mathbf{s}_i$ representing the message symbol m_i. With Equation (5.51) at our disposal, we are now ready to address the basic receiver design problem.

5.5 Coherent Detection of Signals in Noise: Maximum Likelihood Decoding

Suppose that in each time slot of duration T seconds, one of the M possible signals $s_1(t)$, $s_2(t), \ldots, s_M(t)$ is transmitted with equal probability, $1/M$. For geometric signal representation, the signal $s_i(t)$, $i = 1, 2, \ldots, M$, is applied to a bank of correlators, with a common input and supplied with an appropriate set of N orthonormal basis functions. The resulting correlator outputs define the *signal vector* $\mathbf{s}_i$. Since knowledge of the signal vector $\mathbf{s}_i$ is as good as knowing the transmitted signal $s_i(t)$ itself, and vice versa, we may represent $s_i(t)$ by a point in a Euclidean space of dimension $N \leq M$. We refer to this point as the *trans-*

mitted signal point or *message point.* The set of message points corresponding to the set of transmitted signals $\{s_i(t)\}_{i=1}^{M}$ is called a *signal constellation.*

However, the representation of the received signal $x(t)$ is complicated by the presence of additive noise $w(t)$. We note that when the received signal $x(t)$ is applied to the bank of N correlators, the correlator outputs define the observation vector $\mathbf{x}$. From Equation (5.48), the vector $\mathbf{x}$ differs from the signal vector $\mathbf{s}_i$ by the *noise vector* $\mathbf{w}$ whose orientation is completely random. The noise vector $\mathbf{w}$ is completely characterized by the noise $w(t)$; the converse of this statement, however, is not true. The noise vector $\mathbf{w}$ represents that portion of the noise $w(t)$ that will interfere with the detection process; the remaining portion of this noise, denoted by $w'(t)$, is tuned out by the bank of correlators.

Now, based on the observation vector $\mathbf{x}$, we may represent the received signal $x(t)$ by a point in the same Euclidean space used to represent the transmitted signal. We refer to this second point as the *received signal point.* The received signal point wanders about the message point in a completely random fashion, in the sense that it may lie anywhere inside a Gaussian-distributed "cloud" centered on the message point. This is illustrated in Figure 5.7*a* for the case of a three-dimensional signal space. For a particular realization of the noise vector $\mathbf{w}$ (i.e., a particular point inside the random cloud of Figure 5.7*a*), the relationship between the observation vector $\mathbf{x}$ and the signal vector $\mathbf{s}_i$ is as illustrated in Figure 5.7*b*.

We are now ready to state the signal detection problem:

> Given the observation vector $\mathbf{x}$, perform a mapping from $\mathbf{x}$ to an estimate $\hat{m}$ of the transmitted symbol, m_i, in a way that would minimize the probability of error in the decision-making process.

Suppose that, given the observation vector $\mathbf{x}$, we make the decision $\hat{m} = m_i$. The probability of error in this decision, which we denote by $P_e(m_i|\,\mathbf{x})$, is simply

$$\begin{aligned} P_e(m_i|\,\mathbf{x}) &= P(m_i \text{ not sent}\,|\,\mathbf{x}) \\ &= 1 - P(m_i \text{ sent}\,|\,\mathbf{x}) \end{aligned} \tag{5.52}$$

The decision-making criterion is to minimize the probability of error in mapping each given observation vector $\mathbf{x}$ into a decision. On the basis of Equation (5.52), we may therefore state the *optimum decision rule*:

$$\begin{aligned} &\text{Set } \hat{m} = m_i \text{ if} \\ &P(m_i \text{ sent}\,|\,\mathbf{x}) \geq P(m_k \text{ sent}\,|\,\mathbf{x}) \qquad \text{for all } k \neq i \end{aligned} \tag{5.53}$$

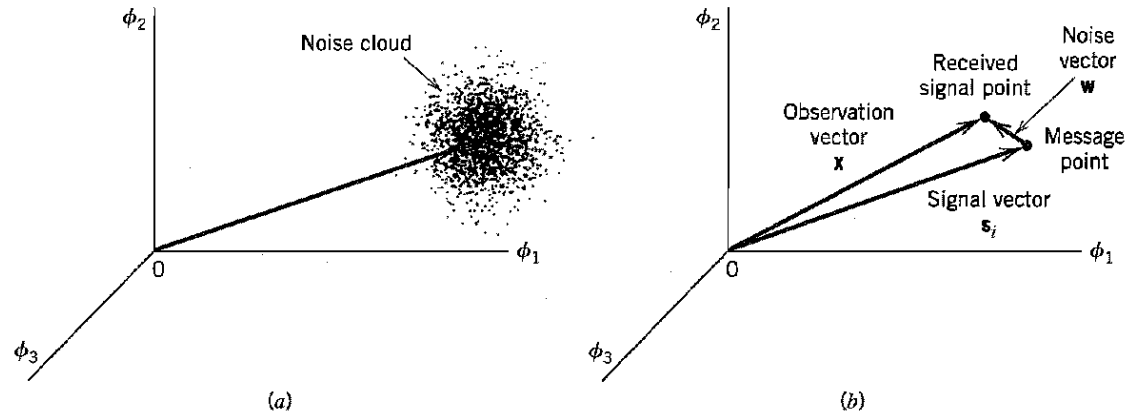

FIGURE 5.7 Illustrating the effect of noise perturbation, depicted in (*a*), on the location of the received signal point, depicted in (*b*).

where $k = 1, 2, \ldots, M$. This decision rule is referred to as the *maximum a posteriori probability (MAP) rule.*

The condition of Equation (5.53) may be expressed more explicitly in terms of the *a priori* probabilities of the transmitted signals and in terms of the likelihood functions. Using Bayes' rule in Equation (5.53), and for the moment ignoring possible ties in the decision-making process, we may restate the MAP rule as follows:

$$\text{Set } \hat{m} = m_i \text{ if}$$
$$\frac{p_k f_{\mathbf{X}}(\mathbf{x}|m_k)}{f_{\mathbf{X}}(\mathbf{x})} \text{ is maximum for } k = i \tag{5.54}$$

where p_k is the *a priori* probability of transmitting symbol m_k, $f_{\mathbf{X}}(\mathbf{x}|m_k)$ is the conditional probability density function of the random observation vector $\mathbf{X}$ given the transmission of symbol m_k, and $f_{\mathbf{X}}(\mathbf{x})$ is the unconditional probability density function of $\mathbf{X}$. In Equation (5.54) we may note the following:

- The denominator term $f_{\mathbf{X}}(\mathbf{x})$ is independent of the transmitted symbol.
- The *a priori* probability $p_k = p_i$ when all the source symbols are transmitted with equal probability.
- The conditional probability density function $f_{\mathbf{X}}(\mathbf{x}|m_k)$ bears a one-to-one relationship to the log-likelihood function $l(m_k)$.

Accordingly, we may restate the decision rule of Equation (5.54) in terms of $l(m_k)$ simply as follows:

$$\text{Set } \hat{m} = m_i \text{ if}$$
$$l(m_k) \text{ is maximum for } k = i \tag{5.55}$$

This decision rule is referred to as the *maximum likelihood rule*, and the device for its implementation is correspondingly referred to as the *maximum likelihood decoder.* According to Equation (5.55), a maximum likelihood decoder computes the log-likelihood functions as metrics for all the M possible message symbols, compares them, and then decides in favor of the maximum. Thus the maximum likelihood decoder differs from the maximum *a posteriori* decoder in that it assumes equally likely message symbols.

It is useful to have a graphical interpretation of the maximum likelihood decision rule. Let Z denote the N-dimensional space of all possible observation vectors $\mathbf{x}$. We refer to this space as the *observation space.* Because we have assumed that the decision rule must say $\hat{m} = m_i$, where $i = 1, 2, \ldots, M$, the total observation space Z is correspondingly partitioned into M*-decision regions*, denoted by $Z_1, Z_2, \ldots, Z_M$. Accordingly, we may restate the decision rule of Equation (5.55) as follows:

$$\text{Observation vector } \mathbf{x} \text{ lies in region } Z_i \text{ if}$$
$$l(m_k) \text{ is maximum for } k = i \tag{5.56}$$

Aside from the boundaries between the decision regions $Z_1, Z_2, \ldots, Z_M$, it is clear that this set of regions covers the entire space of possible observation vectors $\mathbf{x}$. We adopt the convention that all ties are resolved at random; that is, the receiver simply makes a guess. Specifically, if the observation vector $\mathbf{x}$ falls on the boundary between any two decision regions, Z_i and Z_k, say, the choice between the two possible decisions $\hat{m} = m_i$ and $\hat{m} = m_k$ is resolved *a priori* by the flip of a fair coin. Clearly, the outcome of such an event does not affect the ultimate value of the probability of error since, on this boundary, the condition of Equation (5.53) is satisfied with the equality sign.

The maximum likelihood decision rule of Equation (5.55) or its geometric counterpart described in Equation (5.56) is of a generic kind, with the channel noise $w(t)$ being additive as the only restriction imposed on it. We next specialize this rule for the case when $w(t)$ is both white and Gaussian.

From the log-likelihood function defined in Equation (5.51) for an AWGN channel we note that $l(m_k)$ attains its maximum value when the summation term

$$\sum_{j=1}^{N} (x_j - s_{kj})^2$$

is minimized by the choice $k = i$. Accordingly, we may formulate the maximum likelihood decision rule for an AWGN channel as

$$\begin{aligned} &\text{Observation vector } \mathbf{x} \text{ lies in region } Z_i \text{ if} \\ &\sum_{j=1}^{N} (x_j - s_{kj})^2 \text{ is minimum for } k = i \end{aligned} \tag{5.57}$$

Next, we note from our earlier discussion that (see Equation (5.14) for comparison)

$$\sum_{j=1}^{N} (x_j - s_{kj})^2 = \| \mathbf{x} - \mathbf{s}_k \|^2 \tag{5.58}$$

where $\| \mathbf{x} - \mathbf{s}_k \|$ is the Euclidean distance between the received signal point and message point, represented by the vectors $\mathbf{x}$ and $\mathbf{s}_k$, respectively. Accordingly, we may restate the decision rule of Equation (5.57) as follows:

$$\begin{aligned} &\text{Observation vector } \mathbf{x} \text{ lies in region } Z_i \text{ if} \\ &\text{the Euclidean distance } \| \mathbf{x} - \mathbf{s}_k \| \text{ is minimum for } k = i \end{aligned} \tag{5.59}$$

Equation (5.59) states that *the maximum likelihood decision rule is simply to choose the message point closest to the received signal point*, which is intuitively satisfying.

In practice, the need for squarers in the decision rule of Equation (5.59) is avoided by recognizing that

$$\sum_{j=1}^{N} (x_j - s_{kj})^2 = \sum_{j=1}^{N} x_j^2 - 2 \sum_{j=1}^{N} x_j s_{kj} + \sum_{j=1}^{N} s_{kj}^2 \tag{5.60}$$

The first summation term of this expansion is independent of the index k and may therefore be ignored. The second summation term is the inner product of the observation vector $\mathbf{x}$ and signal vector $\mathbf{s}_k$. The third summation term is the energy of the transmitted signal $s_k(t)$. Accordingly, we may formulate a decision rule equivalent to that of Equation (5.59) as follows:

$$\begin{aligned} &\text{Observation vector } \mathbf{x} \text{ lies in region } Z_i \text{ if} \\ &\sum_{j=1}^{N} x_j s_{kj} - \frac{1}{2} E_k \text{ is maximum for } k = i \end{aligned} \tag{5.61}$$

where E_k is the energy of the transmitted signal $s_k(t)$:

$$E_k = \sum_{j=1}^{N} s_{kj}^2 \tag{5.62}$$

From Equation (5.61) we deduce that, for an AWGN channel, the decision regions are regions of the N-dimensional observation space Z, bounded by linear [$(N-1)$-dimensional hyperplane] boundaries. Figure 5.8 shows the example of decision regions for

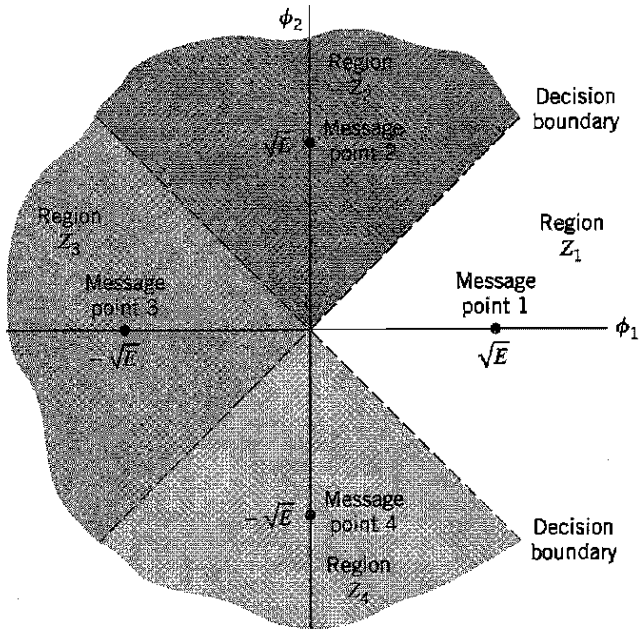

FIGURE 5.8 Illustrating the partitioning of the observation space into decision regions for the case when $N = 2$ and $M = 4$; it is assumed that the M transmitted symbols are equally likely.

$M = 4$ signals and $N = 2$ dimensions, assuming that the signals are transmitted with equal energy, E, and equal probability.

5.6 Correlation Receiver

From the material presented in the previous sections, we find that for an AWGN channel and for the case when the transmitted signals $s_1(t), s_2, \ldots, s_M(t)$ are equally likely, the optimum receiver consists of two subsystems, which are detailed in Figure 5.9 and described here:

1. The *detector* part of the receiver is shown in Figure 5.9*a*. It consists of a bank of M *product-integrators* or *correlators*, supplied with a corresponding set of coherent reference signals or orthonormal basis functions $\phi_1(t), \phi_2(t), \ldots, \phi_N(t)$ that are generated locally. This bank of correlators operates on the received signal $x(t)$, $0 \leq t \leq T$, to produce the observation vector $\mathbf{x}$.
2. The second part of the receiver, namely, the *signal transmission decoder* is shown in Figure 5.9*b*. It is implemented in the form of a maximum-likelihood decoder that operates on the observation vector $\mathbf{x}$ to produce an estimate, $\hat{m}$, of the transmitted symbol m_i, $i = 1, 2, \ldots, M$, in a way that would minimize the average probability of symbol error. In accordance with Equation (5.61), the N elements of the observation vector $\mathbf{x}$ are first multiplied by the corresponding N elements of each of the M signal vectors $\mathbf{s}_1, \mathbf{s}_2, \ldots, \mathbf{s}_M$, and the resulting products are successively summed in accumulators to form the corresponding set of inner products $\{\mathbf{x}^T\mathbf{s}_k \mid k = 1, 2, \ldots, M\}$. Next, the inner products are corrected for the fact that the transmitted signal energies may be unequal. Finally, the largest in the resulting set of numbers is selected, and an appropriate decision on the transmitted message is made.

The optimum receiver of Figure 5.9 is commonly referred to as a *correlation receiver*.

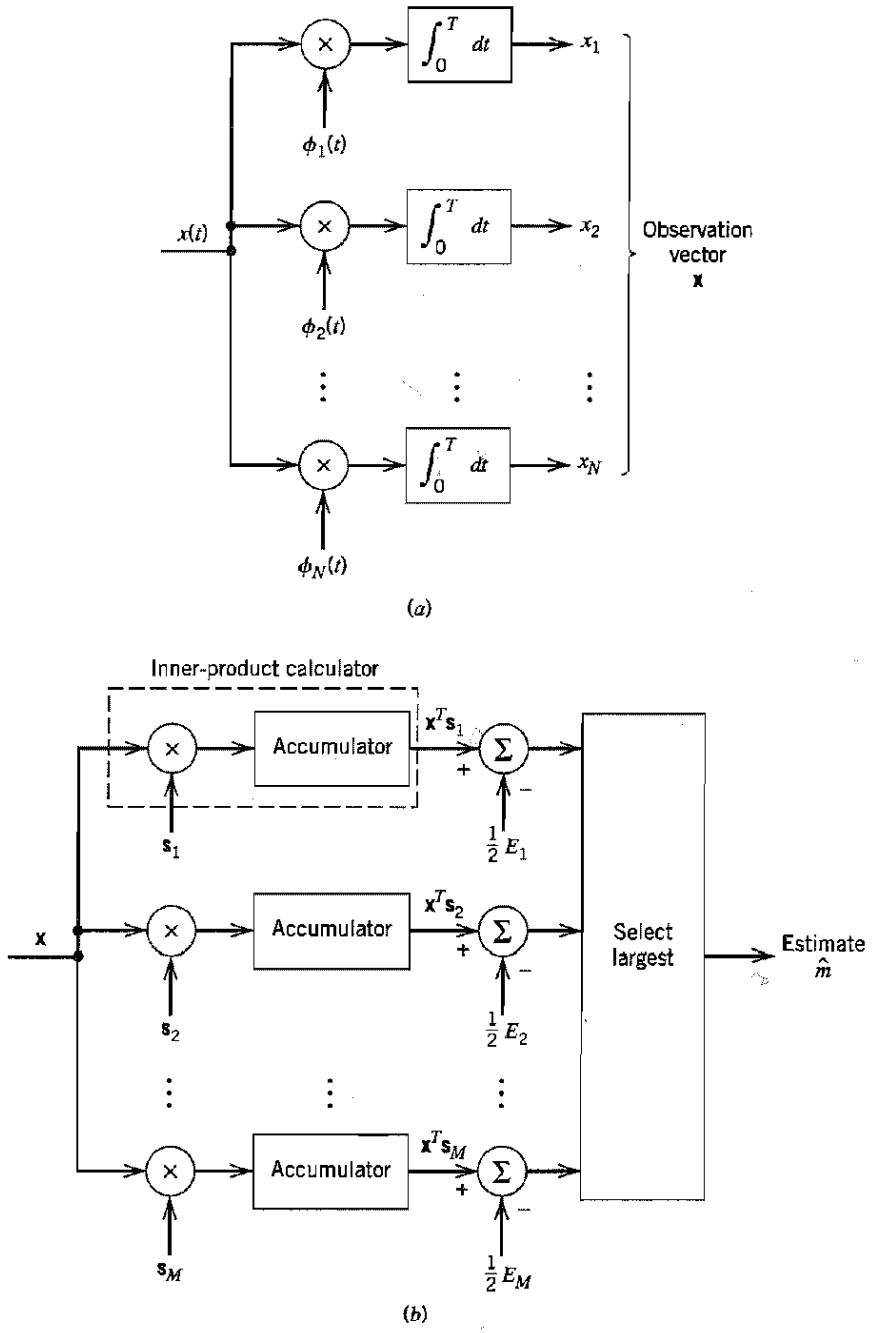

FIGURE 5.9 (*a*) Detector or demodulator. (*b*) Signal transmission decoder.

■ EQUIVALENCE OF CORRELATION AND MATCHED FILTER RECEIVERS

The detector shown in Figure 5.9*a* involves a set of correlators. Alternatively, we may use a corresponding set of *matched filters* to build the detector; the matched filter and its properties were considered in Section 4.2. To demonstrate the equivalence of a correlator and a matched filter, consider a linear time-invariant filter with impulse response $h_j(t)$. With the received signal $x(t)$ used as the filter input, the resulting filter output, $y_j(t)$, is defined by the convolution integral:

$$y_j(t) = \int_{-\infty}^{\infty} x(\tau)h_j(t - \tau)d\tau \tag{5.63}$$

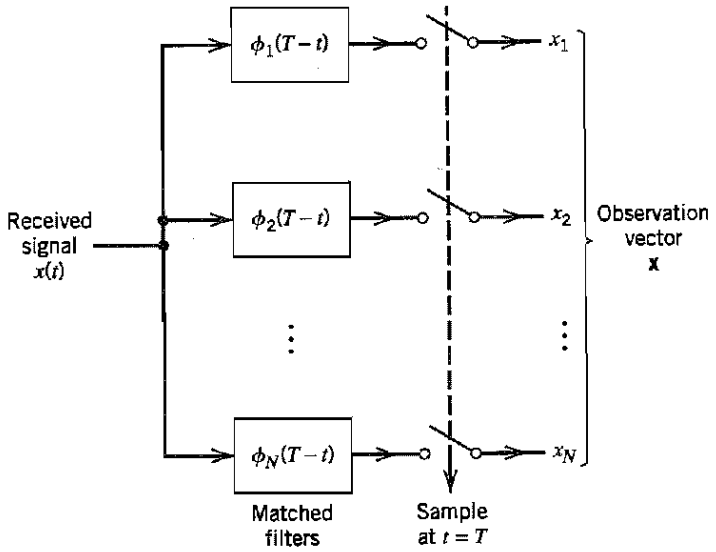

FIGURE 5.10 Detector part of matched filter receiver; the signal transmission decoder is as shown in Fig. 5.9*b*.

From the definition of a matched filter presented in Section 4.2, we recall that the impulse response $h_j(t)$ of a linear time-invariant filter matched to an input signal $\phi_j(t)$ is a time-reversed and delayed version of the input $\phi_j(t)$. Suppose that we set

$$h_j(t) = \phi_j(T - t) \tag{5.64}$$

Then the resulting filter output is

$$y_j(t) = \int_{-\infty}^{\infty} x(\tau)\phi_j(T - t + \tau)d\tau \tag{5.65}$$

Sampling this output at time $t = T$, we get

$$y_j(T) = \int_{-\infty}^{\infty} x(\tau)\phi_j(\tau)d\tau$$

Since, by definition, $\phi_j(t)$ is zero outside the interval $0 \leq t \leq T$, we find that $y_j(T)$ is in actual fact the jth correlator output x_j produced by the received signal $x(t)$ in Figure 5.9*a*, as shown by

$$y_j(T) = \int_0^T x(\tau)\phi_j(\tau)d\tau \tag{5.66}$$

Accordingly, the detector part of the optimum receiver may also be implemented using a bank of matched filters, as shown in Figure 5.10. It is important to note, however, that the output of each correlator in Figure 5.9*a* is equivalent to the output of a corresponding matched filter in Figure 5.10 only when that output is sampled at time $t = T$.

5.7 *Probability of Error*

To complete the statistical characterization of the correlation receiver depicted in Figure 5.9, we need to evaluate its noise performance. To do so, suppose that the observation space Z is partitioned, in accordance with the maximum likelihood decision rule, into a set if M regions $\{Z_i\}_{i=1}^{M}$. Suppose also that symbol m_i (or, equivalently, signal vector $\mathbf{s}_i$) is

transmitted, and an observation vector $\mathbf{x}$ is received. Then an error occurs whenever the received signal point represented by $\mathbf{x}$ does not fall inside region Z_i associated with the message point represented by $\mathbf{s}_i$. Averaging over all possible transmitted symbols, we readily see that the *average probability of symbol error*, P_e is

$$\begin{aligned} P_e &= \sum_{i=1}^{M} p_i P(\mathbf{x} \text{ does not lie in } Z_i | m_i \text{ sent}) \\ &= \frac{1}{M} \sum_{i=1}^{M} P(\mathbf{x} \text{ does not lie in } Z_i | m_i \text{ sent}) \\ &= 1 - \frac{1}{M} \sum_{i=1}^{M} P(\mathbf{x} \text{ lies in } Z_i | m_i \text{ sent}) \end{aligned} \tag{5.67}$$

where we have used standard notation to denote the probability of an event and the conditional probability of an event. Since $\mathbf{x}$ is the sample value of random vector $\mathbf{X}$, we may rewrite Equation (5.67) in terms of the likelihood function (when m_i is sent) as follows:

$$P_e = 1 - \frac{1}{M} \sum_{i=1}^{M} \int_{Z_i} f_{\mathbf{X}}(\mathbf{x} | m_i)\, d\mathbf{x} \tag{5.68}$$

For an N-dimensional observation vector, the integral in Equation (5.68) is likewise N-dimensional.

Invariance of the Probability of Error to Rotation and Translation

The way in which the observation space Z is partitioned into the set of regions $Z_1, Z_2, \ldots, Z_M$, in the maximum likelihood detection of a signal in additive white Gaussian noise, is uniquely defined by the signal constellation under study. Accordingly, changes in the orientation of the signal constellation with respect to both the coordinate axes and origin of the signal space do *not* affect the probability of symbol error P_e defined in Equation (5.68). This result is a consequence of two facts:

1. In maximum likelihood detection, the probability of symbol error P_e depends solely on the relative Euclidean distances between the message points in the constellation.
2. The additive white Gaussian noise is *spherically symmetric* in all directions in the signal space.

Consider first the invariance of P_e with respect to rotation. The effect of a rotation applied to all the message points in a constellation is equivalent to multiplying the N-dimensional signal vector $\mathbf{s}_i$ by an N-by-N *orthonormal matrix* denoted by $\mathbf{Q}$ for all i. The matrix $\mathbf{Q}$ satisfies the condition

$$\mathbf{Q}\mathbf{Q}^T = \mathbf{I} \tag{5.69}$$

where $\mathbf{I}$ is the *identity matrix* whose diagonal elements are all unity and its off-diagonal elements are all zero. Note that according to Equation (5.69), the inverse of a real-valued orthonormal matrix is equal to its transposed form. Thus the signal vector $\mathbf{s}_i$ is replaced by its rotated version

$$\mathbf{s}_{i,\text{rotate}} = \mathbf{Q}\mathbf{s}_i, \qquad i = 1, 2, \ldots, M \tag{5.70}$$

Correspondingly, the N-by-1 noise vector $\mathbf{w}$ is replaced by its rotated version

$$\mathbf{w}_{\text{rotate}} = \mathbf{Q}\mathbf{w} \tag{5.71}$$

However, the statistical characteristics of the noise vector are unaffected by this rotation for the following reasons:

- From Chapter 1 we recall that a linear combination of Gaussian random variables is also Gaussian. Since the noise vector $\mathbf{w}$ is Gaussian, by assumption, it follows that the rotated noise vector $\mathbf{w}_{\text{rotate}}$ is also Gaussian.
- Since the noise vector w has zero mean, the rotated noise vector $\mathbf{w}_{\text{rotate}}$ also has zero mean, as shown by

$$\begin{aligned} E[\mathbf{w}_{\text{rotate}}] &= E[\mathbf{Q}\mathbf{w}] \\ &= \mathbf{Q}E[\mathbf{w}] \\ &= 0 \end{aligned} \tag{5.72}$$

- The covariance matrix of the noise vector w is equal to $(N_0/2)\mathbf{I}$, where $N_0/2$ is the power spectral density of the AWGN $w(t)$; that is,

$$E[\mathbf{w}\mathbf{w}^T] = \frac{N_0}{2}\mathbf{I} \tag{5.73}$$

Hence, the covariance matrix of the rotated noise vector $\mathbf{w}_{\text{rotate}}$ is

$$\begin{aligned} E[\mathbf{w}_{\text{rotate}}\mathbf{w}_{\text{rotate}}^T] &= E[\mathbf{Q}\mathbf{w}(\mathbf{Q}\mathbf{w})^T] \\ &= E[\mathbf{Q}\mathbf{w}\mathbf{w}^T\mathbf{Q}^T] \\ &= \mathbf{Q}E[\mathbf{w}\mathbf{w}^T]\mathbf{Q}^T \\ &= \frac{N_0}{2}\mathbf{Q}\mathbf{Q}^T \\ &= \frac{N_0}{2}\mathbf{I} \end{aligned} \tag{5.74}$$

where in the last two lines we have made use of Equations (5.73) and (5.69).

In light of these observations, we may express the observation vector for the rotated signal constellation as

$$\mathbf{x}_{\text{rotate}} = \mathbf{Q}\mathbf{s}_i + \mathbf{w}, \qquad i = 1, 2, \ldots, M \tag{5.75}$$

From Equation (5.59) we know that the decision rule for maximum likelihood detection is based on the Euclidean distance from the observation vector $\mathbf{x}_{\text{rotate}}$ to the rotated signal vector $\mathbf{s}_{i,\text{rotate}} = \mathbf{Q}\mathbf{s}_i$. Comparing Equation (5.75) to Equation (5.48), we readily see that

$$\| \mathbf{x}_{\text{rotate}} - \mathbf{s}_{i,\text{rotate}} \| = \| \mathbf{x} - \mathbf{s}_i \| \qquad \text{for all } i \tag{5.76}$$

We may therefore formally state the *principle of rotational invariance* as follows:

> If a signal constellation is rotated by an orthonormal transformation, that is,
>
> $$\mathbf{s}_{i,\text{rotate}} = \mathbf{Q}\mathbf{s}_i, \qquad i = 1, 2, \ldots, M$$
>
> where Q is an orthonormal matrix, then the probability of symbol error P_e incurred in maximum likelihood signal detection over an AWGN channel is completely unchanged.

We illustrate this principle with an example. The signal constellation shown in Figure 5.11*b* is the same as that of Figure 5.11*a*, except that it has been rotated through 45 degrees. Although these two constellations do indeed look different, the principle of rotational invariance tells us immediately that the P_e is the same for both of them.

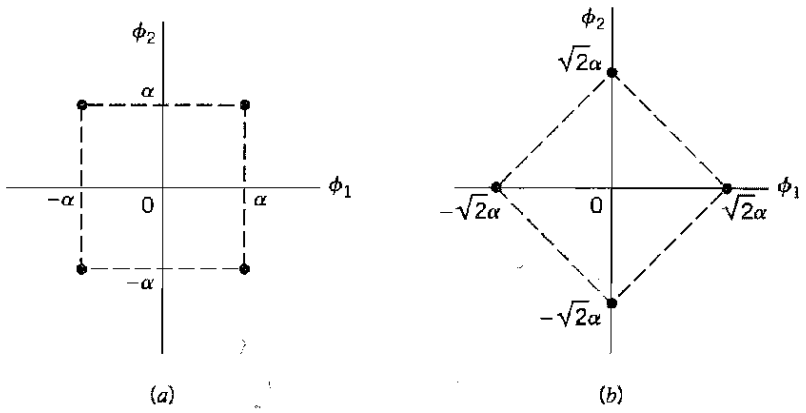

FIGURE 5.11 A pair of signal constellations for illustrating the principle of rotational invariance.

Consider next the issue of invariance to translation. Suppose all the message points in a signal constellation are translated by a constant vector amount **a**, as shown by

$$\mathbf{s}_{i,\text{translate}} = \mathbf{s}_i - \mathbf{a}, \qquad i = 1, 2, \ldots, M \tag{5.77}$$

The observation vector is correspondingly translated by the same vector amount, as shown by

$$\mathbf{x}_{\text{translate}} = \mathbf{x} - \mathbf{a} \tag{5.78}$$

From Equations (5.77) and (5.78) we see that the translate **a** is common to both the translated signal vector $\mathbf{s}_i$ and translated observation vector **x**. We therefore immediately deduce that

$$\| \mathbf{x}_{\text{translate}} - \mathbf{s}_{i,\text{translate}} \| = \| \mathbf{x} - \mathbf{s}_i \| \qquad \text{for all } i \tag{5.79}$$

and thus formulate the *principle of translational invariance* as follows:

> If a signal constellation is translated by a constant vector amount, then the probability of symbol error P_e incurred in maximum likelihood signal detection over an AWGN channel is completely unchanged.

As an example, consider the two signal constellations shown in Figure 5.12, which pertain to a pair of different 4-level PAM signals. The constellation of Figure 5.12*b* is the same as that of Figure 5.12*a*, except for a translation of $3\alpha/2$ to the right along the ϕ_1-axis. The principle of translational invariance says that the P_e is the same for both of these constellations.

■ MINIMUM ENERGY SIGNALS

A useful application of the principle of translational invariance is in the translation of a given signal constellation in such a way that the average energy is minimized. To explore

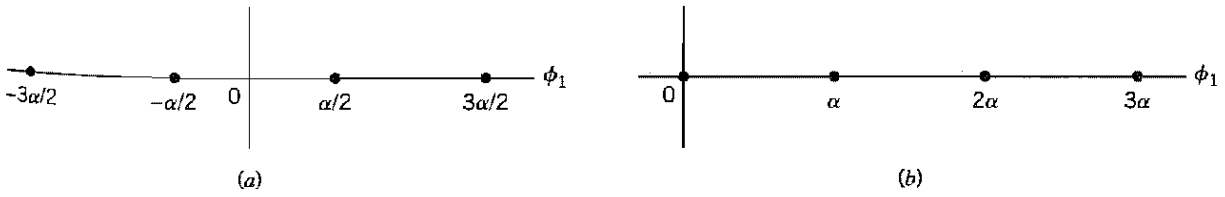

FIGURE 5.12 A pair of signal constellations for illustrating the principle of translational invariance.

this issue, consider a set of symbols $m_1, m_2, \ldots, m_M$ represented by the signal vectors $\mathbf{s}_1, \mathbf{s}_2, \ldots, \mathbf{s}_M$, respectively. The average energy of this signal constellation translated by a vector amount $\mathbf{a}$ is

$$\mathscr{E}_{\text{translate}} = \sum_{i=1}^{M} \| \mathbf{s}_i - \mathbf{a} \|^2 p_i \tag{5.80}$$

where p_i is the probability that symbol m_i is emitted by the source of information. The squared Euclidean distance between $\mathbf{s}_i$ and $\mathbf{a}$ is expanded as

$$\| \mathbf{s}_i - \mathbf{a} \|^2 = \| \mathbf{s}_i \|^2 - 2\mathbf{a}^T\mathbf{s}_i + \| \mathbf{a} \|^2$$

We may therefore rewrite Equation (5.80) in the expanded form

$$\begin{aligned} \mathscr{E}_{\text{translate}} &= \sum_{i=1}^{M} \| \mathbf{s}_i \|^2 p_i - 2 \sum_{i=1}^{M} \mathbf{a}^T\mathbf{s}_i p_i + \| \mathbf{a} \|^2 \sum_{i=1}^{M} p_i \\ &= \mathscr{E} - 2\mathbf{a}^T E[\mathbf{s}] + \| \mathbf{a} \|^2 \end{aligned} \tag{5.81}$$

where $\mathscr{E}$ is the average energy of the original signal constellation, and

$$E[\mathbf{s}] = \sum_{i=1}^{M} \mathbf{s}_i p_i \tag{5.82}$$

Differentiating Equation (5.81) with respect to the vector $\mathbf{a}$ and then setting the result equal to zero, we readily find that the minimizing translate is

$$\mathbf{a}_{\min} = E[\mathbf{s}] \tag{5.83}$$

The minimum average energy of the signal constellation translated in this way is

$$\mathscr{E}_{\text{translate,min}} = \mathscr{E} - \| \mathbf{a}_{\min} \|^2 \tag{5.84}$$

We may now state the procedure for finding the *minimum energy translate*:

> Given a signal constellation $\{\mathbf{s}_i\}_{i=1}^{M}$, the corresponding signal constellation with minimum average energy is obtained by subtracting from each signal vector $\mathbf{s}_i$ in the given constellation an amount equal to the constant vector $E[\mathbf{s}]$, where $E[\mathbf{s}]$ is defined by Equation (5.82).

Recalling that the energy (or power) needed for signal transmission is a primary resource, the minimum energy translate provides a principled method for translating a signal constellation of interest so as to minimize the energy requirement. For example, the constellation of Figure 5.12*a* has minimum average energy, whereas that of Figure 5.12*b* does not.

■ UNION BOUND ON THE PROBABILITY OF ERROR[2]

For AWGN channels, the formulation of the average probability of symbol error, P_e, is conceptually straightforward. We simply write P_e in integral form by substituting Equation (5.46) into Equation (5.68). Unfortunately, however, numerical computation of the integral is impractical, except in a few simple (but important) cases. To overcome this computational difficulty, we may resort to the use of *bounds*, which are usually adequate to predict the signal-to-noise ratio (within a decibel or so) required to maintain a prescribed error rate. The approximation to the integral defining P_e is made by simplifying the integral or simplifying the region of integration. In the sequel, we use the latter procedure to develop a simple yet useful upper bound called the *union bound* as an approximation to the

average probability of symbol error for a set of M equally likely signals (symbols) in an AWGN channel.

Let A_{ik}, with $(i, k) = 1, 2, \ldots, M$, denote the event that the observation vector $\mathbf{x}$ is closer to the signal vector $\mathbf{s}_k$ than to $\mathbf{s}_i$, when the symbol m_i (vector $\mathbf{s}_i$) is sent. The conditional probability of symbol error when symbol m_i is sent, $P_e(m_i)$, is equal to the probability of the *union of events*, $A_{i1}, A_{i2}, \ldots, A_{i,i-1}, A_{i,i+1}, \ldots, A_{i,M}$. From probability theory we know that *the probability of a finite union of events is overbounded by the sum of the probabilities of the constituent events.* We may therefore write

$$P_e(m_i) \leq \sum_{\substack{k=1 \\ k \neq i}}^{M} P(A_{ik}), \qquad i = 1, 2, \ldots, M \tag{5.85}$$

This relationship is illustrated in Figure 5.13 for the case of $M = 4$. In Figure 5.13*a*, we show the four message points and associated decision regions, with the point $\mathbf{s}_1$ assumed to represent the transmitted symbol. In Figure 5.13*b*, we show the three constituent signal-space descriptions where, in each case, the transmitted message point $\mathbf{s}_1$ and one other message point are retained. According to Figure 5.13*a* the conditional probability of symbol error, $P_e(m_i)$, is equal to the probability that the observation vector $\mathbf{x}$ lies in the shaded region of the two-dimensional signal-space diagram. Clearly, this probability is less than the sum of the probabilities of the three individual events that $\mathbf{x}$ lies in the shaded regions of the three constituent signal spaces depicted in Figure 5.13*b*.

It is important to note that, in general, the probability $P(A_{ik})$ is different from the probability $P(\hat{m} = m_k | m_i)$. The latter is the probability that the observation vector $\mathbf{x}$ is

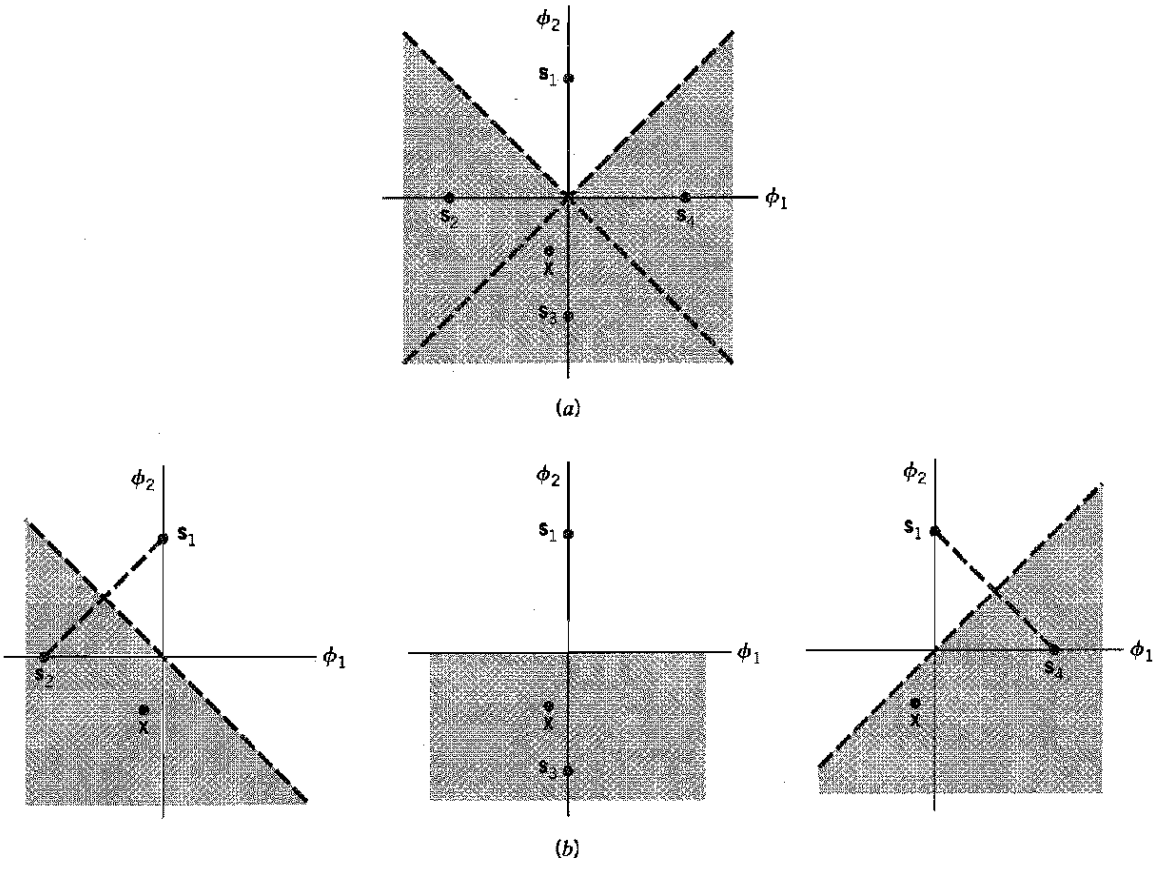

FIGURE 5.13 Illustrating the union bound. (*a*) Constellation of four message points. (*b*) Three constellations with a common message point and one other message point retained from the original constellation.

closer to the signal vector $\mathbf{s}_k$ than every other, when $\mathbf{s}_i$ (or m_i) is sent. On the other hand, the probability $P(A_{ik})$ depends on only two signal vectors, $\mathbf{s}_i$ and $\mathbf{s}_k$. To emphasize this difference, we rewrite Equation (5.85) by adopting $P_2(\mathbf{s}_i, \mathbf{s}_k)$ in place of $P(A_{ik})$. We thus write

$$P_e(m_i) \leq \sum_{\substack{k=1 \\ k \neq i}}^{M} P_2(\mathbf{s}_i, \mathbf{s}_k), \qquad i = 1, 2, \ldots, M \tag{5.86}$$

The probability $P_2(\mathbf{s}_i, \mathbf{s}_k)$ is called the *pairwise error probability* in that if a data transmission system uses only a pair of signals, $\mathbf{s}_i$ and $\mathbf{s}_k$, then $P_2(\mathbf{s}_i, \mathbf{s}_k)$ is the probability of the receiver mistaking $\mathbf{s}_k$ for $\mathbf{s}_i$.

Consider then a simplified digital communication system that involves the use of two equally likely messages represented by the vectors $\mathbf{s}_i$ and $\mathbf{s}_k$. Since white Gaussian noise is identically distributed along any set of orthogonal axes, we may temporarily choose the first axis in such a set as one that passes through the points $\mathbf{s}_i$ and $\mathbf{s}_k$; for three examples, see Figure 5.13*b*. The corresponding decision boundary is represented by the bisector that is perpendicular to the line joining the points $\mathbf{s}_i$ and $\mathbf{s}_k$. Accordingly, when the symbol m_i (vector $\mathbf{s}_i$) is sent, and if the observation vector $\mathbf{x}$ lies on the side of the bisector where $\mathbf{s}_k$ lies, an error is made. The probability of this event is given by

$$\begin{aligned} P_2(\mathbf{s}_i, \mathbf{s}_k) &= P(\mathbf{x} \text{ is closer to } \mathbf{s}_k \text{ than } \mathbf{s}_i, \text{ when } \mathbf{s}_i \text{ is sent}) \\ &= \int_{d_{ik}/2}^{\infty} \frac{1}{\sqrt{\pi N_0}} \exp\left(-\frac{v^2}{N_0}\right) dv \end{aligned} \tag{5.87}$$

where d_{ik} is the Euclidean distance between $\mathbf{s}_i$ and $\mathbf{s}_k$; that is,

$$d_{ik} = \| \mathbf{s}_i - \mathbf{s}_k \| \tag{5.88}$$

From the definition of the complementary error function, we have

$$\operatorname{erfc}(u) = \frac{2}{\sqrt{\pi}} \int_u^{\infty} \exp(-z^2)\, dz$$

Thus, in terms of this function, with z set equal to $v/\sqrt{N_0}$, we find that Equation (5.87) takes on the compact form

$$P_2(\mathbf{s}_i, \mathbf{s}_k) = \frac{1}{2} \operatorname{erfc}\left(\frac{d_{ik}}{2\sqrt{N_0}}\right) \tag{5.89}$$

Substituting Equation (5.89) into Equation (5.86), we get

$$P_e(m_i) \leq \frac{1}{2} \sum_{\substack{k=1 \\ k \neq i}}^{M} \operatorname{erfc}\left(\frac{d_{ik}}{2\sqrt{N_0}}\right), \qquad i = 1, 2, \ldots, M \tag{5.90}$$

The probability of symbol error, averaged over all the M symbols, is therefore overbounded as follows:

$$\begin{aligned} P_e &= \sum_{i=1}^{M} p_i P_e(m_i) \\ &\leq \frac{1}{2} \sum_{i=1}^{M} \sum_{\substack{k=1 \\ k \neq i}}^{M} p_i \operatorname{erfc}\left(\frac{d_{ik}}{2\sqrt{N_0}}\right) \end{aligned} \tag{5.91}$$

where p_i is the probability of transmitting symbol m_i.

There are two special forms of Equation (5.91) that we will find useful in Chapter 6 on passband data transmission:

1. Suppose that the signal constellation is *circularly symmetric* about the origin. Then the conditional probability of error $P_e(m_i)$ is the same for all i, in which case Equation (5.91) reduces to

$$P_e \leq \frac{1}{2} \sum_{\substack{k=1 \\ k \neq i}}^{M} \operatorname{erfc}\left(\frac{d_{ik}}{2\sqrt{N_0}}\right) \text{ for all } i \tag{5.92}$$

2. Define the *minimum distance* of a signal constellation, $d_{\min}$, as the smallest Euclidean distance between any two transmitted signal points in the constellation, as shown by

$$d_{\min} = \min_{k \neq i} d_{ik} \qquad \text{for all } i \text{ and } k \tag{5.93}$$

Then, recognizing that the complementary error function $\operatorname{erfc}(u)$ is a monotonically decreasing function of its argument u, we may write

$$\operatorname{erfc}\left(\frac{d_{ik}}{2\sqrt{N_0}}\right) \leq \operatorname{erfc}\left(\frac{d_{\min}}{2\sqrt{N_0}}\right) \text{ for all } i \text{ and } k \tag{5.94}$$

We may therefore, in general, simplify the bound on the average probability of symbol error in Equation (5.91) as

$$P_e \leq \frac{(M-1)}{2} \operatorname{erfc}\left(\frac{d_{\min}}{2\sqrt{N_0}}\right) \tag{5.95}$$

The complementary error function is itself bounded as[3]

$$\operatorname{erfc}\left(\frac{d_{\min}}{2\sqrt{N_0}}\right) \leq \frac{1}{\sqrt{\pi}} \exp\left(-\frac{d_{\min}^2}{4N_0}\right) \tag{5.96}$$

Accordingly, we may further simplify the union bound on P_e given in Equation (5.95) as

$$P_e \leq \frac{(M-1)}{2\sqrt{\pi}} \exp\left(-\frac{d_{\min}^2}{4N_0}\right) \tag{5.97}$$

Equation (5.97) shows that for a prescribed AWGN channel, the average probability of symbol error P_e decreases exponentially as the squared minimum distance, $d_{\min}^2$.

Bit versus Symbol Error Probabilities

Thus far, the only figure of merit we have used to assess the noise performance of a digital passband transmission system has been the average probability of symbol error. This figure of merit is the natural choice when messages of length $m = \log_2 M$ are transmitted, such as alphanumeric symbols. However, when the requirement is to transmit binary data such as digital computer data, it is often more meaningful to use another figure of merit called the *bit error rate* (BER). Although, in general, there are no unique relationships between these two figures of merit, it is fortunate that such relationships can be derived for two cases of practical interest, as discussed next.

Case 1

In the first case, we assume that it is possible to perform the mapping from binary to M-ary symbols in such a way that the two binary M-tuples corresponding to any pair of adjacent symbols in the M-ary modulation scheme differ in only one bit position. This mapping constraint is satisfied by using a *Gray code*. When the probability of symbol error P_e is acceptably small, we find that the probability of mistaking one symbol for either one of the two "nearest" symbols is much greater than any other kind of symbol error. Moreover, given a symbol error, the most probable number of bit errors is one, subject to the aforementioned mapping constraint. Since there are $\log_2 M$ bits per symbol, it follows that the average probability of symbol error is related to the bit error rate as follows:

$$\begin{aligned} P_e &= P\left(\bigcup_{i=1}^{\log_2 M} \{i\text{th bit is in error}\}\right) \\ &\leq \sum_{i=1}^{\log_2 M} P(i\text{th bit is in error}) \\ &= \log_2 M \cdot (\text{BER}) \end{aligned} \tag{5.97}$$

We also note that

$$P_e \geq P(i\text{th bit is in error}) = \text{BER} \tag{5.98}$$

It follows therefore that the bit error rate is bounded as follows:

$$\frac{P_e}{\log_2 M} \leq \text{BER} \leq P_e \tag{5.99}$$

Case 2

Let $M = 2^K$, where K is an integer. We assume that all symbol errors are equally likely and occur with probability

$$\frac{P_e}{M-1} = \frac{P_e}{2^K - 1}$$

where P_e is the average probability of symbol error. What is the probability that the ith bit in a symbol is in error? Well, there are 2^{K-1} cases of symbol error in which this particular bit is changed, and there are 2^{K-1} cases in which it is not changed. Hence, the bit error rate is

$$\text{BER} = \left(\frac{2^{K-1}}{2^K - 1}\right) P_e \tag{5.100}$$

or, equivalently,

$$\text{BER} = \left(\frac{M/2}{M-1}\right) P_e \tag{5.101}$$

Note that for large M, the bit error rate approaches the limiting value of $P_e/2$. The same idea described here also shows that bit errors are not independent, since we have

$$P(i\text{th and } j\text{th bits are in error}) = \frac{2^{K-2}}{2^K - 1} P_e \neq (\text{BER})^2$$